Ministry of Education and Science of the Russian Federation Federal State Budgetary Educational Institution of Higher Education

"Moscow State Technological University "STANKIN"

Institute of Mechanical Engineering and Engineering

Department of High Efficient Processing Technologies

On the rights of the manuscript

_____ Signed _____

Student's signature

Dhiaa Hameed Chiad Hilfi

"Research and development of plasma-electrolyte surface treatment technology for mechanical engineering products made of valve alloys formed by additive technologies"

Scientific and qualification work in the field of
15.06.01 MECHANICAL ENGINEERING
05.02.07 "Technology and equipment of mechanical and physico-technical processing"

Scientific supervisor		Doctor of Technical Sciences, Professor, Suminov I.V.
	Signed	Academic degree, academic title, full name
The reviewer		is Doctor of Technical Sciences, professor.
	Signed	Academic degree, academic title, full name
Head of the Department		Doctor of Technical Sciences, Professor, Grigoriev S.N.
	Signed	Academic degree, academic title, full name
Director of the Institute		Doctor of Technical Sciences, Professor, M.M. Stebulyanin.
	Signed	Academic degree, academic title, full name

MOSCOW 2024

Table of contents Introduction

Introduction

The relevance of the work.

Currently, work is actively underway in various industries in Russia and abroad and "Technologies and devices based on the method known as 'Additive Manufacturing' are being introduced. (AT) or Additive Manufacturing (AM).

The idea behind the new principle of manufacturing parts is not to cut off excess from blanks or semi-finished products, but to build up the material in layers. This idea is especially attractive in aircraft, shipbuilding and other industries, where the cost of materials is quite high, and complex configurations of parts have high requirements for minimizing weight with maximum strength.

Traditional methods of manufacturing parts, such as casting or volumetric stamping, it is not always possible to realize the complex spatial shapes of parts used in this industry. In addition, traditional methods of production of blanks and parts are completely dependent on technological equipment, the development and manufacture of which is a complex and expensive process, especially in pilot or small-scale production.

Recently, the use of AM methods for the layered synthesis of large-sized products has been expanding. Large-scale installations for complex and large parts for nuclear and other industries are being developed.

The possibility of practical industrial implementation of layer-by-layer expansion appeared only with the development of computer technology, which greatly simplified the development of programs for cutting any parts into a large number of planes.

The layered method of creating parts opens up completely new possibilities provided by this technology, including the creation of a "part in a part", the production of components with varying thickness

of 6

the properties of the material (known as gradient materials), as well as the manufacture of mesh structures that cannot be obtained either by casting or machining. 3D technologies have huge potential in the aerospace industry. This is due to the fact that they can significantly reduce the ratio of the mass of the material required for the production of the part to the mass of the finished product. With

traditional manufacturing methods, this ratio can reach 20:1, whereas with the use of additive technologies, in the worst case, it is 2:1.

The following advantages of additive manufacturing technologies can be distinguished:

Simplification of the production process consists in the possibility of creating complex structures and components, which simplifies and accelerates the production stages and reduces manufacturing costs.

Reducing the number of components in assemblies and assemblies is achieved by integrating multiple functions into one element, which simplifies the design and reduces the number of assembly operations.

Simplification of production stages;

- Refusal to use accessories and accessories;
- Production directly at the place of use;
- Mechanization of the production cycle
- Reduction of labor costs for production;
- Reduction of production time;
- Increase in production accuracy;
- Reducing the mass of products;
- Standardization of the materials used;
- Minimizing waste.
- Specific operating conditions:
- Long service life;
- Increased strength of materials;
- Reliable functioning of the structure;
- Facilitating the repair and replacement of components;

Based on the above, it can be concluded that in recent years there has been a steady trend towards an increase in the proportion of parts produced using additive or 3D technologies, as finished products - direct production (DP).

In recent years, considerable attention has been paid to additive manufacturing (AM) technologies for the manufacture of aluminum and titanium alloy components, as evidenced by a significant number of publications both domestically and abroad.

Currently, titanium is considered one of the most common metals in our time. Titanium alloys are used in many sectors, especially in the aerospace industry. Due to its exceptional properties and relatively low density, titanium is used not only in the manufacture of orthopedic and dental implants, but also in the manufacture of components for modern aircraft and spacecraft.

The widespread use of titanium makes it one of the most sought-after metals on the planet. The popularity of titanium is due to its high resistance to corrosion compared to other metals. Titanium is a very durable and lightweight metal, its density is only slightly higher than that of aluminum. With the same strength, titanium structures are 45% lighter than steel ones.

The degree of development.

Parts manufactured using AM technologies do not always meet the requirements for finished products in terms of protecting them from corrosion, high-temperature influences, the presence of electrical insulating properties, and adaptability to applied loads. In this regard, it is very relevant to give products and structures the above-listed properties formed by additive technologies due to modification of their surface, in particular plasma-electrolyte processing methods (PEO), which allow the full range of these characteristics to be realized.

Plasma electrolytic oxidation The plasma electrolytic oxidation (PEO) process is a new method used to improve the surface characteristics of various metal products. This method, based on conventional anodizing, is closely related to electrochemical mechanisms. PEO allows you to create universal ceramic coatings with various characteristics, such as resistance to corrosion and wear, electrical insulation properties, as well as thermal and aesthetic characteristics. [1]. One of the characteristics of poly (ethylene oxide) (PEO) is the participation of surface microarc discharges in the coating formation process. These discharges play a noticeable and distinctive role in the formation of the resulting coating, which leads to significant differences in the structure and composition of the oxide layers created. As a result, the characteristics of these layers are significantly improved compared to conventional anode films.[2]. The unique features of PEO include its environmentally friendly nature and the absence of the need for complex surface pretreatment and cooling mechanisms to produce thick coatings.

The analysis of the works showed that a fairly large number of works are devoted to the plasma-electrolyte treatment (PEO) of titanium alloys. It should be emphasized

that there is practically no research in the literature on the use of PEO parts made of titanium alloys formed by AT.

 Relevance of the work

in this way, conducting research and on their basis developing a technological process that improves the operational properties of products and structures formed by additive technologies from Titanium alloy (Ti-6-Al-4V) is usually used in various industries, due to surface modification, the plasma electrolyte method remains relevant.

 The purpose of the work

The development of a technological process aimed at increasing wear resistance and corrosion resistance, electrical insulation properties and thermal conductivity of products made of VT6 alloy (Ti-6-Al-4V) formed by additive technologies.

To achieve this goal, the following tasks were solved.

- to conduct a study of the current state in the field of production of products made of VT6 alloy (Ti-6-Al-4V) by methods of additive technologies and surface treatment of titanium alloys by plasma-electrolytic oxidation methods.
-to study the microhardness, surface roughness, wear resistance, and corrosion resistance of Ti-6-Al-4V alloy samples formed AT.
-to study the effect of modes (PEO) on microhardness, wear resistance, surface roughness, corrosion resistance, through porosity of Ti-6-Al-4V alloy samples formed AT.
-on the basis of the conducted research, to develop a technological process of PEO titanium alloy Ti-6-Al-4V.
 Scientific novelty of the work:
- the influence of PEO treatment modes on the increase in surface microhardness has been revealed;
- the influence of the state of the surface layer on the parameters of roughness, porosity and electrical insulation properties after PEO has been determined;
- optimal electrolyte concentrations and modes for PEO treatment of Ti-6-Al-4V alloy have been established.
The practical significance of the work lies in:
- improvement of the performance characteristics of products manufactured using additive technologies from VT6 alloy (Ti-6-Al-4V) and processed by PEO methods;

- creation of a technological process for the production of elements from Ti-6-Al-4V titanium alloy using a combined method of additive technologies and PEO.

 For protection , the following are presented:

- the results of research on the PEO process of processing titanium alloy Ti-6-Al-4V;
- the results of the study of the structure and composition of the modified layers;
- the results of the study of the heredity of the surface layer on the parameters of roughness, porosity after PEO;
- the developed method of manufacturing parts from Ti-6Al-4V titanium alloy using additive manufacturing and plasma-electrolytic oxidation.

 The degree of reliability and approbation of the results

The tasks set in the study were solved using analytical and experimental methods. The principles of physical and technical processing methods, fundamentals of materials science and modern engineering technologies were applied in the work. Experimental studies were carried out according to standard methods using certified instruments and instrumentation.

 Structure and scope of work

The dissertation includes an introduction, four chapters, general conclusions and a list of references.

The first chapter presents an analytical review of the current literature on the state of additive manufacturing.

The second chapter describes the materials used, equipment and methods of experiments.

The third chapter describes the experimental results and the best modes of PEO.

The fourth chapter presents the requirements for the surfaces to be treated, the developed technological process with an operational technological map and the project for the placement of technological equipment for the implementation of the technology.

The research is largely based on experimental data, which contributes to the accumulation of experience and knowledge for the development and implementation of PEO technology for parts manufactured using additive technologies.

CHAPTER 1 Analysis of additive methods and technologies for the production of titanium alloy products and the formation of protective and wear-resistant coatings on them.

1.1 Additive technologies for the formation of titanium alloy products and their advantage over traditional technologies.

Additive manufacturing (AM) is currently a rapidly developing industrial manufacturing industry.

As noted above, the idea behind the principle of manufacturing parts using AT methods is not to cut off excess from blanks or semi-finished products, but to build up the material in layers. This idea is especially attractive in aircraft, automotive, shipbuilding, as well as dentistry, traumatology and other industries where the cost of materials is quite high, and complex configurations of parts have high requirements for minimizing weight with maximum strength, and must also meet the conditions of individuality and bioinertness in the case of medical use.

Table 1.1 shows the industries that are most actively implementing additive technologies.[3]

Table 1.1 Industries benefiting from additive manufacturing

Industry	Applications	Benefits Gained
Aerospace	-Prototyping -Component manufacturing -Reducing aircraft weight -Engine components for the Airbus -Flight-certified hardware -Manufacturing of satellite components	-Produce very complex work pieces at low cost -Allow product lifecycle leverage -Objects manufactured in remote locations, as delivery of goods is no longer a restriction -A reduction in lead-time would imply a reduction in inventory and a reduction in costs On-demand manufacturing for astronauts -Eliminate excess parts that cause drag and add weight -Improve quality
Automotive	-Prototyping Component – manufacturing - Reducing vehicle weight -Cooling system for race car	-Help eliminate excess parts -Speed up time to market -Reduce the cost involved in product development -Reduce repair costs considerably

		-Reduce inventory -Could effectively change the way cars will look and function in the future -Improve quality
Machine Tool Production	-Prototyping -Reducing grip system weight -End-of-arm for smarter packaging	-Quick production of exact and customized replacement parts on site -Allow for designs that are more efficient and lighter
Healthcare and Medical	-Fabricating custom implants, such as hearing aids and prosthetics -Manufacturing human organs -Reconstructing bones, body parts -Hip joints and skull implants -Robotic hand	-Reduced surgery time and cost -Reduced the risk of postoperative complications -Reduced lead-time

A key feature of medicines produced using additive technologies is their ability to work with human organs and tissues due to compatibility. When creating implants and prostheses, it is important to take into account the unique anatomical features of each patient. For example, the production of implants with complex cellular composition, such as implants created using Winger-Seitz technology, contributes to the successful embedding of bone tissue into cells capable of withstanding significant mechanical loads. This development may lead to the opening of a new direction in the field of reconstructive traumatology and surgery. [4].

The first iteration of 3D printing technology appeared in the second half of the 1980s and was first proposed by 3D Systems. Until the mid-1990s, the advent of this technology meant the beginning of Stereolithography, also known as the SLA (stereolithography) process. Initially, these methodologies were called rapid prototyping technologies, but they were mainly used in research and development, in particular for prototyping in the defense industry.[5]

Key terms related to the field of additive technologies (AT) have been defined in ASTM F2792.1549323-1. The term "additive technologies" in this document can be understood as follows. as "a procedure for combining substances to create material

objects based on data from three-dimensional CAD models, usually in a sequential manner, unlike subtractive production methods."[5].

Modern industrial additive manufacturing (AM) technologies vary in performance, layering methods, materials used, and energy resources used during the operation. An illustrative classification of these technologies is shown in the diagram.

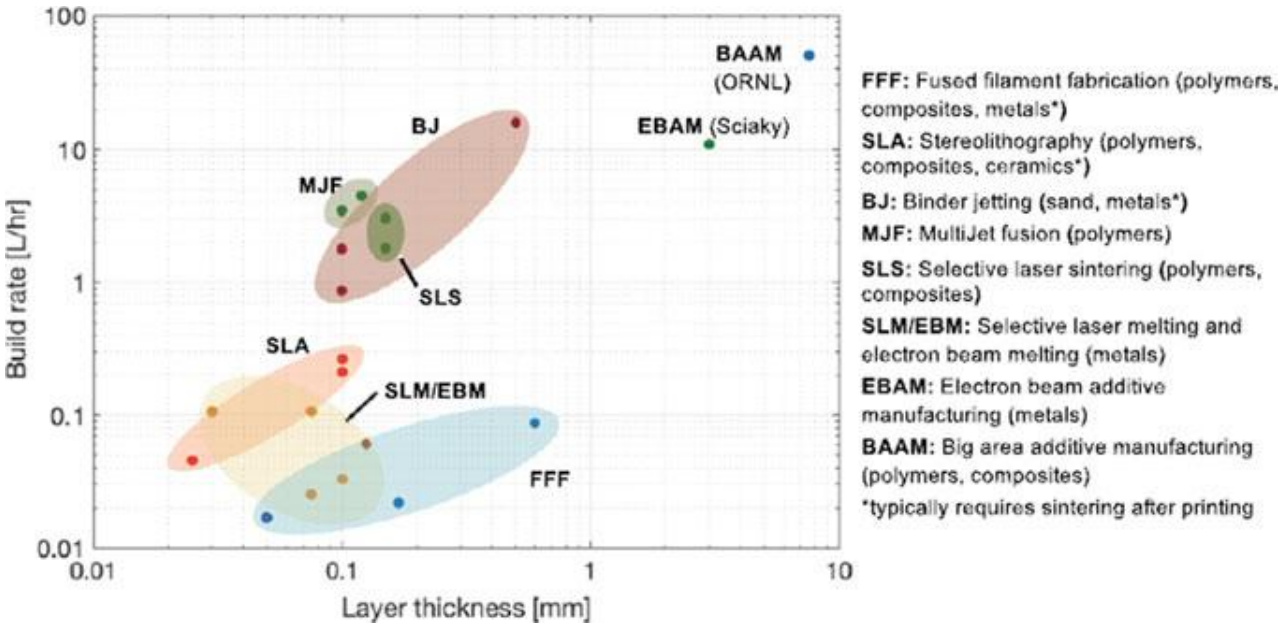

Figure 1.1 – Efficiency of various additive manufacturing technologies. [7].

Additive manufacturing offers many advantages over traditional manufacturing methods. A complete overview of its distinctive features is presented in the table. 1.2.

Table 1.2 Advantages over traditional manufacturing [3]

Areas of Application	Advantages
Rapid Prototyping	Reduce time to market by accelerating prototyping Reduce the cost involved in product development Making companies more efficient and competitive at innovation
Production of Spare Parts	Reduce repair times Reduce labor cost Avoid costly warehousing
Small Volume Manufacturing	Small batches can be produced cost-efficiently Eliminate the investment in tooling
Customized Unique Items	Enable mass customization at low cost Quick production of exact and customized replacement parts on site Eliminate penalty for redesign
Very Complex Work Pieces	Produce very complex work pieces at low cost

Machine Tool Manufacturing	Reduce labor cost Avoid costly warehousing Enables mass customization at low cost
Rapid Manufacturing	Directly manufacturing finished components Relatively inexpensive production of small numbers of parts
Component Manufacturing	Enable mass customization at low cost Improve quality Shorten supply chain Reduce the cost involved in development Help eliminate excess parts
On Site and On-Demand Manufacturing of Customized Replacement Parts	Eliminate storage and transportation costs Save money by preventing downtimes Reduces repair costs considerably Shorten supply chain The need for large inventory is reduced Allow product lifecycle leverage
Rapid Repair	Significant reduction in repair time Opportunity to modify repaired components to the latest design

The diagram shows the various stages of manufacturing products using additive technologies. 1.2.

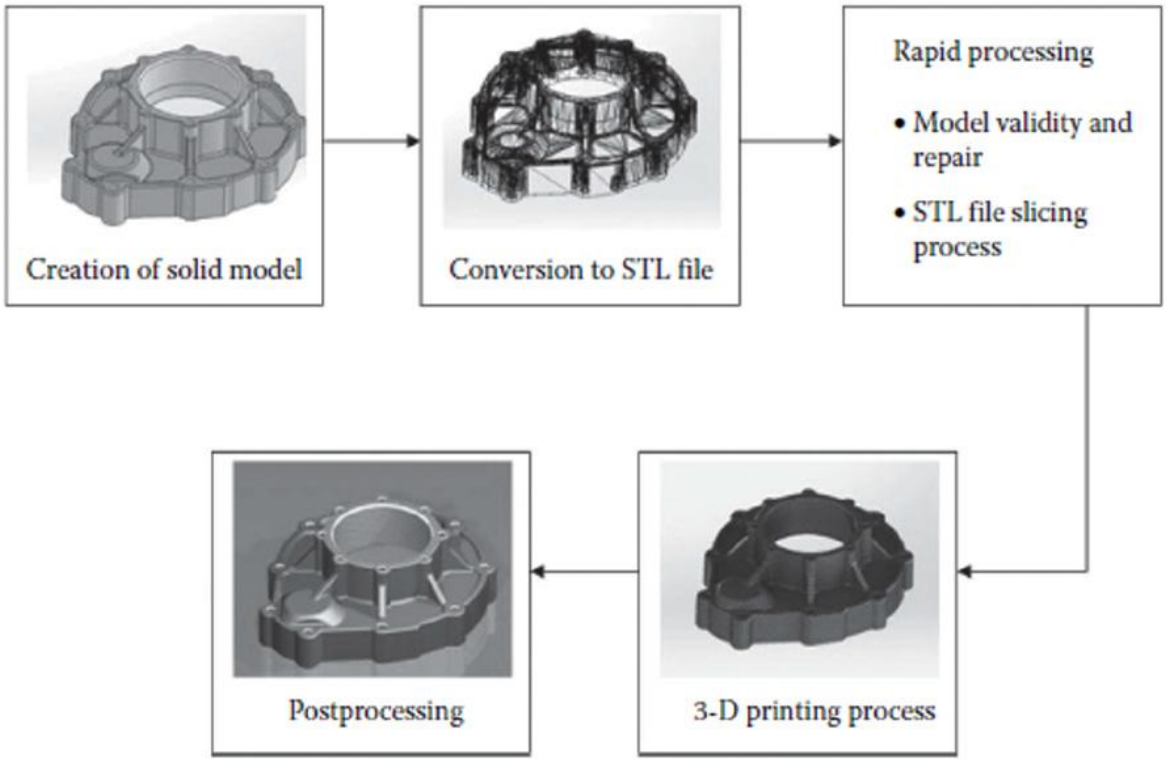

Figure 1.2 shows the successive stages of manufacturing products using additive technologies. [7].

1.2. Features of powder materials used in additive technologies (AT) and the main standards that can be applied to them.

In the industrial sector, the use of additive technologies involves primarily the use of metal powders as the main materials for the production of components. These powders are characterized as bulk materials with a particle size of no more than 1 mm. The classification of these powders depends on their nominal diameter d.

- nanoparticles (d < 0.001 microns);

- ultra–thin (d = 0.01 - 0.1 microns);

- finely dispersed (d = 0.1 – 10 microns);

- small (d = 10 – 40 microns);

- medium (d = 40 – 250 microns);

- large (d = 250 – 1000 microns).

Recently, common criteria have been established for mixtures of metals and powders used in additive technologies. Some manufacturers of additive plants require the use of a specific set of materials supplied by them. The use of powders containing different fractional compositions is obvious in different installations, this minimizes the likelihood of obtaining products with different quality characteristics that may arise when using powders from different manufacturers. However, devices do exist to enable the use of metal powders produced by alternative manufacturers.

Arcam installations using electron beam melting (EBM) technology demonstrate particle size distribution from 45 to 100 microns. Conversely, the standard particle size distribution observed in the selective laser melting (SLM) process ranges from 10 to 45 microns.

The most important and fundamental requirement for powders used in additive technologies (AT) is the requirement to have a spherical shape. This is due to the fact that spherical powders can occupy a certain volume more efficiently and provide a smooth flow with minimal obstacles. Metal powders used in sintering or melting processes are widely used in coatings, fire or plasma spraying.

However, the standards governing the selection of metal powders for additive manufacturing processes are much stricter. These standards include elements such as particle size, shape, and chemical composition. All these elements play a crucial role in ensuring the efficiency and reliability of the process, Powders obtained using

traditional methods such as water spraying may have an incorrect morphology, which makes them unsuitable for use in additive manufacturing, and also allows the powder to be processed in future cycles.

In the field of additive manufacturing, it is important that powders have a predominantly spherical morphology, which makes it possible to create compact and homogeneous layers, as well as ensure uniform fluidity of the material. To eliminate specific disadvantages, it is necessary to limit the moisture content of powders to a maximum of 3%.

At the national level, regulations governing the use of substances in additive technologies have recently been put into effect and protocols for the supervision and evaluation of primary materials have been approved. A structure similar to the internationally recognized ISO 5832-3-2014 standard has been created for the Ti-6Al-4V alloy. This structure describes the properties and suitable evaluation methods of a ductile titanium alloy.

1.3 Various technologies for creating powder materials for additive manufacturing (AM) are considered.

The provision of powder materials is a serious problem that affects both the development of additive technologies and the field of traditional powder metallurgy in general. A common method for the production of metal powders involves the reduction of metal oxides followed by spraying of the resulting melt. Methods such as autoclave and carbonyl treatment, electrolysis of aqueous and saline solutions, diffuse saturation and mechanical grinding are often used.[9]

The diagram, designated as Diagram 1.3, shows the final result of the powder production process.

The main attention in the production of titanium alloy powders for additive technologies is paid to the use of special methods that facilitate the conversion of the starting material into powder with minimal change in its chemical composition. Among the various available methodologies, the melt spraying process is characterized by impressive efficiency, efficiency and the ability to meet the specified requirements of powder mixtures. Most of the powders used in additive manufacturing, the amount of which exceeds 80%, are purchased using these methods. The main methods of production of such powders include gas and centrifugal spraying with subsequent improvement of these methods.[5]

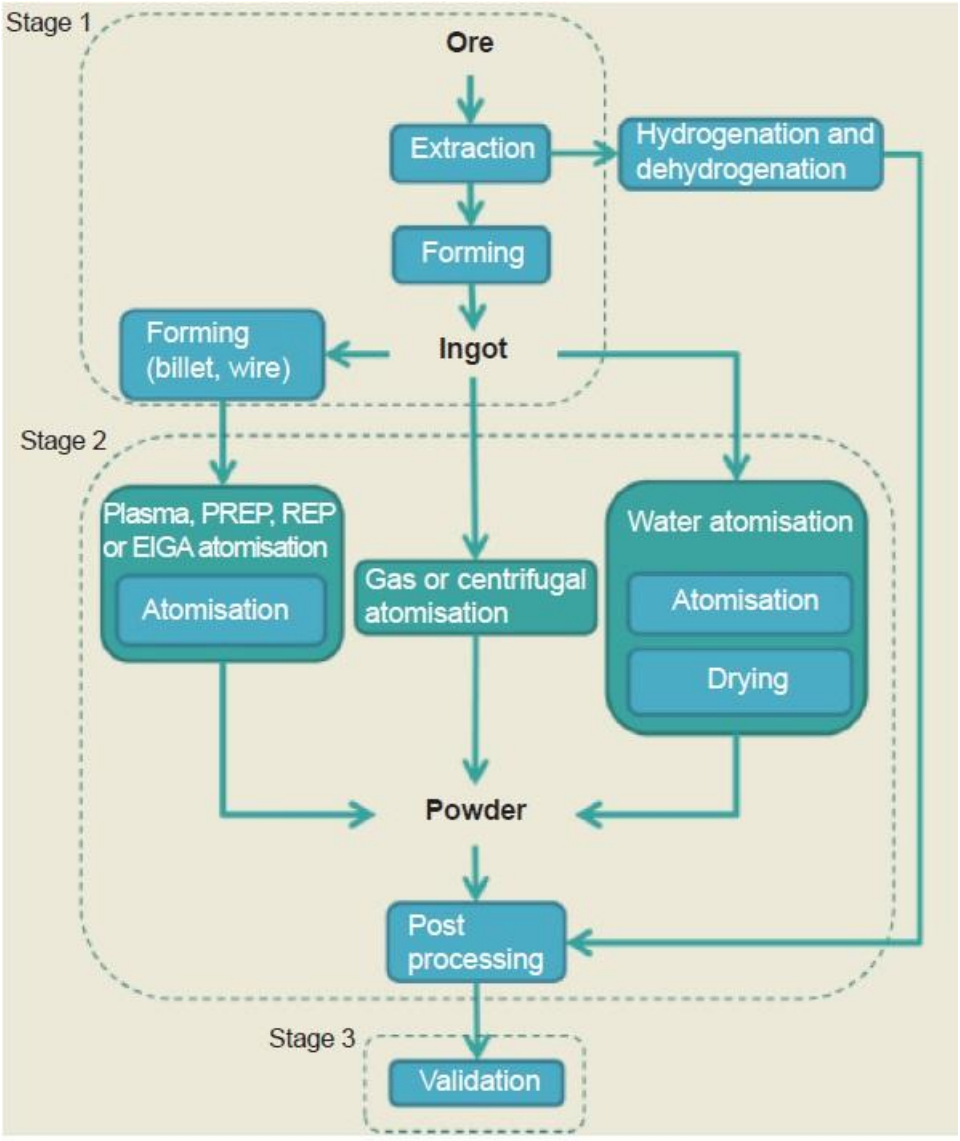

The production procedure for powders obtained from ore substances is shown in the figure.1.3. [10]

1.3.1 The gas spraying process involves the deposition of material using a high-speed gas flow.

One form of gas spraying is revealed using EIGA technology (Electrode Induction Guide), which involves the use of electromagnetic induction in combination with inert gas spraying to produce chemically active metal powders such as Ti, Zr, Hf, V, Pt, Ir, Nb and Mo.

The procedure described in this method (see diagram in Figure 1.4) involves the gradual immersion of a rotating electrode into an annular inductor to inductively

melt the resulting ingots with a diameter of 50 mm and a length of 500 mm. The inert gas is then used to disperse the molten metal droplets through a network of nozzles.

This approach provides a low melt dispersion rate (about 0.5 kg/s), but it allows the dispersion of several tens of kilograms per cycle.[5] This powder production methodology leads to a noticeable increase in efficiency compared to separation devices. In addition, the elimination of consumable ceramic and graphite elements plays a crucial role in reducing the cost of powder production.

The use of an inert gas per 1 kilogram of powder produced is similar to the operation of large sprayers in ceramic vessels. On this particular machine, the workflow demonstrates a higher level of stability compared to crucible sprayers, primarily due to the lack of an initial metal charge. It is known that this initial charge often leads to the ingress of impurities into the powder, such as chips and oxidized particles. Here, the metal is evenly distributed throughout the dispersion process, and the flow of argon through the nozzle is established before the electrode begins to melt.

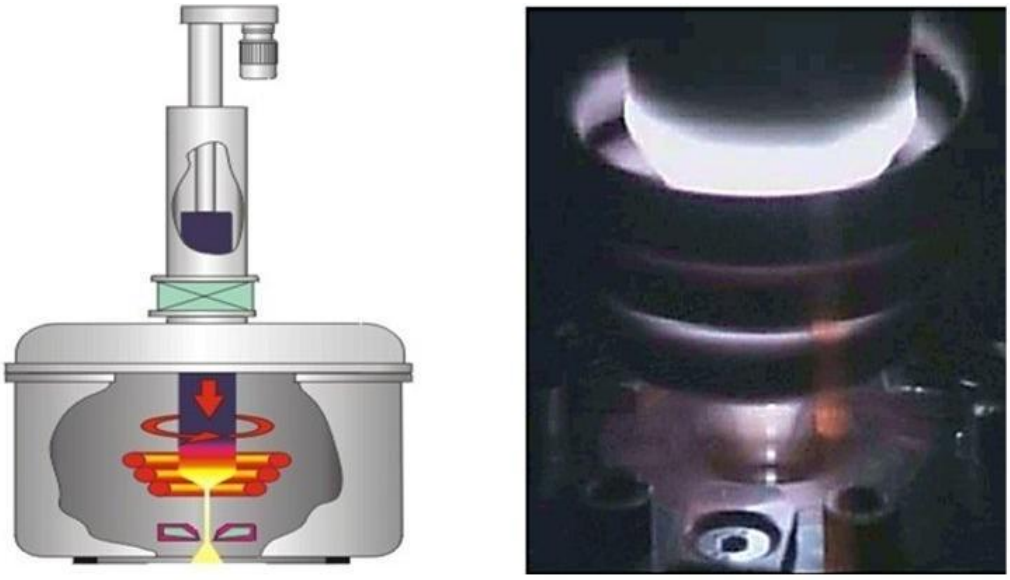

Figure 1.4. – The scheme of the sprayer without crucibles EIGA 50/500 is proposed by ALD Vacuum Technologies GmbH.

1.3.2 The process of centrifugal spraying.

During the production process of creating powders using titanium alloys. Various technological methods are used, with special attention being paid to the REP and PREP processes.

The REP (Rotating Electrode Process) technology, also known as the electrode rotation process, involves the dispersion of a melt formed as a result of an electric arc between a tungsten electrode and a cylindrical titanium alloy ingot.[5].

The resistance projection (REP) process uses a pair of electrodes, one of which is made of tungsten and the other of a certain alloy. The tungsten electrode remains stationary while the spare electrode rotates rapidly. When an electric arc occurs between the electrodes, the material of the initial electrode is subjected to melting. Then, under the action of centrifugal force, the molten metal is dispersed to the periphery, At the point of convergence, the substance turns into tiny droplets, which then take a spherical shape during movement. [13].

A modification of the previous procedure is the Plasma Rotating Electrode (PREP) technology (Plasma Rotating Electrode Process), as shown in Figure 1.5 for the installation option. The ingot is melted by a high-speed flow of inert gas.[5]

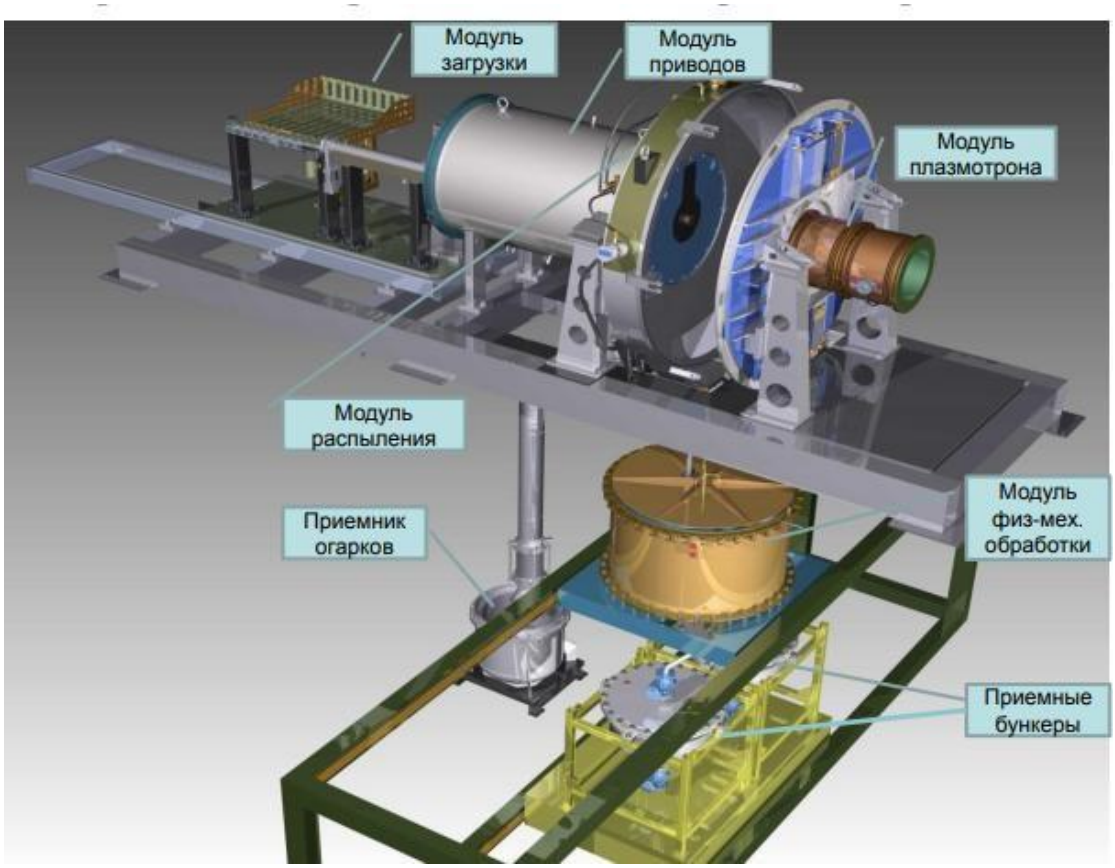

Figure 1.5. – A universal modular generator set is used in the process of powder production by centrifugal spraying. [Source: JSC "WHEELS"]

1. **Модуль загрузки → Loading Module**
   Purpose: Feeds raw material (such as metal bars or granules) into the system.
2. **Модуль приводов → Drive Module**
   Purpose: Powers the rotating components, enabling centrifugal force for material spraying.
3. **Модуль плазмотрона → Plasma Torch Module**
   Purpose: Heats and melts the raw material using plasma energy to create molten metal.
4. **Модуль распыления → Spraying Module**
   Purpose: Uses centrifugal force to atomize molten metal into fine droplets.
5. **Приемник огарков → Scrap Receiver**
   Purpose: Collects excess material or unusable remnants from the spraying process.
6. **Модуль физ.-мех. обработки → Physical-Mechanical Processing Module**
   Purpose: Processes and refines the powder, ensuring uniformity in particle size and shape.
7. **Приемные бункеры → Collection Bins**
   Purpose: Gathers the finished powder product for storage or further processing.

A visual representation illustrating the procedure for using the PREP method can be seen in Figure 1.6. Using this approach involves applying a layer to a molded workpiece 1. Diameter d The object rotates around its axis at a certain angular velocity. Located on the periphery of the workpiece 2. The heat flow is transmitted using a plasma burner 3. Usually, when installing a plasma burner, the deviation h and the specific power. 4 As a result of melting the edge of the workpiece, a surface layer is formed that has undergone a melting process. 5The movement of the melt to the periphery of the limb is caused by centrifugal forces, as a result of which the melt accumulates and forms a kind of "crown". As a result, the melt droplets separate from the surface, which leads to their transformation into granules during crystallization during movement. This phenomenon occurs in an environment rich in inert gases such as argon or helium. [11].

In the process, an inactive gas can be introduced into the container to inhibit oxidation and the introduction of impurities into the material, it is possible to create a vacuum that ensures surface cleanliness and prevents

oxygen exposure. Nitrogen and carbon monoxide are often used for this purpose. The average particle size is. from 40 to 200 micrometers, depending on the parameters of the spraying method. [12].

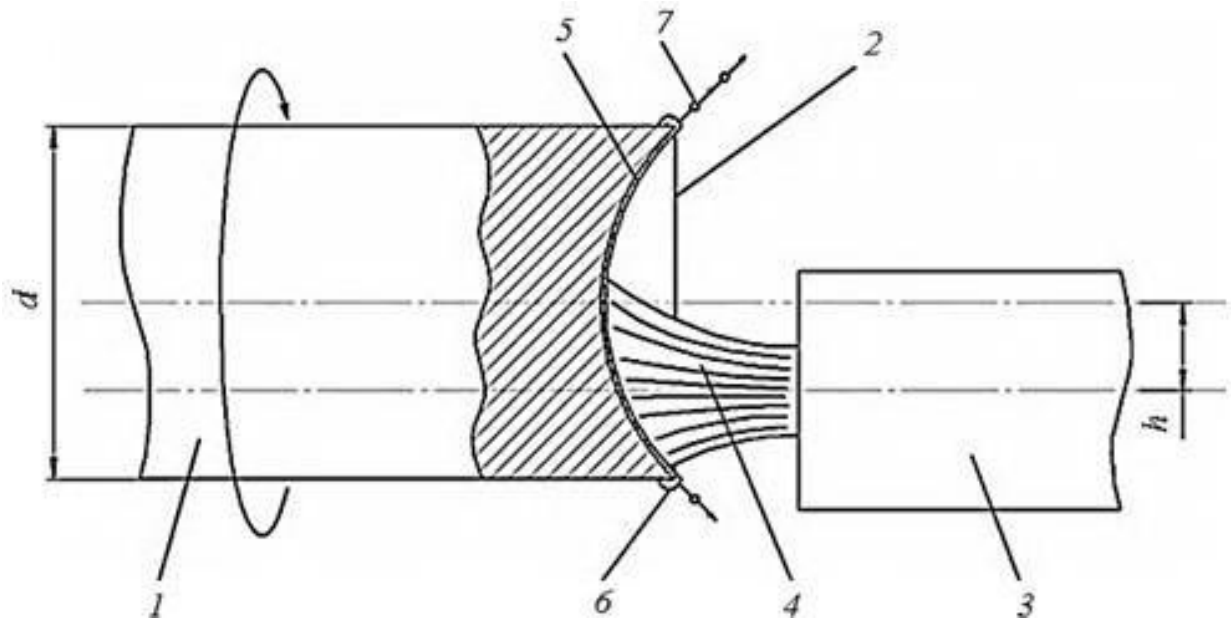

Figure 1.6 shows an image of the PREP process [11].

1 represents the source material with the diameter parameter (d); 2 indicates the end of the source material; 3 means the plasma source with the displacement parameter (h); 4 indicates the thermal flow of the plasma; 5 shows the molten coating; 6 illustrates the creation of an annular structure from the molten material; 7 represents the melt droplets.

The lower limit of the particle size in the powder is 70 microns, the average granule size is about 50 microns, while about 10% of the granules are less than 40 microns in size. Currently, this is the most profitable result of using modern plasma welding systems and centrifugal processing of high-speed cast blanks. [14].

In order to improve the use of powders obtained in the powder metallurgy (PREP) process for additive manufacturing, it is necessary to reduce their size to below 40 microns. The main methods used to reduce the particle size of powders within the framework of the RUP methodology include.[14]:

- An increase in the rotation speed of the formed component leads to a subsequent increase in the velocity of medium-sized particles.

- Increasing the plasma energy level.

- This indirectly affects the particle size, leads to a slight decrease, and also has a significant impact on the technological characteristics and increases the efficiency of the system;

- Minimizing variations in plant operation is crucial to ensure stable performance.

- These fluctuations can negatively affect the granulometric composition of the final powder product, lead to a violation of the uniformity of its composition and, ultimately, this led to a reduction in the production of high-quality materials.

- An increase in the size of the cast workpiece leads to a constant increase in angular velocity, which leads to a decrease in the size of the resulting granules (although an excessive increase in size can lead to increased fluctuations).

Figure 1.7 shows a visual representation showing the distinctive features of Ti-6Al-4V alloy powders obtained using the described methodologies.

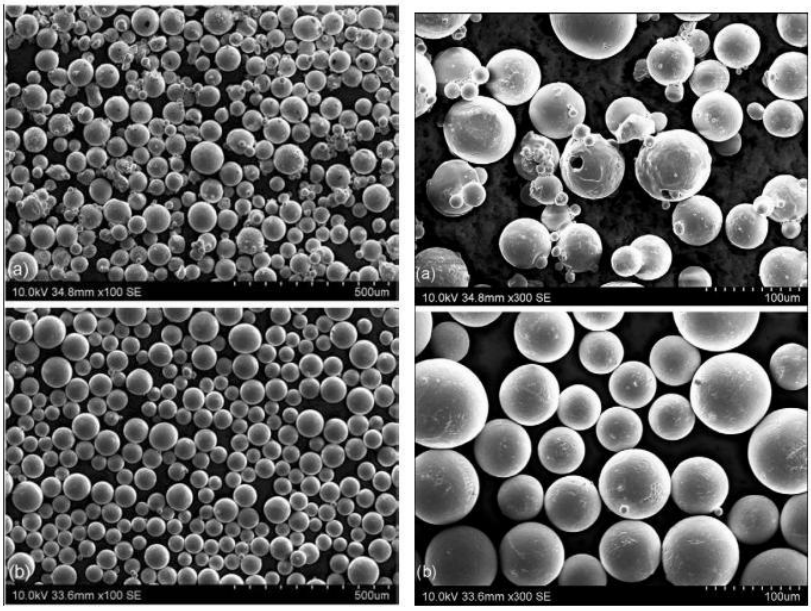

Figure 1.7 shows a visual image of the Ti-6Al-4V powder alloy obtained by two different methods: a) electron beam melting (EBM) and b) powder layer fusion (PBF) [5].

Powders obtained by centrifugal plasma spraying have a more spherical shape with fewer small particles. In addition, powders obtained using PREP technology contribute to electron beam sintering.

1.4 Characteristics of additive manufacturing processes.

1.4.1 Additive manufacturing process, known as selective laser sintering technology.

The advanced technology of selective laser sintering (DMLS) was first used in 1995 by Wilhelm Meiners and Kurt Wissenbach at the famous Institute of Laser Technology founded by A. Fraunhofer. After that, Dieter Schwartz and Matthias Fakele from F&S Stereolithographietechnik GmbH played a crucial role in the project, as a result of which the method was patented.[5].

Selective laser melting (SLM) technology was created to meet the need to create robust integrated structures of complex geometry with mechanical characteristics comparable to cast or forged parts, which leads to a reduction in production time [5]. A schematic representation of the workflow of the selective laser melting method can be seen in Figure 1.8.

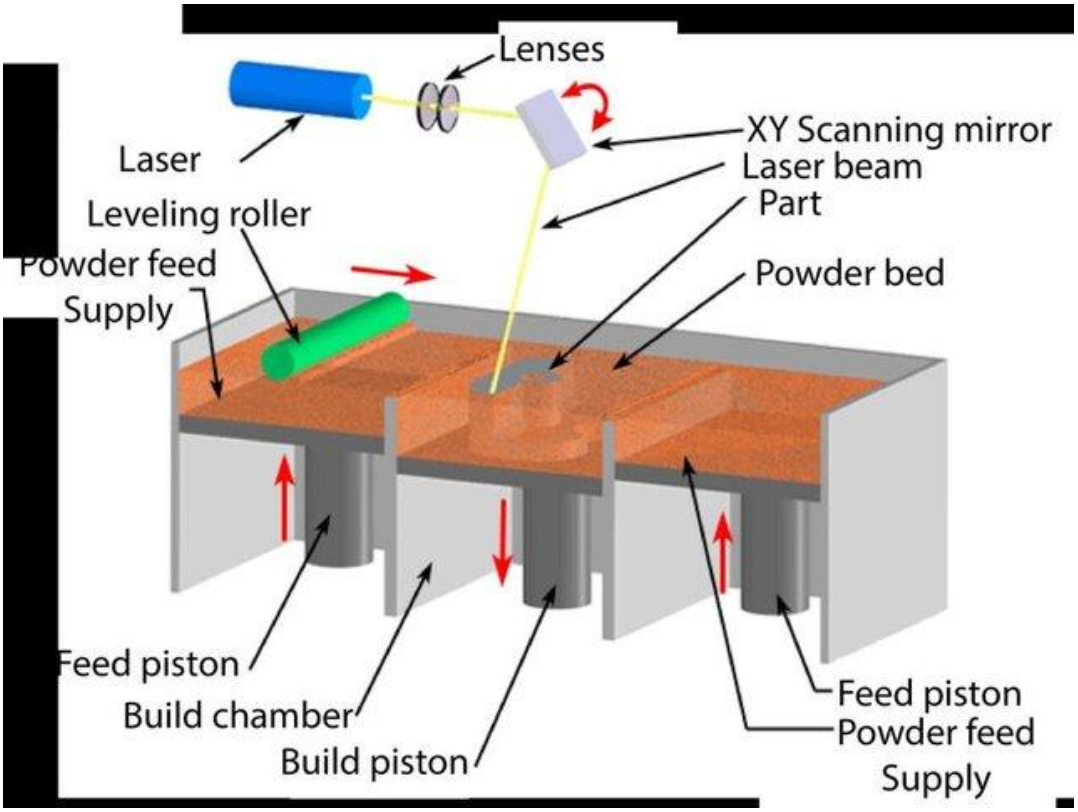

Figure 1.8 illustrates the selective laser melting (SLM) process. [5]

Depending on the configuration of the installation, a squeegee or roller is used to evenly distribute the powder layer to the required thickness on a preheated steel platform. The laser beam then acts on certain areas of the powder layer surface based on the current layer structure described in the CAD model and the assigned laser irradiation plan. After this stage, the platform is adjusted according to the thickness of the powder layer, a new layer of powder is applied, and then smoothed. [15].

Various types of lasers are widely used in the field of additive technologies, with fiber lasers known as YAG (yttrium-aluminum garnet) lasers in which neodymium activation becomes the main option due to their increased reliability, compact design and relatively economical maintenance costs. The laser beam is concentrated on the surface of the material with sufficient energy to achieve the required degree of melting of the particles. Adapting the laser power to a specific material is of paramount importance, since it requires taking into account the absorption and reflection coefficients of radiation. In addition, the characteristics and wavelength of the radiation are crucial factors in determining the degree of energy absorption. [16].

The laser system scans the surface along established trajectories, known as tracks. The operating power of the laser is about 90% of the rated power due to the loss of energy in the optical system. To avoid the formation of oxide and nitride compounds in the metal frame, the process is carried out in a carefully controlled atmosphere of inert gas. [17].

The thermal energy of the laser beam causes the granules of the powdered material to transform, as a result of which they become liquid. As a result, the laser beam passes through the surface of the layer, as a result of which the previously applied powder melts on the substrate. The individual trajectories of the laser beam form separate trajectories called tracks, which are schematically shown in Figure 1.9.

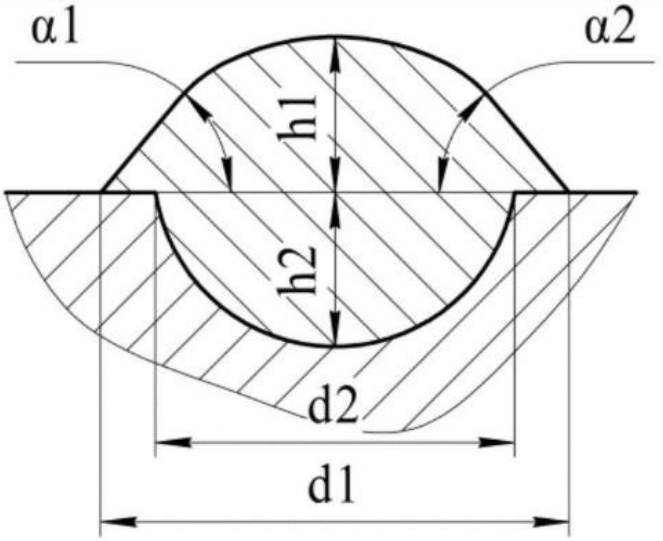

Figure 1.9 shows the geometric attributes of a certain trajectory in a segment of the liquid layer. The parameter h1 represents the vertical distance of the trajectory from the base, and h2 means the melting depth in the underlying layer. In addition, d1 indicates the width of an individual path, and d2 corresponds to the width of the molten area. In addition, α1 and α2 determine the angles at which the molten substance penetrates the surface in the area exposed to laser irradiation.

There are various strategies for controlling laser radiation during layer fusion (Fig. 1.10). These approaches can be divided into two main groups: entry-level strategies and mid-level strategies. The next section discusses basic entry-level strategies that serve as the basis for mid-level strategies. In the field of entry-level strategies, four main methods have been recognized as the basis for the production of products by selective laser melting.

The basic tactics can be divided into two well-defined sets. The initial set consists of single-pass techniques, while the next group includes methods of double passage of a laser beam through a layer of material, which contributes to the achievement of increased sample density (porosity less than 1%).

• In the initial approach, the scanning process occurs periodically at a predetermined interval, designated as h, so that each individual track is located in close proximity to each other at a distance equal to or greater than the diameter of the laser focal point on the surface of the substrate or fused layer d1.

• The second strategy refers to a situation where the distance h is less than d1. Such methods are rarely used, since the increased porosity of the samples leads to a

decrease in their mechanical characteristics. These methods, known for their high efficiency, can significantly reduce the production time of the product; however, the quality of the microstructure of the sample often deteriorates. These approaches often serve as the basis for the creation of advanced technologies at the secondary school level. [18].

• The method, which in modern literature is called the "double zone" method, consists of a two-phase process of processing each layer of powder material with a laser beam. Initially, the layer is processed at a certain interval that coincides with the width of the track of the molten material. The laser beam then passes between the already processed tracks, effectively combining two adjacent tracks.

• The fourth methodology, known in English literature as the "cross-scanning" methodology, The premise of this method is that each layer is examined perpendicular to the scanning trajectory of the previous layer. One of the key advantages of this methodology is its ability to prevent the occurrence of a repetitive wave configuration. This phenomenon becomes more and more noticeable as each newly obtained layer is added.

The choice of the laser treatment method in the process of selective laser melting plays a crucial role in influencing the mechanical properties and porosity of the samples. In addition, it also affects the production time of individual layers and the final product as a whole.. [19].

To reduce porosity, it is necessary to fine-tune the Technological parameters that need to be taken into account include the power and speed of scanning the laser beam, the thickness of the layer of molten powder material and the determination of the optimal scanning step between adjacent tracks.

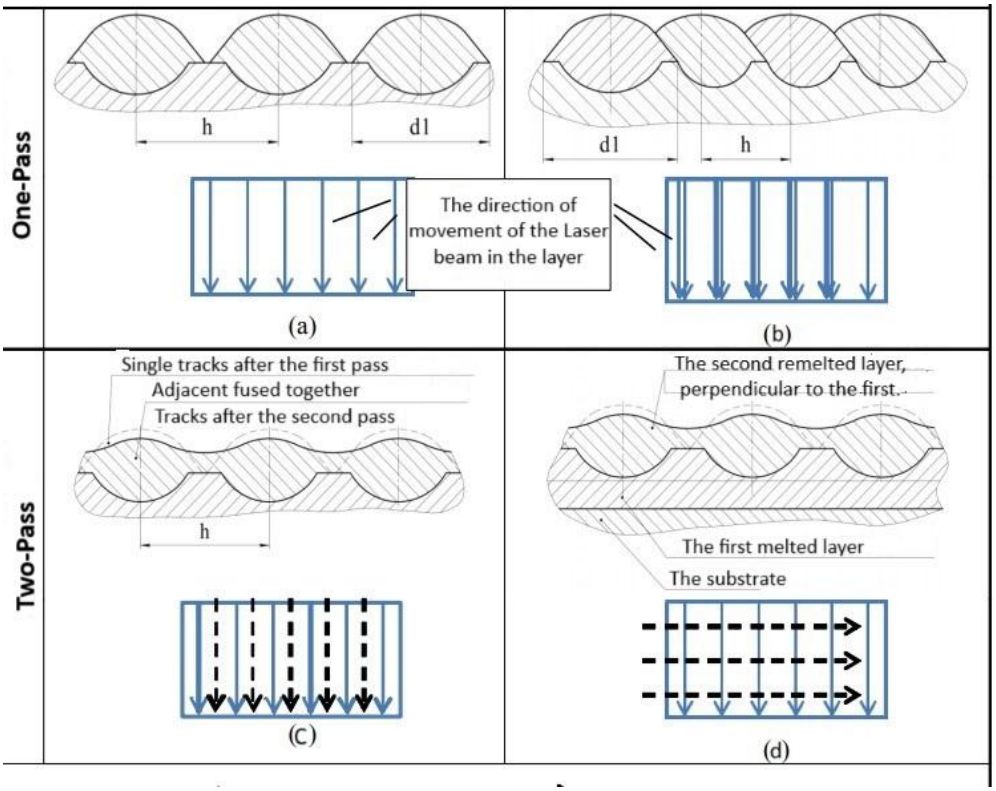

Figure 1.10 shows various approaches to laser processing [18].

The blue lines in the diagram indicate the primary direction of the laser beam, and the black lines indicate the secondary direction. Strategy (a) uses a simple one-pass scanning method with scan intervals between tracks where the parameter h exceeds d1. Conversely, strategy (b) is an improved single-pass method with a reduced scan interval, where h is less than d1. Strategy (c) implements a two-pass procedure called "double zones", whereas strategy (d) uses a two-pass procedure called "cross-shading". In these methodologies, h stands for the magnitude of the scanning step, and d1 stands for the diameter of the laser beam in the molten layer.

The quality of the obtained layers is greatly influenced by various factors, while the main attention is paid to the characteristics of the raw materials and the parameters of the melting process. The main characteristics of materials in the initial stages include their granular structure, chemical composition, density, flowability and a special surface area of the powdery form. [19, 20].

The parameters used in the sintering process include variables such as laser power, speed of movement, radiation intensity, pulse frequency, type of gas medium and duration of exposure. The properties of the resulting layers are influenced by factors

such as extreme dimensional accuracy, uniform density and a range of layer thickness. [19].

A shortage may occur during the product formation process. The main task of the melting stage is to disperse the initial powder and remove empty spaces and partially molten particles.

The properties of an effective heat emitter created by the interaction of a laser with a powder layer differ markedly from the properties of thermal radiation emitted by a solid metal object. The interaction of radiation with the opaque metal surface of an object affects the distribution of energy due to the relationship between the ability of the material to absorb radiation and its thermal conductivity. The ability of the powder layer to absorb liquid is influenced by both the physico-chemical characteristics of the powder and its bulk density, which often exceeds the density of the solid.

In the process of laser melting, part of the electromagnetic radiation is purposefully absorbed by particles located on the surface of an insufficiently compacted powder layer. In addition, the radiation penetrates through the empty spaces between the particles and interacts with the particles underneath them. Standard heat transfer mechanisms regulate the thermal dispersion in the powder layer. The level of laser radiation decreases as it penetrates deeper into the powder layer [21].

Each metal has different properties related to radiation absorption, surface energy, and fluidity in the molten state. Therefore, in order to improve the melting procedure, it is necessary to have a deep understanding of the physico-chemical characteristics of individual metals in order to minimize the risk of instability. [18].

The effect on the occurrence of defects is shown in Figure 1.11. This includes the stages of defect development, insufficient refining and flocene formation. The presence of pores is associated with changes in the intensity of the laser, the speed of the beam along the surface of the material, the size of the focal area and additional variables.

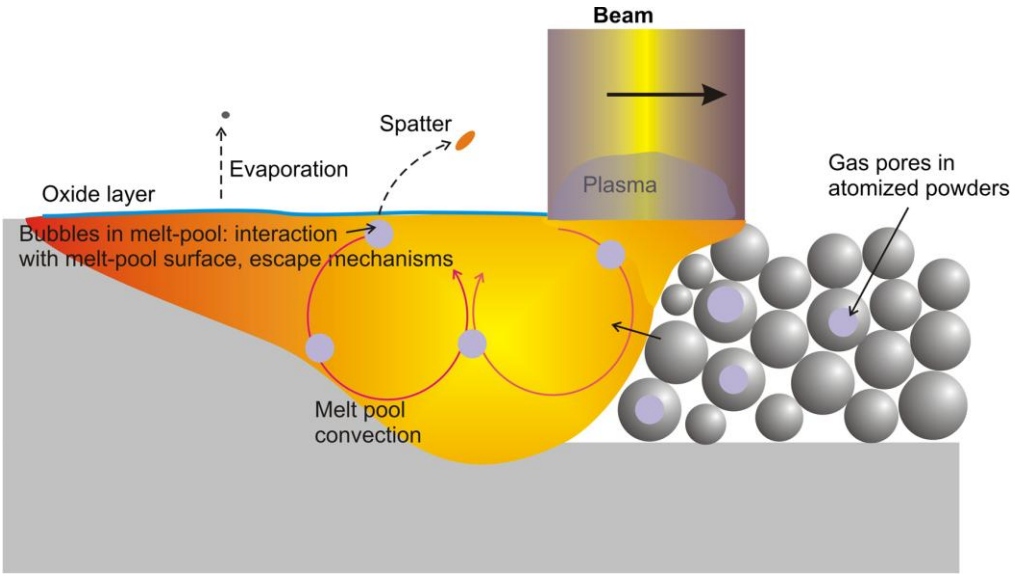

Fig.1.11. Schematic illustration of melt pool phenomena during powder bed melting.

The increase in scanning speed is inherently associated with a reduction in production time; however, it is important to recognize that such an increase is possible only by increasing the intensity of radiation and reducing the time interval between successive scans. Otherwise, achieving the required minimum porosity level of the final product may be a difficult task. A slight decrease in laser power, for example, by 10 watts, can lead to a significant increase in pore volume [17].

Porosity estimation can be achieved through processes involving consolidation and fusion of powdered substances, such as amalgamation of liquefied particles. This leads to a decrease in volume and an increase in density. The effect of thermocapillary forces becomes apparent during the melting of the powder particles. The presence of pores and air cavities negatively affects the mechanical characteristics of the products obtained, the presence of stress concentration at the sample boundary, especially in wedge-shaped samples, can lead to a noticeable decrease in strength in the presence of a separate defect, which can lead to the formation of a crack.

The abundance of pores in the material plays a crucial role in reducing its strength and affecting its elastic properties, viscoplastic properties and other properties. As a result, this prevents the practical use of products manufactured by selective laser welding. [18].

There are cases of porosity in Figures 1.12 and 1.13. The formation of floccins is inextricably linked to the moisture content in the presented powder material. When interacting with a laser beam, water molecules undergo a splitting process, which leads to the absorption of released hydrogen in a liquid medium. Due to the high crystallization rate of the molten material, the process of removing gases is difficult [22]. The research conducted by scientists [23] made it possible to determine the optimal operating parameters of the laser melting apparatus, as a result of which the porosity level is 0.5%. These settings require the use of a 200 W carbon dioxide laser in combination with a duration of exposure of 150 microseconds per coordinate while maintaining a constant layer thickness and line length of 50 microns (see Figure 1.14).

Figure 1.12 shows several areas in which the powder sintering process has not yet been fully completed, as noted in the previous study [16].

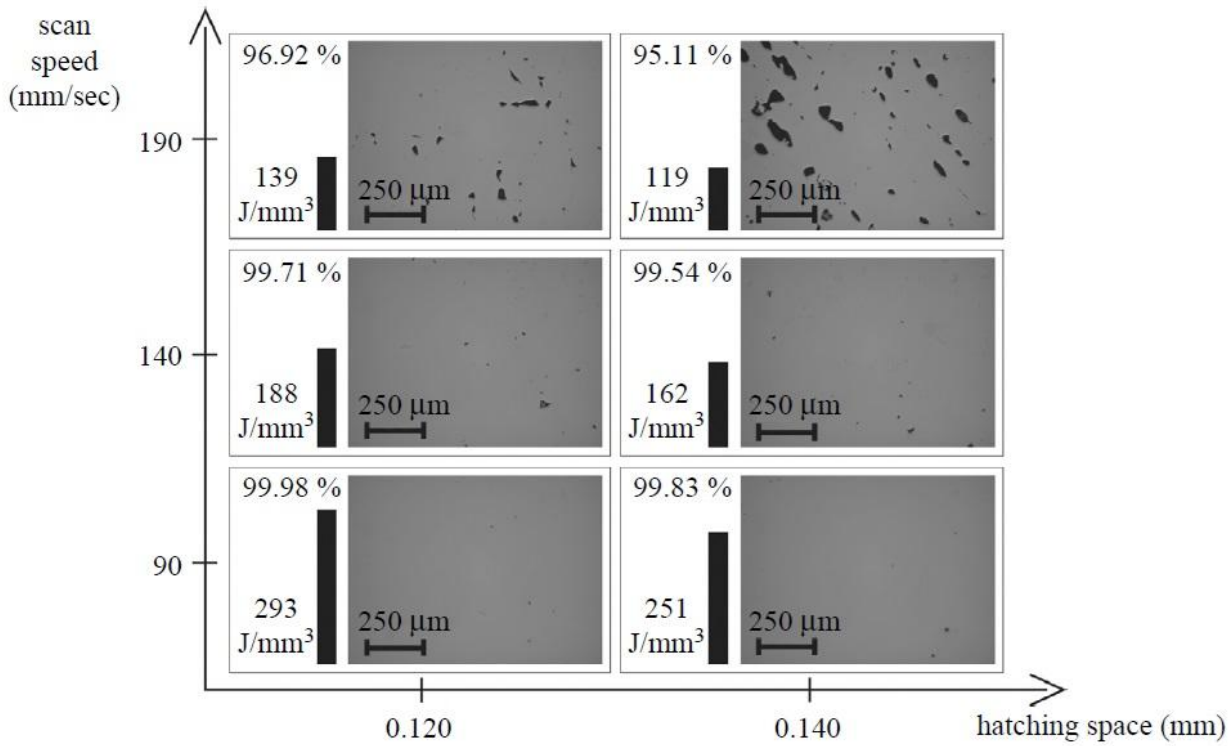

Figure 1.12 shows micrographs of alloy samples with the highest density depending on the scanning speed and impact intensity, with special emphasis on the effect of using an ytterbium laser [24]

Increasing the intensity of the laser beam while maintaining other operational factors (for example, scanning speed and layer depth) can lead to the formation of a wave-like structure on the surface. [17]. The main strategy for reducing the impact of these effects is to use specialized processing methods such as "The two zone method" and "cross-shading". [26].

The main strategy for reducing these impacts is to use the processes of stroke formation and spheroidization — the main processes of additive manufacturing. It is recommended to use a high level of laser power, as this increases flexibility in adjusting the scanning speed and thickness of the powder layer. The increased energy level, especially in conditions of high laser power and low scanning speed, can lead to an increase in the volume of the molten bath during selective laser melting (SLM) operations and, consequently, to instability of the printed tracks. [27].

An analysis of the process of creating a single track from metal powders by selective laser melting (SLM) showed that the method has a noticeable threshold characteristic: a stable region characterized by consistent and uniform melting of the material by a laser, and an unstable region in which there are interruptions in the formation of the track. Instability occurs when the scanning speed is insufficient, resulting in distortions and defects, or when the speed is too high, resulting in spheroidization. The range of ideal scanning speeds can be expanded by increasing the laser power and using materials with high thermal conductivity. The incorporation of thermal energy into the base material leads to increased durability and the creation of continuous separate paths. Examples of these disadvantages are shown in Figure 1.14.

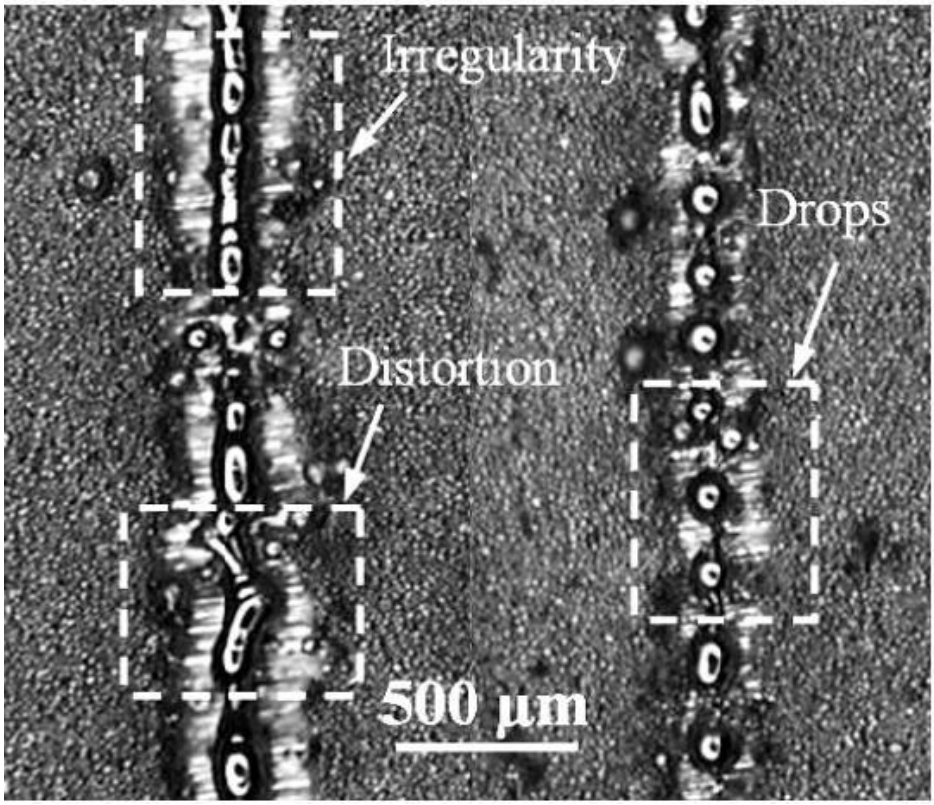

Figure 1.14 shows the cases of spheroidization and strokes marked on the surface of the powder layer, as indicated in the source [27].

Advantages of selective laser melting (SLM) technology [17, 28]:

• An important advantage lies in the simplicity of the laser device design;

• Several products of different shapes can be made in one production cycle.

• Hardware software provides ready-made models designed to improve the arrangement of elements in the work environment using virtual assemblies displayed on a monitor screen using fully automated procedures.

• Laser devices are characterized by exceptional accuracy, which ensures a high standard of product surface quality.

• The device is equipped with additional components, including nitrogen generators, dust collectors and powder separators.

• This makes it possible to produce products of complex shapes (with a significant surface area, but limited volume, complex structures, internal cooling channels and finished components) that cannot be manufactured using traditional methods.

• There is a significant level of powder usage, as well as the possibility of its subsequent use.

Complex internal channels can be created provided they are subsequently cleaned of powder residues at the next processing stages.

The disadvantages of the SLM process are particularly high.

• A comprehensive understanding of the physical and chemical principles of additive manufacturing, as well as 3D model development procedures, is necessary to maximize technological capabilities.

• There is an urgent need for complete standardization of additive manufacturing procedures, as differences in identical procedures currently serve as competitive advantages for manufacturers of additive equipment;

• Disadvantages may arise due to insufficient optimization of the melting process and poor quality of powder materials, which leads to deformations, cracks, persisting porosity and spheroidization in the molten areas.

• Strict standards are applied to the quality of the powder, since changes in its properties can affect the appearance of defects and the overall surface quality of the final product. The cost of powder materials is especially high — from 10,000 rubles per kilogram.

• This process is characterized by a relatively low level of efficiency, since no material costs are required when mixing old and new powder, so the only acceptable option is to use sorted powder.

• The accuracy of the design is influenced by the size of the laser spot, the size of the powder particles and the location of the component in the workspace.

• Although high processing speeds and a larger laser spot diameter can increase productivity, they can also lead to lower product quality. This leads to the production of end products with anisotropic properties, which limits their use in critical scenarios.

• In addition, these products have internal stresses that require heat treatment or hot isostatic pressing.

• Finished products require additional processing, including mechanical surface treatment and chemical etching.

1.4.2.Electron beam melting EBM.

Electron beam melting (EBM) technology, originally created in the early 2000s by the Swedish firm Arcam AB, This method uses a high energy density electron beam, similar to laser methods, instead of photons. The procedure involves the focused release of electrons. IBM equipment has the ability to generate a focused electron beam that causes melting in certain areas of the metal. The scheme of electron beam production in the system is shown in Figure 1.15 [29].

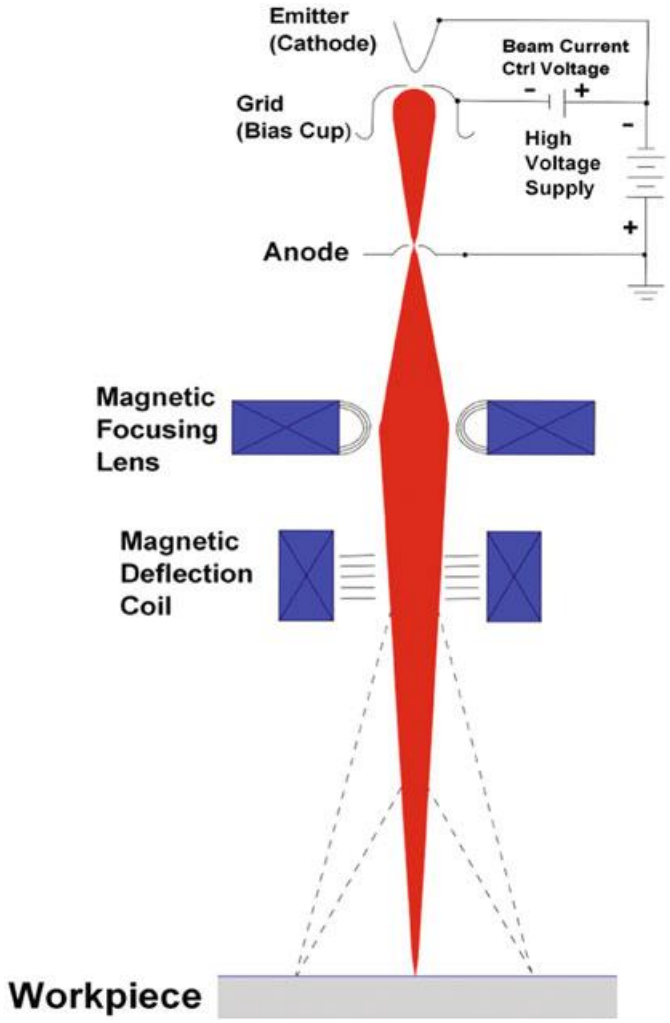

Figure 1.15 shows the concept of operation of an electron beam cannon, described in the link [4].

An increased amount of electric current is supplied through a mesh bowl and a positively charged anode. An electron-emitting cathode, heated and negatively charged, undergoes thermionic emission, releasing electrons. These electrons are then focused and amplified in a mesh bowl, and then sent through the anode to the working chamber. In the working environment, electromagnetic lenses are used to precisely focus the electron beam carrying the charge, and a magnetic deflection coil is used to fine-tune the trajectory. The electronic cannon device is capable of generating beams with a voltage in the range from 60 to 150 kV and an output power from 3 to 30 kW. The concentration of the electron flux converges to a tiny focal point a few millimeters in size. The energy is introduced in a high vacuum environment (below 1·10-4 MBAR). The material used in this process must contain a small amount of oxygen and hydrogen and must be completely dehydrated to avoid the formation of water vapor.[29]

Figure 1.16 shows a diagram showing the layout of electron beam melting (EBM) equipment using electrons created using an electron gun (1), the electrons are accelerated to a voltage of 60 kV, after which they are focused through electromagnetic lenses (2). and controlled by a coil that deflects them (3) Along the path defined by the program. The electron beam is directed to the surface in several passes with a scanning speed of about 10^4 mm/s and a significant beam current of about 30 mA. As a result of this process, the temperature of the powder layer increases by 0.8 times compared to the melting point of the alloy. After the preheating stage, the layer is then processed at a speed of approximately 10^2mm/s using a beam current in the range from 5 to 10 m. The beam crosses the x-y coordinates, which leads to the complete integration of certain sections of the layer. Successive segments of powder materials are supplied from containers (4). In the operational area (6), Adjustments are made depending on the thickness of the layer formed to create a new layer. A squeegee (5) is used to level the surface of the layer. The addition of helium to the working medium leads to an increase in pressure up to 10^{-2}mbar, which increases the thermal conductivity and cooling efficiency of various components of the system. [30].

Figure 1.17 shows the range of factors influencing the successful completion of the electron beam melting procedure.

Performing the operation in vacuum conditions is a disadvantage, since the presence of gas particles can lead to dispersion of the electron beam. In addition, the

movement of electrons leads to the formation of X-rays, which poses a danger to technicians working with equipment. [29].

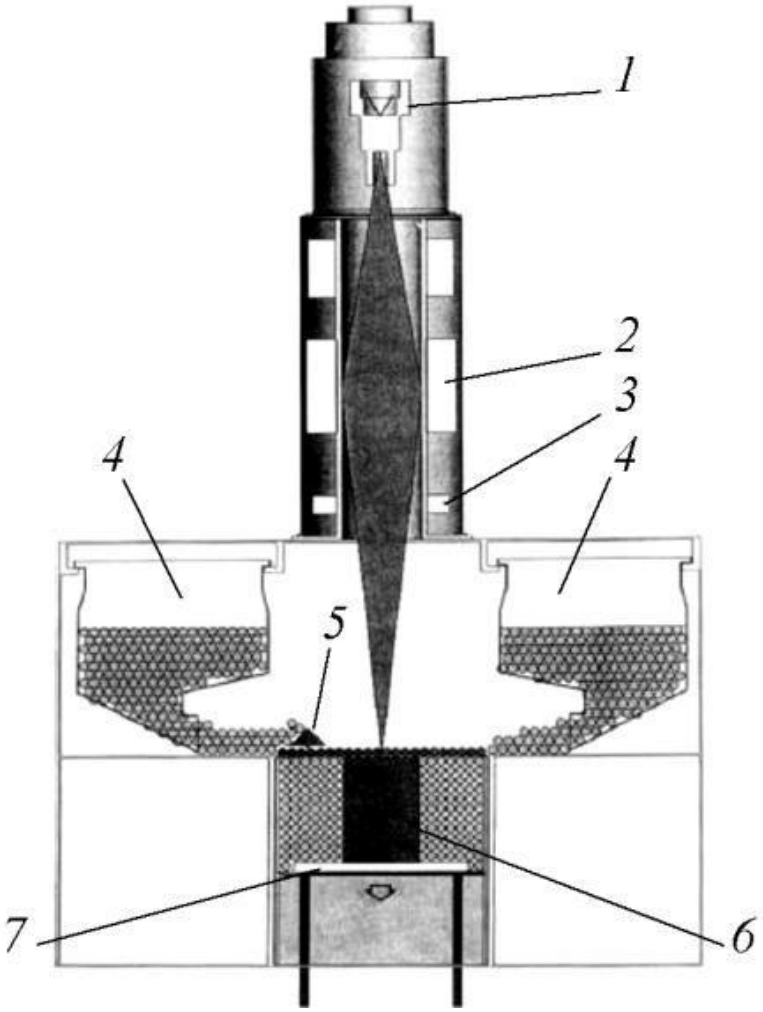

Figure 1.16 — Diagram of the EBM device [29]

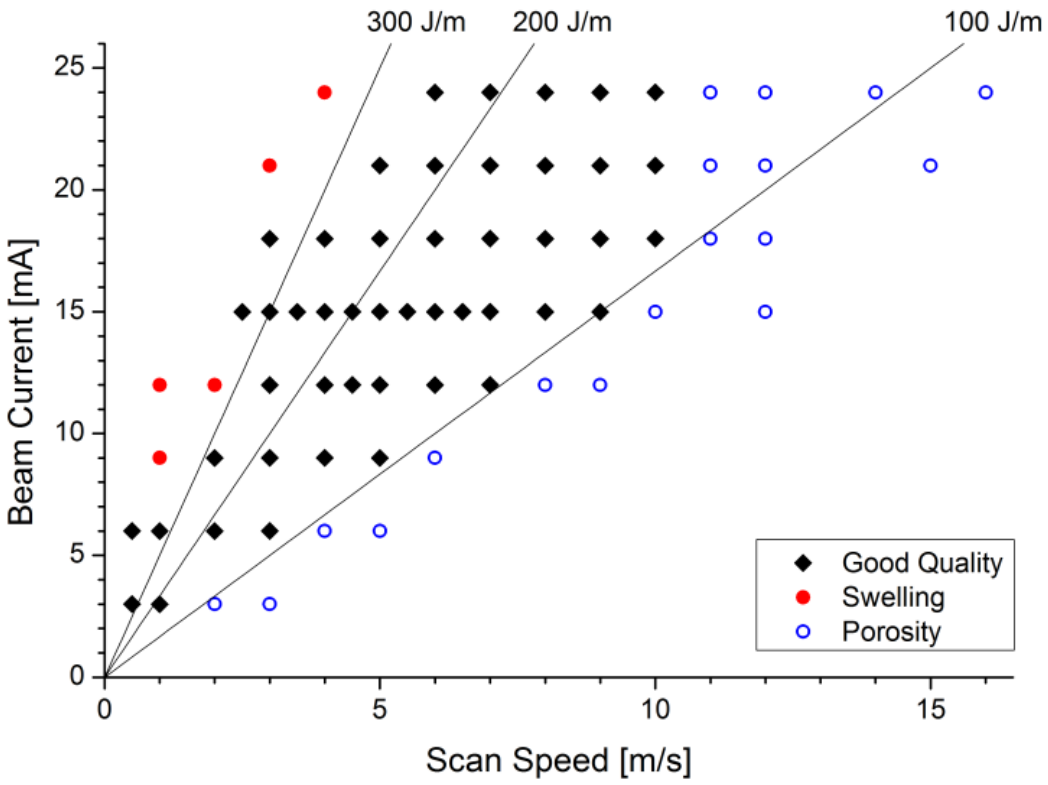

Figure 1.17 shows the evidence-based medicine (EBM) process applied to the (Ti-6Al-4V) alloy, as reported in reference [31].

Advantages of electron beam melting (EBM) technology [29, 33]:

• The need for supporting structures is reduced;

• This approach involves the process of increasing the temperature of powders to 700°C, which reduces thermal and residual stresses, minimizes shrinkage and achieves uniformity of phase formation in products.

• As a result, the need for maintenance of the graphical user interface (GUI) is reduced.

• Successful completion of the process;

• Obtaining powders directly from the equipment supplier guarantees the reliability of the process.;

• The mechanical characteristics of the manufactured parts are very similar to cast or forged analogues.

• Further heat treatment or hot isostatic pressing increases the fatigue properties of the material.

Disadvantages of the electron beam melting (EBM) method [29, 33]:

• The cooling procedure of the working chamber takes a long time, but is necessary to create a stable microstructure and completely eliminate internal stresses.

• However, this method also increases the cost of maintaining the required vacuum level.The choice of materials is limited exclusively to titanium and cobalt-based alloys.

• However, this method also increases the cost of maintaining the required vacuum level.

• The variety and size of products that can be manufactured are limited by the limited capacity of the equipment.

• The use of powders containing larger particles is important because electrostatic repulsion between small granules can interfere with the adhesion of the final layer, which leads to a decrease in the accuracy of the final product compared to laser technologies (which require a minimum particle size of 45 microns).

• It is extremely important to prioritize the safety of printing equipment, given the important role of radiation in the printing process.

Table 1.3 presents an in-depth study of the characteristics of additive manufacturing technologies.

Table 1.3 – Comparison of technical characteristics of SLM and EBM additive manufacturing plants [32, Arcam AB, Farsoon High-tech Co., Ltd]

Model	A2X	FS271M
Cost, million rubles.	55	28,5
General information		
Manufacturer	Arcam AB	Farsoon High-tech Co., Ltd
Country of origin	Sweden	KNR
Application	Industrial	Industrial
Technical specifications/construction parameters		
Printing technology	EBM	SLM
The radiation source	Электронно-лучевая пушка	Yb-волоконный лазер
Construction speed, cm3/h	55 – 80	5 – 20
The size of the construction area, mm	200 · 200 · 380	275 · 275 · 320
Number of ray spots	1 – 100	1
Beam power, W	50 – 3500	500
The minimum diameter of the beam spot, microns	200	20
Roughness of finished products	Ra25/Ra35	
Accuracy of construction, microns	До 130	До 200
Vacuum level, mbar	$5 \cdot 10^{-4}$	—
Protective gas	Helium (optional)	Argon, nitrogen
Protective gas consumption l/min	—	~ 3
Scanning speed, m/s	8000	15
Guaranteed accuracy of parts, mm	± 0.13 – ± 0.2	± 0,2
Supported materials	Metal Powders: Ti6Al4V (Grade 5) Ti6Al4V ELI (Grade 23) Titanium CP (Grade 2) ASTM F75 CoCr IN718	Metal powders: 316L, 17-4PH, IN 625, IN718, AlSi10Mg Ti 6Al 4V, Co-Cr, 18 Ni 300, Cu90Sn10, Ta, W
Hardware Parameters		
File Formats	STL, SLC	STL
Installation dimensions, mm	1850 · 900 · 2200	1740 · 1430 · 1860
Weight, kg	1420	2033
Type of power supply	3·400 W, 7 KV	380 W, 8 KV

When studying selective laser melting (SLM) and electron beam melting (EBM) methods, it is important to emphasize that the costs associated with selective equipment are significantly reduced, EBM installations, unlike SLM installations, are able to melt a wide range of materials without the need for protective shields due to the unique characteristics of the energy source.

The improved performance of the EBM unit indicates a noticeable increase in operating speed. Using thermal processes, this device effectively solves the problem of internal stress associated with the manufacture of parts.

Unlike the selective laser melting (SLM) method, the need for heat treatment has been eliminated to improve mechanical properties and reduce residual stresses. Nevertheless, maintaining the necessary vacuum conditions leads to increased costs.

1.5 Methods of technical improvement of the performance characteristics of additive manufacturing parts made of titanium alloys.

It is noteworthy that titanium and its alloys are highly resistant to corrosion, however, the formation of pitting corrosion on their surface is possible in the presence of active agents and oxidants in the environment. In particular, chlorine ions can act as active agents in chlorine-containing solutions, which underlines the importance of this phenomenon for titanium and its alloys. In addition, it is important to emphasize that Titanium exhibits instability in the presence of certain non-acidic mineral acids, including hydrofluoric, sulfuric and phosphoric acids, especially in conditions of elevated concentrations and temperatures. Corrosion of titanium and its alloys usually leads to uniform wear of the entire surface, unlike some other metals that are subject to local pitting.[6].

Taking into account the above factors, it is possible to use titanium alloy components by coating work surfaces. The resistance of such coatings to chemical influences, wear, strong adhesion to the substrate and increased heat resistance is of paramount importance.

However, there is a problem related to the fact that many wear-resistant coatings have a higher hardness compared to the base metal, which makes them susceptible to contact loads, This difficult situation creates problems with strengthening the base material, especially for parts subjected to shocks and high loads.

Thus, the durability and reliability of VT6 products increases. Using technological approaches remains the most important task in the field of mechanical engineering. In the next discussion, various strategies for solving this problem will be considered.

Currently, the sector covers a wide range of technological approaches designed to increase the durability of titanium alloy components. In addition, new innovative technologies are being developed to protect titanium alloys from mechanical influences and aggressive chemical environments.

Figure 1.18 shows the classification of common application methods for functional surface treatment of titanium and its alloys. [34,35].

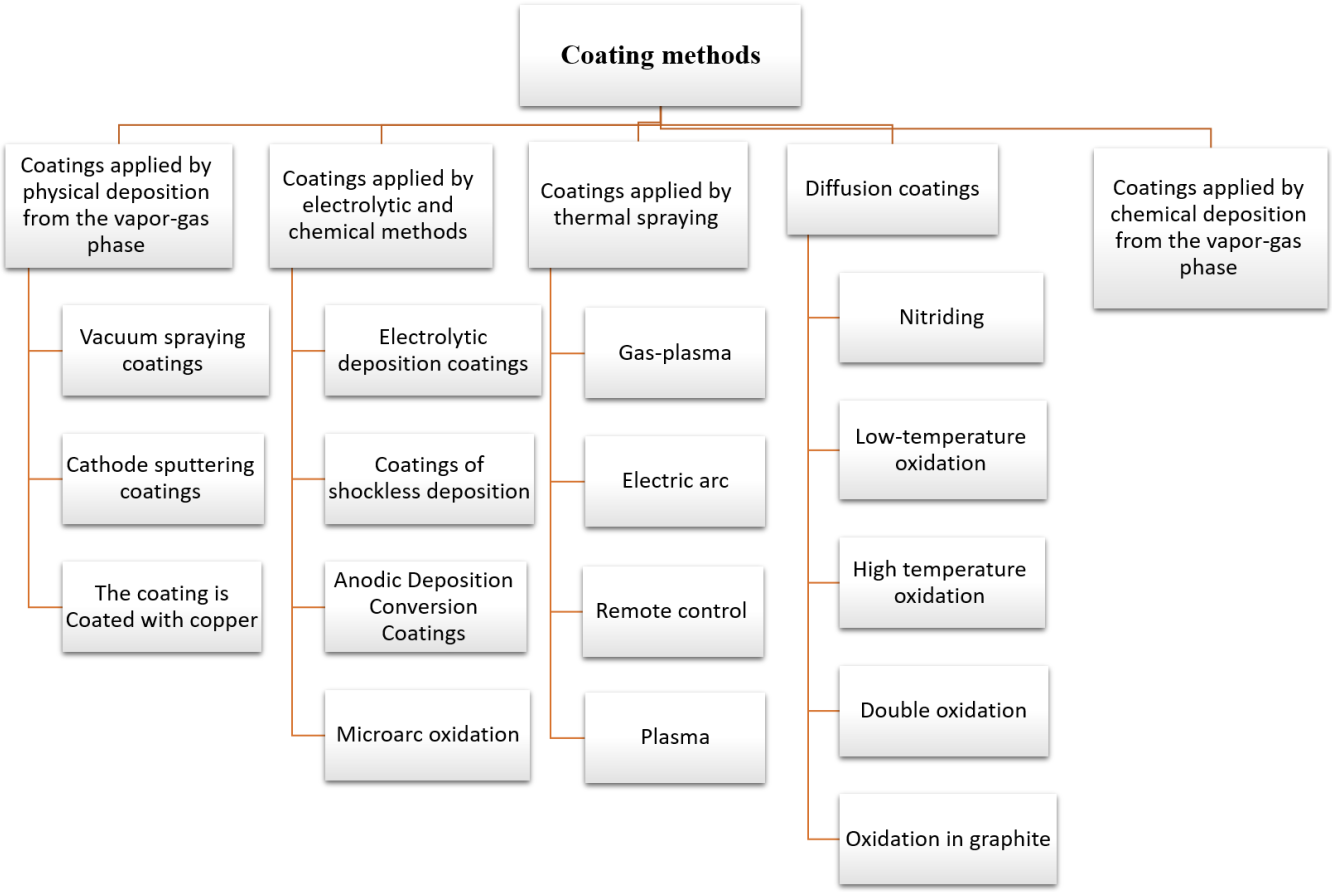

Figure 1.18 shows the classification of the main methods used in the application of functional coatings on titanium and related alloys, as indicated in the sources [34].

Table 1.4 Matrix of the use of coating for various types of wear							
	Coating applied by electrolytic and chemical methods			Coating applied by thermal spraying	Coating applied by physical deposition from combined cycle gas phases	Diffusion coating	Coating applied by chemical deposition from the vapor-gas phases
	Electrolytic shockless deposition coating	Deposition coating	Anodic Deposition conversion coating				
Adhesive wear	+		+			+	
Erosive wear				+	+	+	+
Vibrating			+				
Abrasive wear	+	+		+	+	+	+

Table 1.4 shows the suitability of thermally coated coatings for various wear categories. However, this method has several significant drawbacks. In particular, the adhesion between the coatings and the surface of the component is relatively weak. The mechanical clutch is primarily responsible for this. In addition, this approach does not particularly contribute to environmental sustainability, since particles in the air formed during the spraying process can pose a danger to the health of workers. In addition, it turns out to be ineffective in processing small components due to significant material losses.

Alternatively, the focus is on diffusion coatings and their production methods, including oxidation at various temperatures. However, these approaches are not without their limitations. An illustration of this is the absence of additional solid components in the coatings, such as aluminum oxide, resulting in a solid solution with oxygen. This phenomenon can lead to brittleness of the surface layers of α-titanium alloys and deterioration of their plastic characteristics.The use of these coatings is limited, which leads to limitations in their use, especially in situations involving wear due to vibration.

All alternative coating technologies have inherent advantages and significant disadvantages that require consideration within a specific production framework. These factors may lead to the rejection of a particular method, even if it has outstanding functional characteristics in the field of acquired coatings. In addition,

many of the mentioned methods often do not meet all the contradictory criteria for the surface of the component at the same time.

Among the discussed methods, plasma electrolyte treatment (PEO) is a potentially effective strategy for increasing the durability of titanium alloy parts exposed to both friction and corrosive environments. The plasma electrolyte (PEO) treatment process focuses on converting the outer layer of materials into oxide ceramics using electroplasm. This approach makes it possible to create multifunctional coatings on titanium surfaces, characterized by increased resistance to wear, corrosion, high adhesion and excellent electrical insulation characteristics. [34,35,36].

Electrodeposition leads to the formation of a metal layer that is not completely saturated with dissolved oxygen, and the prevention of deterioration of the mechanical and corrosion-mechanical properties of titanium parts is achieved through the use of titanium alloys [37]. In addition, no scale is formed on titanium alloy components. [38].

In addition, plasma electrolytic oxidation (PEO) technology is characterized by its technological simplicity, as it eliminates the need for etching, degreasing and surface cleaning; In addition, it uses environmentally friendly electrolytes, as shown in Figure 1.19. Consequently, this leads to minimizing the need for equipment, reducing the use of chemicals and eliminating toxic and volatile elements [39].

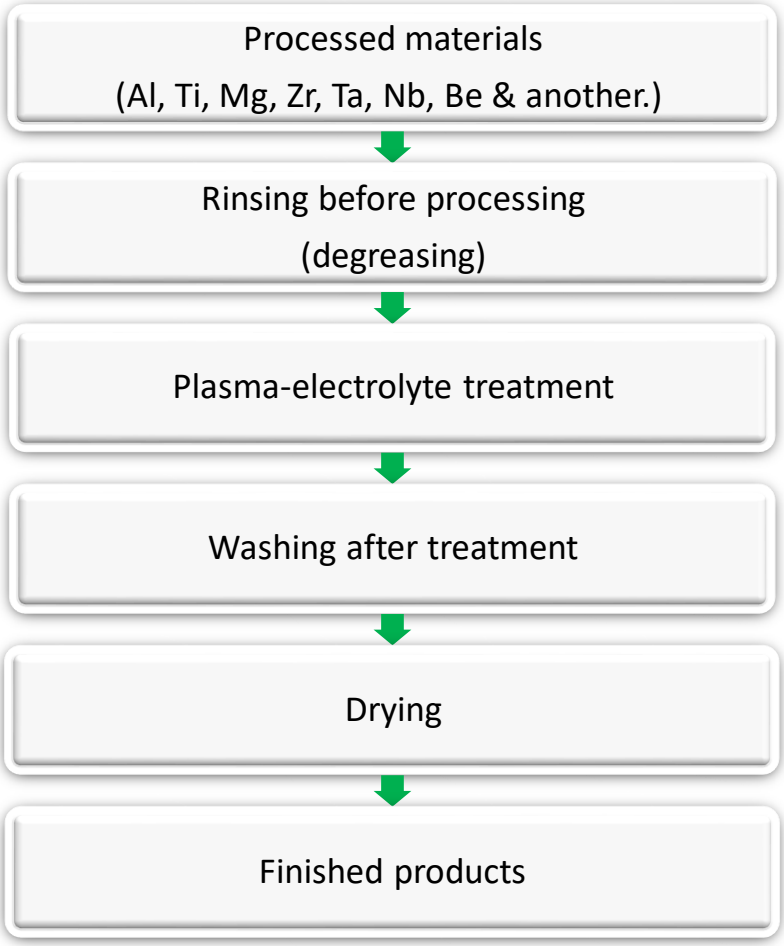

Figure 1.19 shows the chronological sequence of technological processes associated with the plasma electrolytic oxidation (PEO) process.

Among the PEO methods shown in Figure 1.20, the use of titanium alloys to obtain universal coatings on aircraft engine components is particularly interesting. Studies on the use of the PEO process with titanium alloys were conducted by P.S. Gordienko, S.B. Gnedenkov, O.A. Khrisanfova, A.E. Rosen and V.V. Bakovedom [34, 35, 37-44].

The theoretical aspect was considered in the above-mentioned works on PEO titanium alloys, the study of technological patterns, the description of operational characteristics and the compilation of various compositions of electrolytes. However, the spectrum of electrolyte component concentrations and current densities proposed for the PEO process has yet to be determined, the use of this approach for the manufacture of multifunctional coatings on titanium components obtained using additive manufacturing is very diverse and requires additional

tailoring. In addition, the influence of various parameters of the PEO process on the structure, sizing mechanisms, microhardness of coatings, as well as the influence of the structure and surface roughness of parts on the thickness, microhardness and composition of the coating has not yet been studied. The analysis of the distribution of oxides in coatings, residual stresses and durability of the coating under contact loads was noticeably absent. Moreover, the optimization of PEO settings to produce coatings with excellent wear resistance and corrosion resistance in harsh environments has not been thoroughly studied. Solving these technological problems is necessary for the effective integration of the PEO process into the production of titanium alloy aviation components.

1.5.1. The mechanisms underlying the creation of oxide coatings by electrodeposition and the mechanisms regulating their formation remain unexplored.

Coatings obtained using the method of plasma oxidation of electrolytes (PEO) usually consist of oxide layers formed as a result of exposure to an electric microarray in a certain electrolytic solution. This method is especially effective for metallic materials characterized by oxide coatings with increased levels of density and hardness.

When carrying out the electrooxidation procedure, it is necessary to establish the circumstances under which the predominance of the flow of electric current in one direction over the opposite is ensured, a phenomenon known as the diode effect. Titanium, which has diode characteristics, meets these criteria.

The use of titanium's diode properties makes it possible to form oxide layers under the action of alternating voltage.

The process of electrolytic oxidation (PEO) is based on the principle of electrolysis, in which a substance passes from an electrolyte into a solution discharge, simultaneously experiencing high-temperature chemical reactions in the discharge zones and on the electrodes. During microplasma processes, the formation of oxide layers can occur due to thermochemical changes involving electrolyte elements on the metal surface, followed by melting and oxidation of the metal underneath.

At the level of electrooxidation, there is a complete understanding of the primary processes taking place. The anodic reaction is initiated by the release of hydroxyl ions or oxidation of the anode metal and manifests itself in the form of semi-reactions. [45]:

$$40H^{-} \rightarrow\leftarrow 0_2 + 2H_20 + 4e^{-} \quad (1.1)$$

$$M + xH_2O \rightarrow\leftarrow MOx + 2xH^{+} + 2xe^{-} \quad (1.2)$$

At the molecular level, the mechanisms involved in the PEO process have been comprehensively clarified. The anode reaction is caused by the release of hydroxyl ions or the oxidative transformation of the anode material, which is described in semi-reactions [45].

The fundamental principles of oxidation include the following components: [46-50]:

• In order to develop and increase the thickness of coatings, layers with insulating or barrier characteristics are formed at the first stage.

• In order to develop and increase the thickness of coatings, at the first stage it is necessary to create layers with insulating or barrier characteristics.

• It is possible to change the chemical composition of the coatings by adjusting the substrate or introducing soluble or insoluble elements into the electrolyte.

The sequence of plasma chemical oxidation events includes the formation of a dielectric oxide film on the oxidized surface when the voltage exceeds the threshold value of the arc discharge. Consequently, the oxidation process occurs exclusively in areas where the film is thinner, which leads to sparks, dips and microarc discharges.

In the case of titanium oxides, the destruction process mainly occurs under the influence of thermal energy.

This statement can be confirmed by the observation that during the spark oxidation of titanium, the anatase phase of titanium oxide noticeably turns into a kind of rutile, which is accompanied by an increase in temperature.

The temperature range at which the transition reaches equilibrium is usually from 700 to 1200 °C.

In addition, it is important to emphasize that the specific titanium oxide formed is influenced by the anionic composition of the electrolyte.

The interaction of processes contributing to the electrical destruction of the barrier layer and the formation of molten oxide at the sites of destruction leads to an increase in the thickness of the initial barrier layer and the displacement of the bulk charge region further into the coating. The movement of the bulk charge region in the coating anticipates the beginning of the plasma electrochemical oxidation process, in which microplasma discharges cannot reach the boundary between metal and oxide. The barrier properties of the metal-oxide-electrolyte system are influenced by various conduction pathways: ionic conductivity in the anode direction and electronic conductivity in the cathode direction.[47].

The temperature in the arc zone reaches about 3000 °C, while the temperatures of the electrolyte and anode remain low. In this particular working environment, the oxide film reaches a sufficient degree of conductivity, which leads to the formation of metal oxide in the discharge zone. This leads to an increase in the thickness of the dielectric layer, as well as its electrical resistance. Then the discharge moves to areas covered with a thinner film, which leads to an inhomogeneous distribution of microarc craters on the surface of the part, As soon as the voltage reaches a stable state, the process stops because the breakdown voltage coincides with the oxidation voltage, as a result of which the PEO coating is evenly distributed over the component. [44].

The growth of the oxide layer occurs due to the movement of metal ions inside the oxide layers towards the bulk charge region, while the electrolyte particles move in the opposite direction under the action of an electric field in the discharge region. Usually, the outer layers grow faster compared to the inner layers.

An increase in the thickness of the coating leads to a gradual sealing of micropores, an increase in the size of microarc discharges and a decrease in their number. When a certain threshold value of the critical voltage is reached, microarc discharges are replaced by arc discharges.

This shift is determined by a decrease in the frequency of discharges, an increase in their intensity and a change in their trajectory along the surface. The energy generated by arc discharges can increase the temperature of the base material, melt the PEO coating and create depressions on the metal surface, which leads to degradation of the PEO coating. Therefore, microplasma treatment methods can be divided into spark, microarc and arc processes depending on discharge characteristics.[47].

Taking into account the polarization characteristic, all electrochemical microplasma processes can be divided into three separate groups. The main category refers to reactions occurring at the working electrode during anodic polarization and discharge. The next category includes reactions occurring at the working electrode during cathodic polarization. The latter category includes reactions occurring at the working electrode when the voltage polarity and discharge type change, especially in the case of PEO involving the anode and cathode.[38,47].

Cathodic polarization is characterized by the formation of an oxide-hydroxide layer without discharges, which facilitates the transfer of electrons through the oxide layer to the coating while reducing the discharge power. As a rule, obtaining excellent coatings using this polarization method can be a difficult task.

In the process of coating production using the mode of anodic-microarc oxidation, in certain areas where discharges are absent for a long time, paths are laid similar to those that occur during conventional electrochemical oxidation. This increases the electrical stability of these zones compared to areas where emissions have recently stopped. Consequently, water discharges resume at the points where they stopped, which contributes to further expansion of the coverage area. [47].

To mitigate this limitation, a certain number of pulses of positive polarity are interspersed with numerous pulses of negative polarity. Consequently, destruction occurs with high accuracy in areas devoid of discharges for a long time, since coatings formed under typical electrochemical conditions At a lower voltage threshold in the negative polarity of the coating are destroyed, which leads to a more uniform growth over the entire surface.

The process of creating a surface layer during microarc oxidation at both the anode and the cathode begins with repeated application of voltage, including alternating positive and negative pulses.

A protective layer is formed in anode and cathode microarc discharges. Microarc discharges of the anode occur at the interface of the protective film with the electrolyte, while cathode discharges occur at the boundary between the metal and the oxide layer.The inclusion of a cathode element plays an important role in ensuring the minimum porosity of protective coatings,

exceptional adhesion and composite nature, possessing outstanding physical and mechanical properties.[51].

The plasma electrooxidation process consists of four main stages, occurring both at the anode and at the cathode, as indicated earlier. The duration of the anodizing and spark oxidation processes can vary from a short period to several minutes, depending on the composition of the alloy and the reactivity level of the electrolyte used. [52].

One of the features of the process of creating a PEO coating using the anode and cathode method is the delayed onset of the formation of a compact layer, which requires a certain duration of the process. The greatest increase in the coating thickness occurs mainly at the stages of spark and microarc oxidation.[45,52,54].

Plasma electrooxidation at the anode and cathode makes it possible to obtain coatings characterized by increased thickness and reduced porosity. Currently, this approach is the main method of plasma electrolytic treatment.

1.5.2. Properties and performance characteristics of coatings created by plasma electrooxidation on titanium alloys.

Reliable adhesion of coatings to the substrate is a crucial factor determining their ability to withstand contact loads. As the film thickness increases, more metal is involved in the oxidation process, which leads to a subsequent increase in adhesive strength. The layer formed as a result of plasma electrooxidation has a significant ability to penetrate into the material to a considerable depth. Due to changes in voltage and electrolyte composition, it is possible to obtain coatings with different properties, which are influenced by both the base material and the composition of the electrolyte. [53].

Rutile has an advantage over toilet bowl in the field of wear resistance among various types of titanium oxide. Anatase is formed as a result of the connectivity of octahedral complexes at the vertices, and rutile is formed due to connectivity at the edges.

The use of sodium aluminate makes it possible to eliminate heterogeneity and significant macrodefects from coatings obtained in sulfate electrolytes. At a pH level of up to 11.9, sodium aluminate promotes the dissolution of its own oxides present on the metal surface, which are characterized by amphoteric properties and solubility in an alkaline medium. This process leads to gradual erosion of the oxide film during the application of the plasma electrolytic oxidation (PEO) method, which ultimately leads to the creation of a more durable coating. In addition, the fusion of aluminum

oxide, formed as a result of the decomposition of aluminate, with titanium oxide causes the formation of the compound Al2TiO5.

Thus, electrolytes obtained from phosphates and aluminates create coatings with increased electrical insulation characteristics and minimal gas permeability, whereas electrolytes obtained from sulfates and aluminates provide a coating with excellent wear resistance. [35,36].

In order to increase the wear resistance of titanium alloys, it is advisable to carry out the procedure in environments that promote the development of the inner layers of the coating. The most durable films are observed on alloys containing aluminum additives. [37,45].

In the study of electrolytes for plasma electrooxidation of titanium alloys, sodium aluminate is an important and noteworthy component. The presence of an increased amount of alkali in the sodium aluminate solution subsequently increases the pH level, thereby causing the decomposition of the resulting oxide film. [55,56-60].

When studying the characteristics of coatings obtained as a result of plasma electrooxidation, it is necessary to take into account that differences in the microhardness of individual coating layers indicate their different composition, as shown in Figure 1.20.

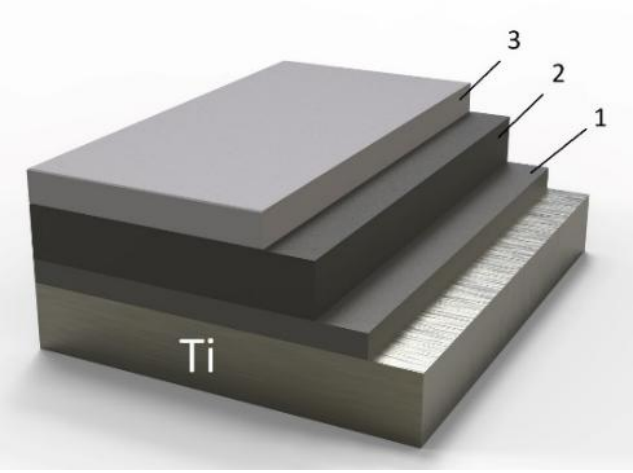

Fig.1.20. The structure of PEO coatings on titanium alloys.

when: 1 is the transition layer, 2 is the main, working layer, 3 is the technological layer.

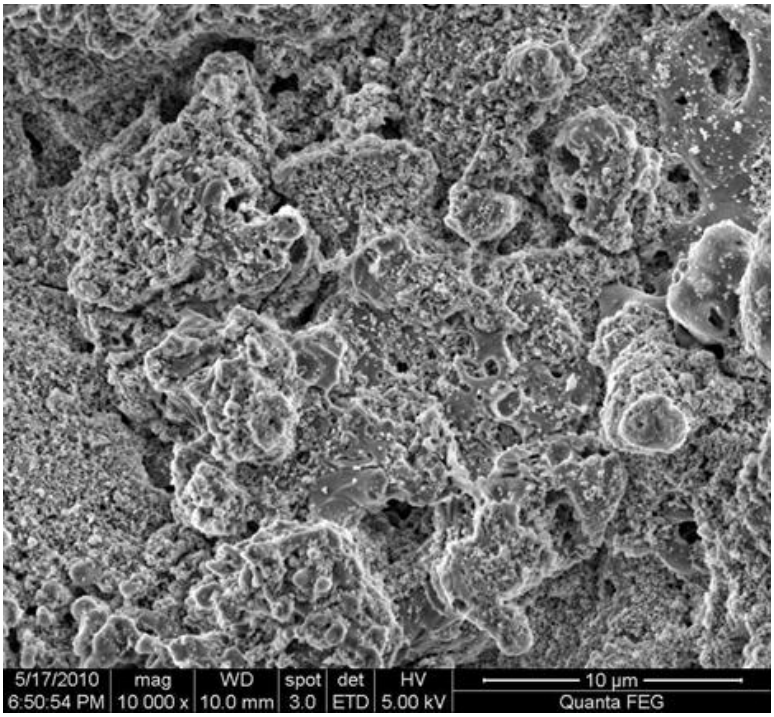

Figure 1.21. The surface of the oxide layer on the titanium alloy Ti-6Al-4V.

Round pores of various sizes with diameters from fractions of a micrometer to several micrometers are present in the thickness of the coating, as shown in Figure 1.21. An increase in the number of pores, especially small pores, was found in the inner regions of the oxide film. As the current density increases, there is a noticeable increase in the number of medium-sized pores, while larger pores practically disappear. [40,75].

At the stage of arc oxidation after PEO treatment, the pores in the coating grow, which leads to a decrease in its electrical elasticity. However, at the same time as the coating thickness increases, a high degree of microhardness remains.

The progress of ceramics undergoing plasma electrooxidation is influenced by many factors, such as the composition and concentration of the electrolyte, electrical properties and inherent characteristics of the material. These variables play a key role in determining the diverse prospects of plasma electrooxidation in the formation of the structure and composition of coatings.

An essential quality of oxide ceramics is its ability to maintain noticeable strength properties even at elevated temperatures exceeding the melting point in the range from 0.8 to 0.9. [57,66-69].

PEO does not affect short-term strength and toughness. The metal substrate under the coating obtained using this technology retains its plasticity. Such coatings have a minimal level of defects, since they do not have interconnected voids and small cracks [37]. VT6 corrosion cracking is the result of embrittlement caused by hydrogen. Coatings obtained by plasma electrooxidation have reduced hydrogen diffusion, which, as a result, increases their corrosion resistance and mechanical properties.

During the oxidation of titanium alloys, a thin layer consisting of oxide and metal is formed, leading to an increase in microhardness. The microhardness values of the metal layers located in the immediate vicinity of the coating demonstrate a striking similarity with the parameters of the source material.

Having studied the above-mentioned literature sources, it can be concluded that a significant amount of research has been conducted on the treatment of titanium alloys by plasma electrolytic oxidation (PEO), in particular the VT6 alloy (TiAl6V4). However, there are noticeably few studies devoted to the processing of PEO components of TiAl6V4 manufactured using additive manufacturing technologies.

Conclusions to chapter 1

1. From the analysis of the literature data, it follows that EBM technology is more preferable for the creation of titanium parts in aerospace engineering. Devices using EBM demonstrate significant superiority in production speed. The thermal operation of these devices reduces internal stress, thereby eliminating the need for heat treatment to improve mechanical properties and reduce residual stresses. unlike the SLM method. Maintaining an appropriate vacuum level also entails additional financial costs.

2. Increasing the durability and reliability of titanium alloy products using technological approaches is an important task in the field of mechanical engineering. Among the studied methods aimed at creating protective and abrasion-resistant layers, plasma electrooxidation (PEO) should be noted, an effective method is used to improve parts made of titanium alloys, in particular those that are subjected to intense friction and aggressive chemical environments.

3. Plasma electrooxidation (PEO) is an electrochemistry method that is used to convert the outer layer of materials into ceramic oxides. This approach makes it possible to create universal coatings for titanium products with increased wear resistance, corrosion resistance, high electrical insulation characteristics and reliable adhesion.

4. The use of the anode-cathode mode in plasma electrooxidation (PEO) makes it possible to obtain coatings with increased thickness and reduced porosity. Currently, this method is the predominant approach in the field of plasma electrooxidation.

5. According to the results of an analytical review of literary sources, insufficient elaboration of the chosen research area has been revealed, which confirms the relevance of this work.

GOALS AND OBJECTIVES OF THE WORK

The purpose of this work is to develop a technological process that improves the performance characteristics of products manufactured using additive technologies from titanium alloy (Ti-6Al-4V) by means of PEO processing

To achieve this goal, it is necessary to solve the following tasks: the development of experimental methodologies.

1. Conduct experimental studies of the effect of PEO parameters on surface roughness, microhardness and wear resistance of the surface layer.

2. Conduct experimental studies to assess the impact of the characteristics of the electrooxidation process on the surface parameters, microhardness and wear resistance of the upper layer of the material.

3. Based on the results of the conducted research, formulate a technological procedure for plasma electrolytic oxidation (PEO) of the components of the Ti-6-Al-4V titanium alloy obtained using additive manufacturing technologies.

CHAPTER 2. MATERIALS, EQUIPMENT AND METHODS OF CONDUCTING EXPERIMENTS

2.1 RESEARCH MATERIALS

2.1.1. Attributes of titanium alloys and their distinctive features.

Titanium alloys represent the main category of structural materials used in various industries. The reason for their widespread use is due to their unique characteristics, including increased durability, resistance to corrosive substances, lack of magnetic properties and high temperature resistance at temperatures from 500 to 600 degrees Celsius.

Improved use of titanium alloys can be achieved by reducing the costs associated with the production of intermediate and final products. Various technological methods, including casting, cold processing, welding, machining and heat treatment, are crucial to influence the overall economic efficiency of the product.

Each of the above operations is influenced by various process features such as casting, deformation, welding, machining and annealing. [57,58,59]. The tables below provide a comprehensive overview of the nomenclature of titanium alloys and their respective mechanical properties.

Alloy grade	Average chemical composition of the alloy, by weight%	Mechanical properties, not less than				
		$\sigma_в$, МПа	$\sigma_{0,2}$ МПа	δ, %	ψ, %	$a_н$, МДж / м^2
ВТ1Л	Technical Titanium	343	294	10	20	0,49
ТЛ-3	Ti-4,5Al	588	539	8	16	0,4
ВТ5Л	Ti-5,2Al	686	627	6	14	0,3
ВТ20Л	Ti-5,5Al-2Zr-1Mo-1V	932	823	5	13	0,25
ВТ21Л	Ti-6Al-5Zr-1V-0,7Mo-0,35Cr-0,2W	981	902	4	8	0,2
ВТ6Л	Ti-6Al-4V	882	804	5	12	0,25
ВТ3-1Л	Ti-6Al-2,5Mo-1,5Cr-0,2Si-0,5Fe	932	814	4	8	0,25
ВТ9Л	Ti-6Al-3,3Mo-1,5Zr-0,3Si	932	855	4	8	0,2
ВТ14Л	Ti-5Al-3,5Mo-1,5V-0,3Cr-0,4Fe	883	785	5	12	0,25
ВТ23Л	Ti-5,5Al-2Mo-4,5V-1Cr-0,7Fe	990	880	4	8	0,25
ВТ18УЛ	Ti-6,5Al-4Zr-3Sn-1Nb-0,7Mo-0,2Si	905	821	12	24	0,3
ВТ35Л	Ti-3Al-15V-3Cr-3Sn-1,2Zr-1Mo	1110	980	6	16	0,25
ВТЛ1	Ti-5Al-1Si	835	736	5	12	0,15

Table 2.1 shows the chemical composition, as well as the guaranteed mechanical properties, as indicated in the reference [59],

The technological characteristics of titanium alloys differ markedly from structural alloys based on iron and aluminum, which is primarily due to differences in their respective physical properties (see Table 2.2).

Table 2.2 presents the basic physical data on aluminum, titanium and iron, detailed in the source. [59],

Properties of metals	**Aluminum**	**Titanium**	**Iron**
Density, kg / m3	2698	4540	7874
Melting point, T_m, °C	660	1665	1535
Thermal conductivity, λ, W/m×k	238	15.5	72.4
Coefficient of thermal expansion, $\alpha \times 10^6, 1/°C$	23.86	8.35	11.70
Heat capacity, c, j/ g×k	0.90	0.52	0.45
Electrical resistivity, nOm×m	26.5	420	97.1
Modulus of elasticity, E, GPa	70.6	103	200

Various important elements play a significant role in the development of technologies and the choice of processing methods for titanium alloys. A key aspect to consider is the significant reduction in the thermal conductivity of titanium and its alloys compared to aluminum and iron alloys, which, respectively, is about 15 and 5 times lower. While technology can improve our society and improve everyday life, it is crucial that it is used ethically. The coefficient of thermal conductivity, heat capacity and density of titanium alloys are crucial factors in heat transfer processes due to their markedly reduced thermal conductivity. This difference is about 15 times less than that of aluminum alloys, and 3.5 times less than that of steels. The occurrence of noticeable temperature fluctuations of ingots and workpieces during their heating can lead to thermal stress and cracking. In situations where induction heating conditions are not ideal, there is a possibility of melting of the subsurface layer and the release of liquid metal during subsequent deformation of the ingot. When titanium alloy workpieces are subjected to a cooling process, the rapid hardening of sharp corners and thin sections makes it difficult to achieve uniform deformation and increases cracking resistance. Consequently, this characteristic imposes restrictions on the achievable shapes of the profiles of workpieces and products, as well as on deformation methods, speed and equipment selection. In addition, low thermal conductivity negatively affects the hot deformation process, potentially causing overheating in areas with high deformation intensity, affecting the structure and properties of the material. This problem is especially evident in processes such as forging workpieces, rolling rods and profiles,

which require careful selection of schemes and deformation modes to reduce the risk of overheating. [59],

Titanium and its alloys are widely used in mechanical engineering due to their excellent mechanical strength, resistance to elevated temperatures, corrosion and heat, as well as remarkable specific strength and low density. The increased price of this metal and its derivatives is often offset by their increased efficiency. In some cases, they represent the only acceptable option for the manufacture of equipment or structures capable of operating under certain conditions. [57-59].

Titanium alloys are mainly used in the aviation and rocket industries, as well as in shipbuilding. The use of technical titanium is evident in the manufacture of a wide range of products, including tanks, reactors, pipes, fittings, pumps, valves and other components designed to operate in corrosive conditions.

Titanium alloys make a significant contribution to the development of the aviation sector and are aimed at creating lightweight structures with the required strength. Materials obtained from titanium are used in the production of linings, fasteners, chassis components, as well as various components. In addition, they are used in the design of jet engines, as a result of which their mass is reduced by 10-25%. Components such as compressor discs, blades, air intake elements and guides are made of titanium alloys and are used in various engine parts.[59].

2.1.2 Titanium alloy VT6 (Ti 6Al 4V) VT6 alloy (Ti 6Al 4V)

was selected for research, which is actively used in various sectors due to its high specific strength, corrosion resistance and excellent compatibility. with biological tissues. [122-123]. Examples of the use of Ti6Al4V alloy in various industries are shown in Fig.2.1., the chemical composition of the alloy in Fig.2.2, and the physical properties in Fig.2.3.

Figure 2.1. Examples of Ti6Al4V alloy application in various industries, [122,123].

chemical properties % material Ti-6Al-4V (GOST 19807 - 91)

Fe	C	Si	V	N	Ti	Al	Zr	O	H	Impurities
To 0.6	To 0.1	To 0.1	3.5-5.3	To 0.05	86.45-90.9	5.3-6.8	To 0.3	To 0.2	To 0.015	Other 0.3

Note: Ti is the basis; the percentage of Ti is given approximately

Table 3. Physical properties of the Ti-6Al-4V material						
Temperature, T	Modulus of elasticity of the first kind, E 10^{-5}	Coefficient of thermal (linear) expansion (range 20^{o} - T), a 10^{6}	Coefficient of thermal conductivity, I	Material density, r	Specific heat capacity of the material, C	Electrical resistivity, R10^{9}
Degree	MPa	[1/ Degree]	[V/(m· Degree)]	[kg/m3]	[j/(kg· Degree)]	[Ом·м]
20	1.15		8.37	4450		1600
100		8.4	9.21			1820
200		8.7	10.88		0.586	2020
300		9	11.7		0.67	2120
400		10	12.56		0.712	2140
500			13.82		0.795	
600			15.49		0.879	
T			I	r	C	

Table .2.3. Physical properties of Ti 6Al 4V alloy (VT6), [58.59].

The alloy has a very high quality, thanks to alloying additives. The alloy includes aluminum, which has a beneficial effect on the heat resistance and strength of products, as well as vanadium, which can increase the strength of the alloy and make it more ductile.

2.2. Research equipment

2.2.1. Equipment for the production of samples by additive methods

As described in the first chapter, the production of titanium alloy products involves two different approaches: selective laser sintering (SLS) and electron beam sintering (EBS), also known as the EBM procedure. The main advantage of these approaches compared to traditional technologies is that they allow you to manufacture a product in one copy in accordance with the computational plan.

The ELS method involves the use of high-energy electron beams for gradual sintering of the material. ELS is the preferred approach to additive manufacturing of chemically reactive metals, such as titanium alloys, under high vacuum conditions. In addition, ELS provides increased efficiency (approximately 80 cm3/h) compared to SLS (20-30 cm3/h), as well as increased adaptability when choosing the size of powder particles (20-45 microns for ELS, 45-105 microns for SLS). [29].

Considering the above, the ELS method implemented on the Arcam A2 installation was used to create samples for research, Fig.2.4.

Figure 2.4. Arcam A2 electron beam melting unit

a-the appearance of the installation; b-the device of the vacuum chamber

2.2.2 Plasma electrolyte treatment (PEO) equipment.

Plasma electrolytic oxidation was carried out at an installation developed by the staff of the STANKIN Moscow State Technical University, which allows setting a wide range of parameters and processing modes. Figure 2.5 shows the device diagram.

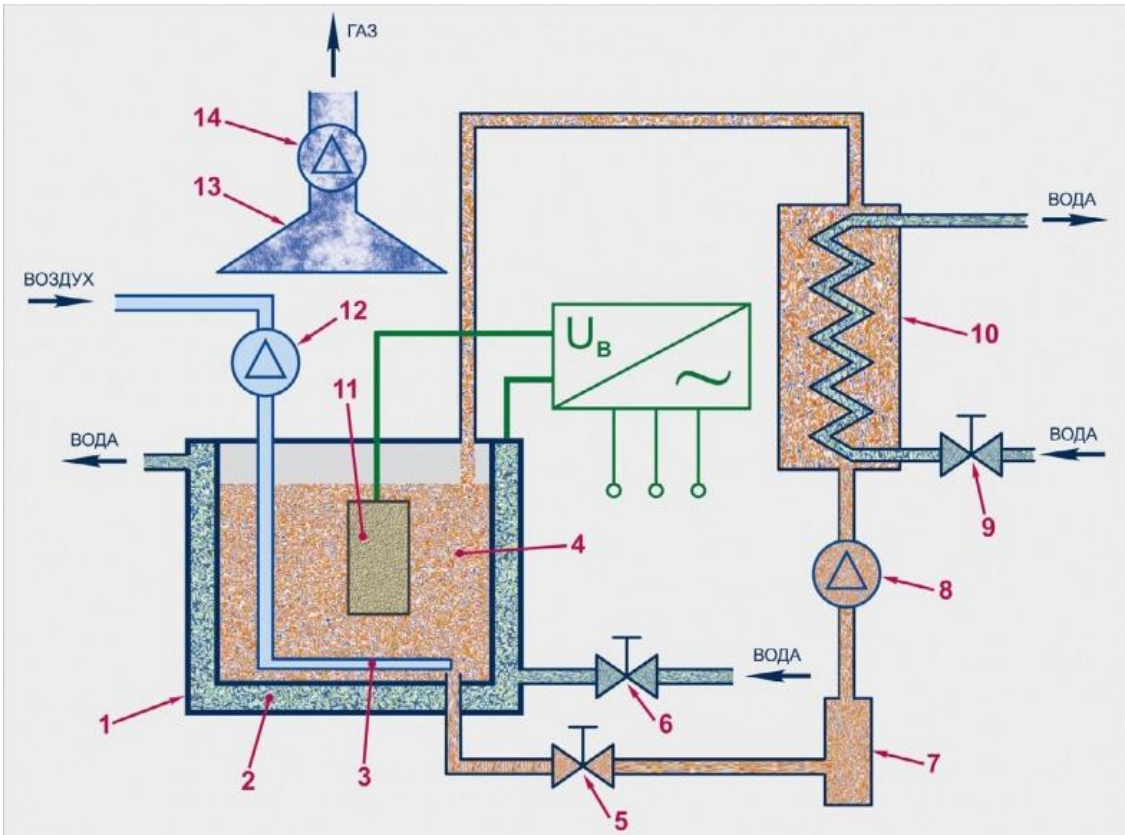

Figure 2.5. Scheme of the electrolyte-plasma oxidation installation: 1 – "Bath for the electrolyte process", 2 – "Shell for cooling with water", 3 – Bubble, 4 – electrolyte, 5,6,9 – Gate valve and valves, 7 – filter, 8 – Liquid pump, 10 – Container with heat transfer device, 11 – element, 12 – Compressor for air compression, 13 – Air removal device, 14 – Ventilation device for air removal [60].

To achieve the necessary coating parameters, it is necessary to ensure an even distribution of the electrolyte components over the volume of the electrolyte bath, which is achieved by the electrolyte mixing system.

Figure 2.6 shows a diagram of an electrolyte bath and a diagram of the circulation of electrolyte flows or the trajectory of dispersed particles [60].

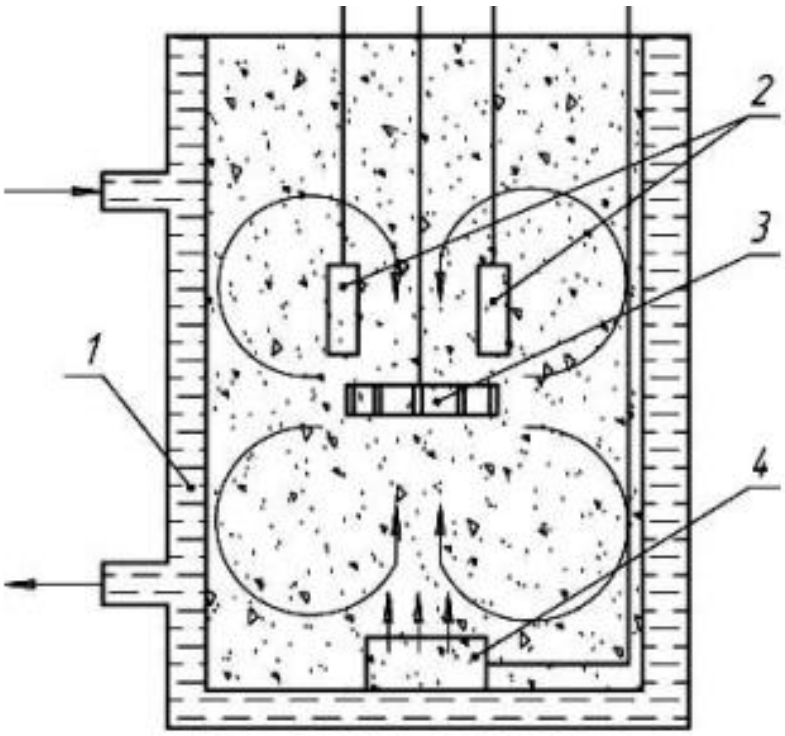

Figure 2.6. Electrolyte circulation laughter during PEO treatment [55]:

1 – cooling jacket of the bath; 2 – parts; 3 – turbine agitator; 4 – compressor.

During mixing, uniform and symmetrical circulating flows occur, which ensure a uniform concentration of particles in the electrolyte [60].

One of the main nodes of the PEO installations that ensure the production of multifunctional coatings is a technological current source (TIT), the appearance of TIT is shown in Figure 2.7, developed by specialists of MSTU STANKIN. TIT allows you to select any polarity of the processing mode, as well as adjust the ratio of the anode and cathode current within the widest limits. TIT control is carried out from the operator's touch panel (Figure 2.8.), and diagnostics throughout the entire technological process is carried out by the Monitor software package.

Fig. 2.7. Appearance of the TIT installation.

n 

Figure 2.8 shows a visual representation of the monitoring system with an operator panel. The electrolyte container is made of stainless steel and loaded with a pre-prepared electrolyte solution consisting of silicates and hypophosphites.

The method was implemented using a soft anode and cathode configuration using a combined anode and cathode current density of 10 A/dm2 during treatment for 10 minutes. The location of the samples in the PEO treatment solution can be seen in Figure 2.9, and the procedural steps of sample processing are shown in Figure 2.10.

Figure 2.9. Arrangement of samples in the bath.

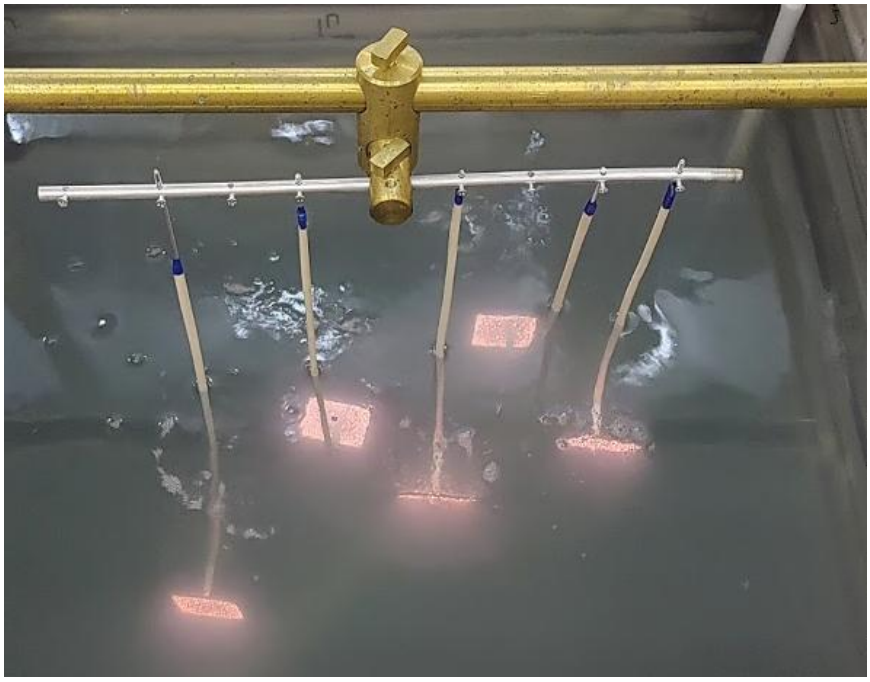

Figure 2.10. The process of PEO sample processing.

2.3. Research methods

2.3.1 Method of measuring the thickness of PEO coatings.

To study the thickness of the coatings, a VT-201 thickness gauge was used, designed to quickly and accurately measure the thickness of the coating on the part. The image of the device is shown in Figure 2.11.

The measurement process proceeds as follows: the sensor of the device is installed on the surface of the part, after which the received electrical signal and the measured amplitude are converted into a numerical value of the measured surface thickness. This value is displayed on the device's display in micrometers [61].

Fig. 2.11. Thickness gauge VT-201 [61]

To obtain correct measurements of the coating thickness, the device is pre-calibrated according to the attached instructions.

2.3.2. Method of measuring microhardness.

Currently, the most popular method of analyzing and studying the strength characteristics of various materials is the measurement of microhardness. Hardness refers to the ability of a particular material or alloy to resist elastic or plastic deformation. Measuring the indicator of this material property is considered one of the most famous types of mechanical testing of metals. To date, 3 methods of static measurement of the hardness of a material are most common: according to Brinell, according to Vickers, and according to Rockwell [62].

In this work, the measurement is carried out on a QNESS Q10A hardness tester shown in Figure 2.12. The Qness Q10A microhardness meters are designed to measure the hardness of metals and alloys using the Vickers and Knoop methods and are used in laboratory metallographic studies. The advantage of Vickers microhardness meters manufactured by Qness is a wide range of loads from micro to macro (0.25 gs - 62.5 kgf/ 0.00245-613.1 N) supported by a single device, while using a modern electronic loading system (load cell) over the entire load range, which ensures high measurement accuracy. The Qness microhardness meter consists of a bed, a loading unit, an object table and a control unit based on an integrated or external PC with the Windows operating system.

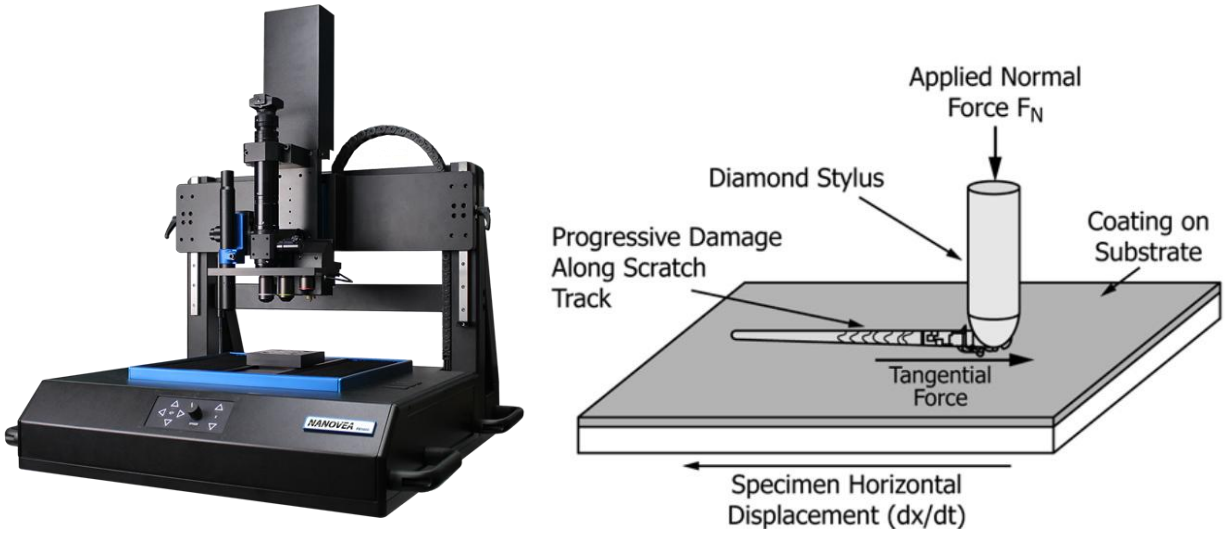

(A) (B)

Fig. 6. (A)Nanovea scratch tester hardness tester., (B).A schematic diagram of the test.

To perform the tests, the following model parameters should be set:

Type of test: Progressive Load test.

Indenter: Select the appropriate type of indenter from the list. The approach speed and contact load depend on the selected indenter.

Initial load: 0.050 N.

Final load: 13 N.

Load increase rate: 1 N/min.

Scratch length: 5 mm.

Scratching speed: XXX mm/min.

2.3.3. The method of measuring the microhardness of PEO coatings.

This study used the Vickers microhardness measurement method [62]. This method uses the application of a static load to a diamond indenter on the sample surface to create an impression for a certain period of time. Then the characteristics of the resulting print are evaluated and the value of the microhardness Hm is determined using a special mathematical expression.

$$H_{\mu} = \frac{1{,}854\boldsymbol{P}}{\boldsymbol{d}_{ср}{}^{2}}\ 10^{6},\ \text{Kg/mm}^2, \qquad (1)$$

where P is the force acting on the diamond indenter, measured in kilograms;
d_{cp} is the average value calculated based on measurements of the two diagonals of the print, designated as d1 and d2, expressed in micrometers, called the arithmetic mean (see Figure 2.13).

(a) (b)

Fig. 2.13. Diamond indenter (a) and its imprint (b) when measuring microhardness

For a lens with a focal length of F = 6.3 and an aperture of A = 0.60:

$$d\ [\mu] = d\ [\text{divisions}]/7{,}9. \qquad (2)$$

In the experiments, a diamond indenter with a square base and an angle of 136° between the faces at the vertex a was used. The penetration depth of the indentation is equal to one seventh of the diagonal of the impression *d*. In accordance with the recommendations set out in GOST 9450-76, the following considerations should be taken into account:

-The distance between the center of the printed image and the edge of the sample should not be less than two diagonal lengths of the printed image d.

- The distance between the centers of consecutive prints should be three times the length of the diagonal of the print d.

- The minimum thickness of the sample or the test layer should exceed ten times the penetration depth of the indenter.

2.3.4. The method of studying the penetrating porosity of MDO layers

Porosity is a fundamental aspect of coatings, which are divided into open and closed porosity, and open porosity is also classified as through and dead-end porosity.

In the case of coatings resistant to chemical influences, such as PEO coatings, the main parameter determining their corrosion resistance and ability to withstand high temperatures (high temperature gas corrosion) is the through porosity Ps.

In the field of corrosion protection of PEO coatings, through-porosity estimation involves calculating the ratio of the total through-hole area to the total surface area of the coated sample (expressed as a percentage), rather than comparing the through-hole volume with the coating volume.

This study used a rapid method to evaluate the permeability of PEO coatings and similar dielectric coatings by analyzing the electrical resistance in a two-electrode electrochemical cell. One of the electrodes of this installation consists of a metal sample coated with PEO, with pores that ensure the conductivity of the system. The second electrode serves a dual purpose as a metal counter electrode and a component of an electrochemical cell.
A schematic representation of the corresponding measuring circuit is shown in Figure 2.14.

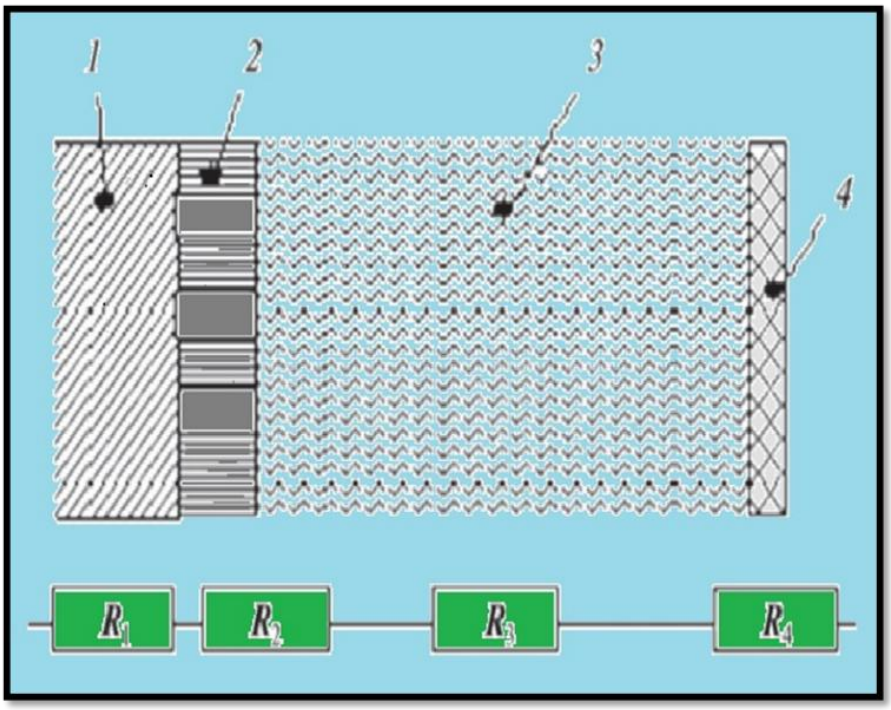

Figure 2.14 shows a schematic representation of the measuring circuit, which is considered equivalent. The following components are included: 1 — base metal; 2 — dielectric PEO coating with through pores; 3 - electrolyte; 4 — metal counterelectrode (electrochemical cell); R1 — transient resistance at the interface between the phases of the base metal and the electrolyte; R2 — electrolyte resistance in the through pores of the dielectric coating; R3 — electrolyte resistance in areas between the coating and the counter electrode; R4 is the resistance of the electrolyte in the area between the coating and the counter electrode between the electrolyte and the counter electrode.

The total resistance of the system can be quantified:

$$\boldsymbol{R_{total} = R_1 + R_2 + R_3 + R_4.} \qquad \textbf{(3)}$$

The resistance, denoted as R1, can be mathematically represented as:

$$\boldsymbol{R_1 = r_{м–э}/S_д,} \qquad \textbf{(4)}$$

Resistance $\boldsymbol{r_{м–э}}$ The term "refers to the electrode" refers to the transient resistance at the interface between the phase of the base and the electrolyte, Expressed as a single unit of area, measured quantitatively. in Ом·дм². $\boldsymbol{S_д}$ - The total base area of the through pores is quantified in terms of its expression. in dm^2. The resistance of the $\boldsymbol{r_{м–э}}$ result depends on many variables, with the main factors being the composition

of the alloy, the composition and temperature of the electrolyte, the polarity, and the magnitude of the applied voltage. Under identical conditions, the $r_{м–э}$ remains constant. The parameter *R1* primarily describes the permeability of the coating. The conductivity of the solution in permeable channels.

$$R_2 = \rho_э \cdot h_{пк} / S_{\sum п}, \quad (5)$$

where $\rho_э$ is the resistivity of the electrolyte, primarily influenced by its composition and temperature, Ом·дм; $h_{пк}$; cod is the coating thickness, дм; $S_{\sum п}$: is the total cross–sectional area of the open channels, dm^2:

$$S_{\sum п} = S_{ср.\ п} \cdot n, \quad (6)$$

where $S_{ср.\ п} \cdot n$ is the average cross–sectional area of the passing pore, dm^2 ; n is the number of through pores.

The resistance of the electrolyte in the area located between the coating and the counter electrode:

$$R_3 = \rho_э \cdot l_{п–п} / S_{ср.\ п–п}, \quad (7)$$

where $l_{п–п}$ is the spatial extent of the area located between the protective layer and the opposite electrode, *dm*; $S_{ср.\ п–п}$ is the average cross–sectional area of this particular region, dm^2. The resistance *R3* of the sample and the counter electrode in the measuring cell consistently remain stationary.

The resistance R4 can be represented using the concept of equivalent resistance. $r_{э–п}$:

$$R_4 = r_{э–п} / S_п, \quad (8)$$

where $r_{э–п}$ is the transient resistance at the interface between the electrolyte and the metal of the counter electrode was minimized to a level measured per unit area of the electrode, Ohms · dm^2; $S_п$ is the surface area of the counter electrode, dm^2.

Under conditions of constant temperature, polarity and applied voltage, the value of R4 remains unchanged for this particular combination of electrolyte and counter electrode. According to equation (5), the coating thickness affects the element R2, which leads to an error in the actual resistance of the system R, which is characterized by porosity. The main determinant affecting R is R1, which, as

indicated in equation (4), is determined by porosity over the entire area of the pore bases. The effect of the R2 deviation in this scenario is more positive than unfavorable, as it allows us to get an idea of the permeability of the coating. Thus, the recorded value of the electrical resistance of the system not only reflects the usual porosity of the coating, but also serves as an exhaustive indicator of the corrosion resistance of the inert MDO coating, which indicates its importance. Within this methodology, the term "through porosity" refers to this particular characteristic.

The aqueous NaCl solution serves as an electrolyte, being a powerful electrolyte and depassivator. The NaCl concentration was optimized in order to minimize the electrical resistance of the system, which includes a "sample (VT6 alloy with PEO coating) - electrolyte — counterelectrode", which made it possible to reproduce the conditions in a highly corrosive environment. This optimization also improves measurement stability by reducing the influence of diffusion and polarization mechanisms in the electrolyte. The resistance of the system at a constant electrolyte temperature of 45 °C is constantly decreasing in the concentration range from 0 to 3.5 g/l and eventually reaches stability at concentrations close to the solubility threshold. Thus, the most appropriate concentration of 4 g/l was determined.

The method for estimating the through-porosity of PEO coatings is shown in Figure 2.15. The test sample is placed in a cylindrical electrolytic cell made of stainless steel, which performs the function of a counter electrode. The temperature of the electrolytic cell is regulated using a laboratory thermostat UT-15. To measure the resistance, the RLC E7-8 universal meter is used, designed to operate on alternating current with a frequency of 1000 Hz, which reduces the effect of polarization effects on the measurement data obtained.

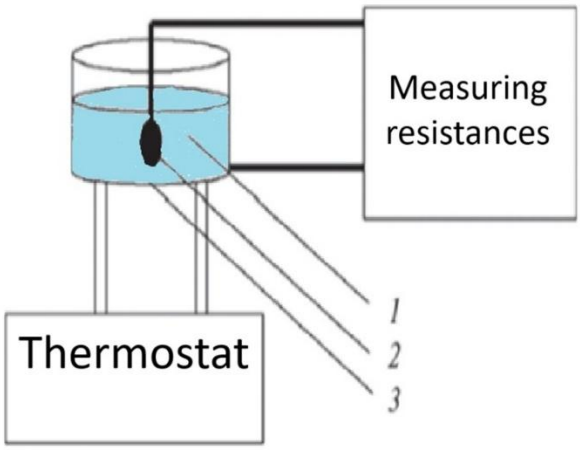

Figure 2.15. Design of a device for determining the total porosity of electrodeposited coatings, source [62]:
1 – electrolytic solution; 2 – test sample; 3 – electrolytic cell (counter electrode).

It is most preferable to investigate the measurement results using the conductivity of the device. $G_{изм}$, the term "is defined as the inverse of the quantitative value of resistance." $R_{изм}$:

$$\boldsymbol{G_{изм} = 1/R_{изм}\ [См].} \qquad \textbf{(9)}$$

Before starting the measurements, it is necessary to prepare the measuring equipment, which includes a number of steps: the initial preparation of the electrolyte solution, ensuring sufficient heating of the thermostat and placing the test samples on insulated electrodes. Then it is necessary to adjust the rack mechanism responsible for moving the sample in the electrolyte to zero on the scale, as well as completely removing the sample from the electrolyte.

Before starting the measurements, the technique is coordinated using a standard uncoated sample with specified dimensions, and one of its dimensions significantly exceeds the others. For example, it can be a thin plate. It is extremely important that the standard uses the same alloy composition as the polyurethane-coated test sample. The choice of standard sizes depends both on the surface area of the sample under study and on the calibration range required to measure porosity. For example, a washer with a diameter of 25 mm and a thickness of 6 mm with a surface area of Sob = 14.7 cm2 is used together with a standard surface area of 2 cm2 to calibrate porosity measurements in the range from 1 to 14%.

The refined and fat-free reference is completely immersed in the electrolyte and subjected to a 5-minute calibration of the measuring instrument measurements. Then, using a rack system with an accuracy of 0.5 mm, the standard is systematically extracted from the electrolyte, which leads to a decrease in the permeability index.

At each stage, the surface area of the reference is measured, which is still immersed in the electrolyte. (Sэт), Important factors to consider are the conductivity of the measuring system and the corresponding values. (G). The collected data is used to build a calibration correlation. G = f (Sэт), At the stage of direct measurements of through porosity, it is necessary to immerse the sample in an electrolyte for 5 minutes to achieve thermodynamic equilibrium in the system. After this period, a universal meter is used. RLC E7-8 The conductivity of the measuring system is quantified $G_{обр}$.. The value is determined using a calibration curve Sэт, Related to these changes $G_{обр}$. And understanding the surface area of the sample is very important. $S_{обр,}$ The total porosity of the test sample is determined.

$$\mathbf{П_с = (S_{эт}/S_{обр})100\ [\%].} \qquad (10)$$

2.3.5 Method for determining surface roughness

Surface roughness is an integral technological characteristic of machine parts. It is a collection of irregularities along the entire length of the surface and is measured in micrometers (microns). It is assigned after analyzing the working conditions of the product surface and technological requirements during the design of the product (machine parts).

In this work, the roughness parameter of VT6 titanium alloy samples was measured using the Micro CAD premium+ optical system (GFM, Berlin, Germany).

This device is designed to measure the roughness parameters of various surfaces of machine parts. The device includes a base unit carrying a measuring transducer (IP), a microprocessor and a drive. The principle of probing the surface of the product under study with a diamond probe, followed by the conversion of mechanical vibrations into voltage changes, is the basis of the device's operation. The result of the measurement is displayed on the display or on an external personal computer for further research and calculations.

The IP is an inductive sensor. A different set of probes for the device provides an expanded range of applications. The probes vary in shape and size, which makes it possible to use the device in holes with a diameter of 3 mm, grooves, as well as on various profiles of gears.

A distinctive feature of the device is the possibility of installing the device when measuring in an inverted position and when the sensor is positioned at an angle of 90 °. This feature allows you to measure the roughness parameter of the surfaces of parts such as the crankshaft.

2.3.6. Test procedure for friction and wear

The development of surface coatings, as a rule, requires them to have increased wear resistance. There are many test methods that allow the use of a rotating sphere (pin) test, also used to measure coating thickness, as a test for small-scale abrasive wear. The ability of the test to measure the internal wear resistance of thin coatings is demonstrated together with a new analysis method that allows simultaneous assessment of the wear resistance of both the base material and the coating based on their combined wear characteristics in a single test.

The aim of the study is to obtain basic data on the surface wear properties of uncoated and PEO-coated titanium samples, which can be used to assign restrictions and develop techniques for their operation.

The studies were carried out using a DOM POD-4.0 high-temperature tribometer, Fig.2.16.

The preliminary preparation of the studied samples is carried out as follows, the samples are cleaned, this procedure is necessary to minimize the influence of foreign particles on the quality of the studied surface of the samples. The samples are washed with alcohol. For the studied samples, washing in an ultrasonic bath is also effective. DOM POD-4.0 allows tribological tests to be performed in rotational motion mode, which are usually present in practically used devices.

The contact body, made in the form of a ball, needle or rod, is attached to the test sample with a certain load and at a given distance from the center of rotation, see Fig.2.16. During movement, the contact body forms a wear groove on the surface of the sample. The coefficient of friction is determined using an accurate load sensor and can be calculated for any selected point or area in each test cycle.

In addition, a fast and smooth control of the rotation speed is available in the range from 0.1 to 2000 revolutions per minute, which allows you to analyze the dependence of the coefficient of friction on the rotation speed. Speeds up to 0.1 rpm are critically important for the study of friction in static conditions and for understanding the process of transition from static to dynamic coefficient of friction. The wear rate can also be determined from the 2D or 3D profile of the wear groove.

Fig.2.16. DUCOM POD-4.0 friction unit

The test samples can be made in a variety of shapes, including cylindrical. The length of the nasal passage is adjusted before starting measurements. With the start of testing, the tip forms a linear wear track.

The friction forces are fixed both when moving forward and when moving backwards. The speed of movement corresponds to the shape of a sine wave, reaching its maximum values in the middle of the track. The amount of friction varies at each point of the track depending on the speed and direction of movement. The wear rate for the contact body and the sample is calculated based on the mass of the lost material.

The DOM POD-4.0 tribometer is equipped with Widcomm 2010 software compatible with Windows 10.

Software Characteristics:

- The study is controlled by the software using the parameters provided by the user. Before starting the test, information about the sample is entered to facilitate the preparation of an experiment report.
- The WinDUCOM software provides a complete overview of the main factors of the experiment, including rotation speed, wear, temperature and velocity, friction force, sliding speed, friction path and duration of the test.
- Graphical representation of experimental data online allows you to visualize data in both graphical and Excel format.

2.3.7. Test procedure for adhesive strength of coatings.

The adhesive strength of coatings is an important parameter for the use of products as various friction applications, such as pulleys for driving power elements (compressors, superchargers, etc.), where torque is actually transmitted through the coating and coating failure is critical in this combination.

The adhesive strength is determined according to the ASTM C1624-05 standard. (2010) on a Nanovea scratch tester hardness tester (Nanovea Scratch Tester, Figure 2.17 (A)) according to the scheme shown in Figure 2.17 (B)

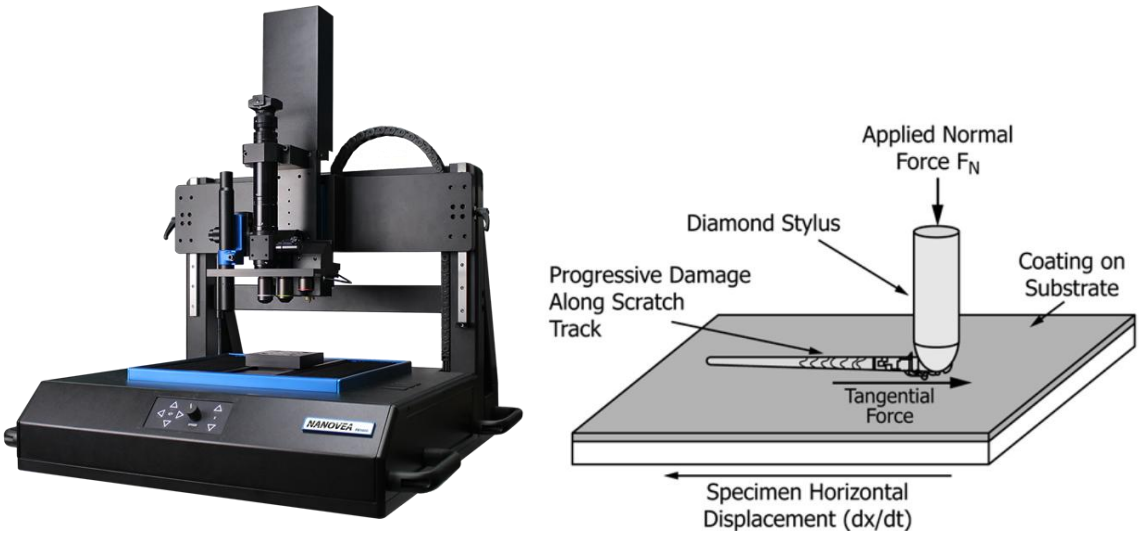

(A) (B)

Fig. 6. (A)Nanovea scratch tester hardness tester., (B).A schematic diagram of the test.

To perform the tests, the following mode parameters should be set:

Type of test: Progressive Load test.
Indenter: Select the appropriate type of indenter from the list. The approach speed and contact load depend on the selected indenter.
Initial load: 0.050 N.
Final load: 13 N.
Load increase rate: 1 N/min.
Scratch length: 5 mm.
Scratching speed: XXX mm/min.
For testing with increasing load, any 4 of the 5 parameters can be set, the 5th parameter is calculated from the following equation: (Final velocity - Initial load) * Scratch rate, Scratch length*, Load increase rate

- To analyze the result in the Image Acquisition window that opens, use the buttons of the coordinate pen to move the sample along the scratch area to identify critical loads. All received images are saved and marked in the graphical test window (Figure 2.18). Each received image automatically saves the location of the scratch, as well as the corresponding values of normal force, friction force, coefficient of friction and depth.

- To create a report, the File Menu opens -> Print Preview command (Figure 2.18). In this window, a panoramic image of the resulting scratch is created (Figure 2.19). Comparing the data from the diagram and the panoramic image, we determine the critical load Lc, which led to the abrasion of the coating to the substrate.

By comparing the data with the diagram and the panoramic image, we determined the critical Lc load causing wear of the coating on the substrate.

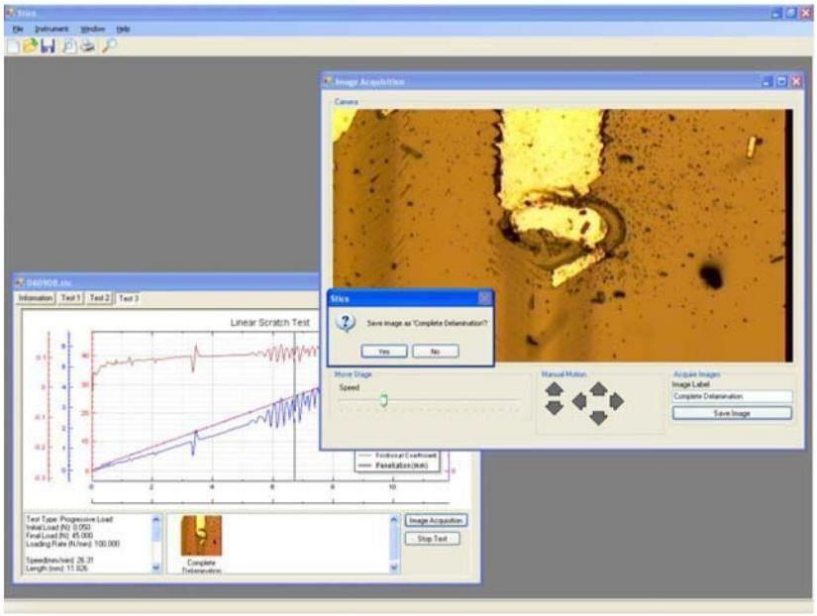

Fig. 7. The result of the scratch test.

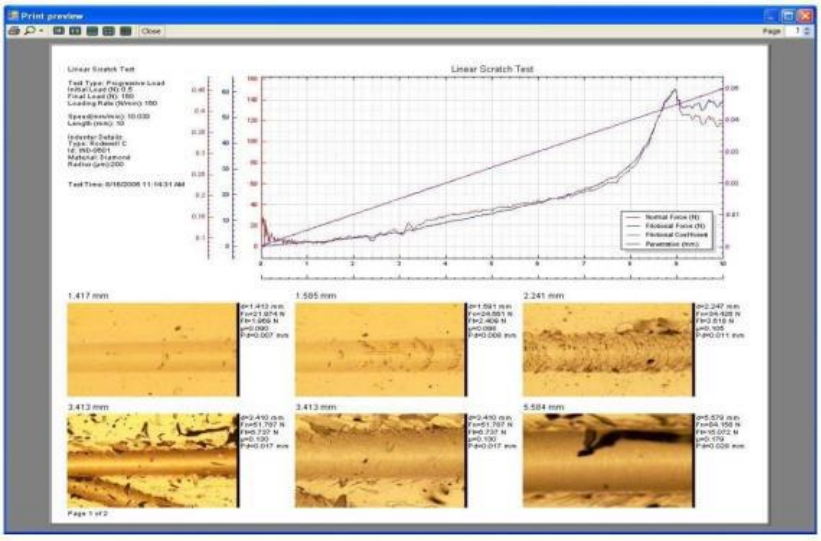

Fig. 8. The result preview window.

Figure 9. Panoramic shot of the resulting scratch.

Figures 2.21-2.22 show typical protocols for measuring the adhesive strength of MDO coatings according to the ASTM C1624-05 (2010) standard and panoramic images of the resulting scratches.

During the experimental procedure, various physical characteristics are measured when the material is exposed to an external force, and the length of the scratch is documented. The point of failure of the adhesive coating is determined by visual inspection after testing, using an optical microscope connected to a digital camera, or by changing the acoustic emission parameter. indenter penetration depth and longitudinal force (Figure 2.15).

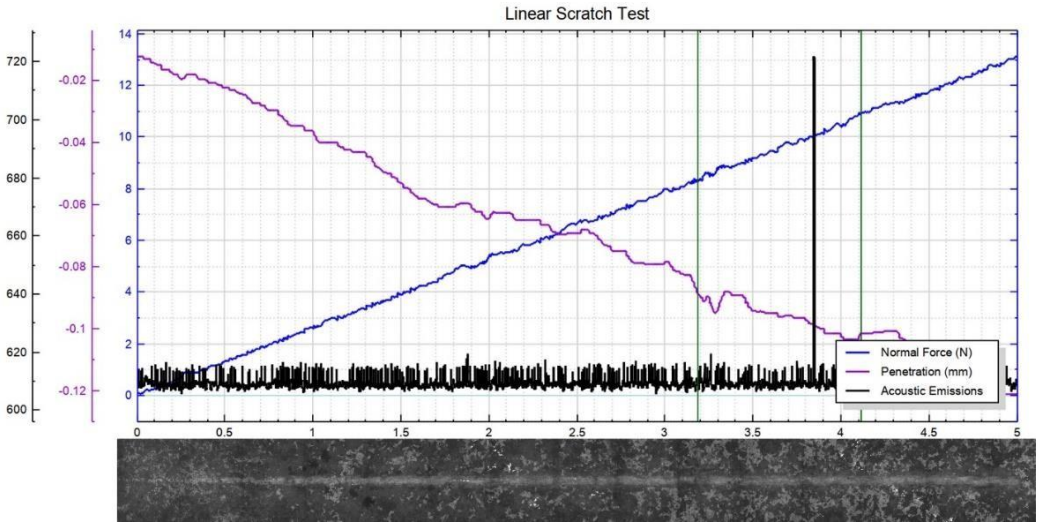

Figure 2.21. Diagram of the test performed with a panoramic image, Acoustic emission (black), indenter penetration depth (purple), longitudinal force (blue)

Comparing the data from the diagram and the panoramic image, we find the Lc value in H (Figure 2.22).

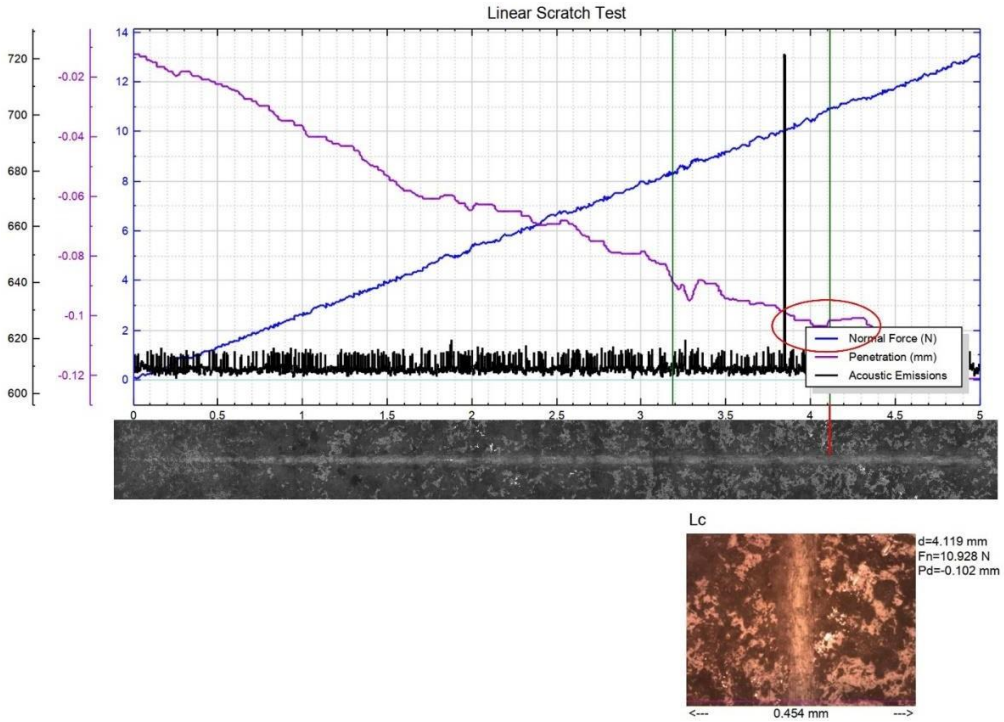

Figure 2.22. Comparison of chart data and panoramic image.

In this case (Fig. 2.16), Lc was 10.928 N. Lc is found similarly for the remaining samples.

2.3.8. Determination of dielectric properties.

A special measuring cell was developed and manufactured to measure the electrical parameters of the samples. The preliminary design of the cell is shown in Figure 2.23.

After developing the preliminary design, a 3-D cell model was developed with some design improvements, in particular, the measuring electrode is pressed without a spring, but with a ball joint, to reduce friction in the joint, conductive dry graphite grease can be used. The clamp itself is also made of bronze, has an external m10 thread, and the ball in the joint has a radius of

7.9 mm. In the upper part of the clamp of the measuring electrode there is a hole for the m6 thread for the possibility of attaching a conductor, the sample clamps are made of m4 pins with plastic tips. The 3D model of the cell is shown in Figure 2.23.

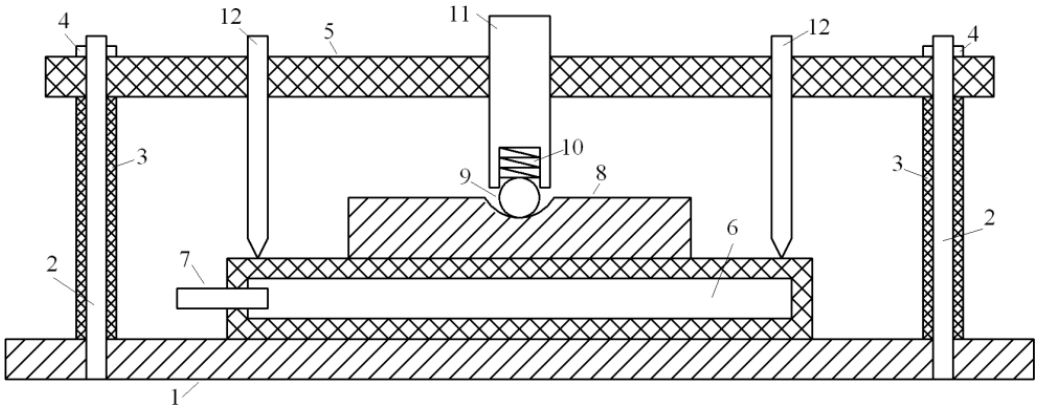

Figure 2.23. Preliminary design of the measuring cell

1 – metal base (3 mm, steel, aluminum or bronze); 2 – threaded studs (4-6 pcs, steel, M6); 3 – ceramic (plastic) tubes (4-6 pcs); 4 – M6 nuts; 5 – fiberglass (15-20 mm); 6 – test sample (minimum circle or square diameter / side 7 cm); 7 – electrode (aluminum) fixed in the hole of the current supply; 8 – measuring electrode (circle with a diameter of 5 cm, thickness 1-2 cm, bronze), the lower surface is leveled and polished; 9 – ball (steel); 10 – spring (steel); 11 – screw for clamping the electrode (steel); 12 – screws for fixing the sample (8 pcs, hard plastic).

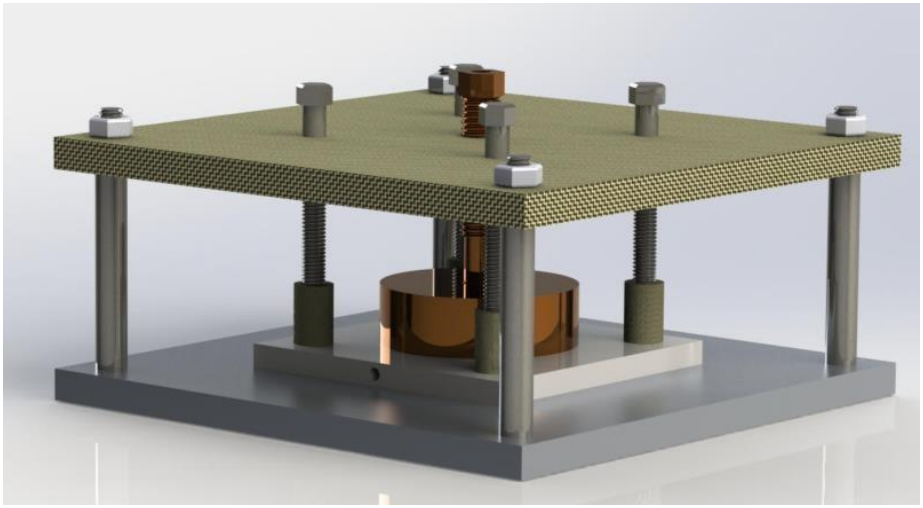

Figure 2.24 3-D model of the measuring cell.

After the final adjustments of the 3-D model, the components of the measuring cell were manufactured using CNC turning and milling. Final view.

The measuring cell is shown in Figure 2.25.

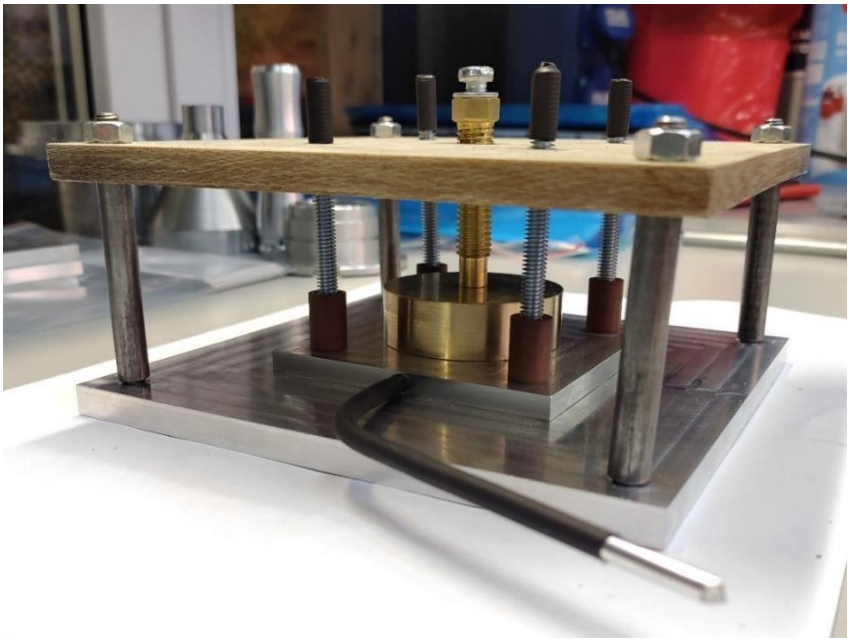

Fig.2.25. The final view of the manufactured measuring cell.

The use of the developed cell allowed conducting research on the electrical resistance of PEO coatings on VT6 alloy, as well as determining the breakdown voltage of PEO coatings.

CONCLUSIONS FROM CHAPTER 2

1. Based on the study of titanium alloys used in the aviation industry, VT6 alloy (Ti6Al4V), widely used in various industries, was selected for research.

2. The equipment suitable for conducting the planned experiments was successfully selected. This equipment can be used in industrial processes related to additive manufacturing, plasma-electrolytic oxidation, as well as their integration.

3. The samples for the study and the parameters of the PEO technological processes, including current density, composition and concentration of electrolytes, as well as the duration of treatment, were determined taking into account the experimental methods and the functionality of the equipment used.

4. The tools and equipment necessary for a complete analysis of the experimental results have been selected. They allow measuring the thickness of PEO coatings, microhardness and surface roughness, wear resistance, as well as determining the structure, phase composition and distribution of oxides in coatings.

5. The selected tools and devices can be used in industry to carry out the processes of additive manufacturing of titanium alloy products and their subsequent processing by plasma-electrolytic oxidation, which corresponds to one of the key research objectives.

CHAPTER 3 Investigation of the effect of plasma-electrolytic oxidation process parameters on the characteristics and operational properties of an oxide coating.

3.1. Production of experimental samples for research.

To study the evolution of various structural components and alloying elements on titanium alloy Ti6Al4V, samples were produced using electron beam melting (EBM) technology at the Arcam A2 installation in the form of disks ∅ 20×10 mm, Fig.3.1.

The thickness of the powder layers reached about 50 microns, the power of the electron beam was set at 900 watts, and its travel speed was 4350 mm/s. All operations were performed in a vacuum chamber using helium as a protective atmosphere.

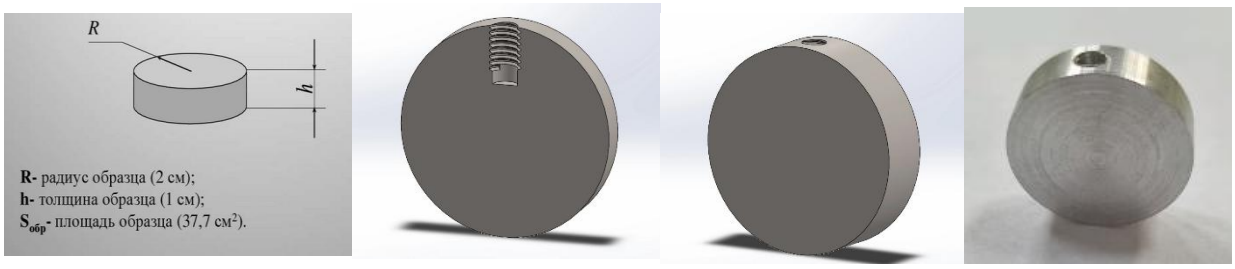

Fig.3.1. Samples for studies of plasma-electrolyte processes in titanium alloy Ti 6Al 4V.

Before applying the PEO coating, the surface of the samples was degreased with acetone. After imaging the PEO process (see Figure 3.2), the samples were subjected to a comprehensive analysis.

The illustration in Figure 3.2 shows samples of titanium alloy Ti 6Al 4V after the PEO process, intended for research.

3.2. Investigation of the dependence of coating properties on the technological parameters of the PEO process.

As a result of a preliminary analysis of the experimental data obtained, it was found that obtaining PEO coatings with a given thickness and adhesion strength of the coating to the base material is possible in a range of technological parameters.:

- Electric current density j, A/dm2: 6-16;

- The ratio between the currents at the cathode and the anode. Ik/Ia: 0,7 - 1,45;

- duration of the process, min.: 5 - 35;

- KOH concentration in aqueous electrolyte C, g/l: 0.5 - 5.

These parameters were chosen as the parameters beyond which it is limited to obtain the required properties of PEO coatings on titanium alloys.

It should be noted that the sampling intervals of the technological parameters of the process are related to the design of the equipment and are the minimum possible, i.e. sampling with a smaller step is impossible.

The properties of MDO coatings were studied in the following sequence:

1) Thickness measurement;

2) measurement of through porosity;

3) measurement of the MDO bond strength.

The data obtained during the study of coating properties (i.e., the output parameters of the PEO process) was processed in two stages. At the first stage, the primary statistical processing was carried out. At the second stage, experimental data were approximated and the dependence of coating properties on the technological parameters of the PEO process was analyzed.

The research results are presented in Tables 3.1 – 3.6 and Figures 3.3 – 3.6.

Table 3.1.

Alloy	Concentration, CONC. g/l	τ, min.	j, A/d^2	I_k/I_a	$H_{coating}$, µm	Porosity, %	$\sigma_{adhesion}$, MPa
Ti-6Al-4V	2,0	5	10	1	2,1	2,0	-
		10			4,8	2,5	-
		15			8,6	3,6	43
		20			9,8	4,2	41
		25			11,1	5,2	40
		30			14,9	5,8	39
		35			18,8	6,1	37

Fig. 3.3. The dependence of the thickness, through porosity and adhesion strength of the coating on the duration of the process.

Table 3.2.

Alloy	Concentration, CONC. g/l	τ, min.	j, A/d^2	I_k/I_a	$H_{coating}$, µm	Porosity, %	$\sigma_{adhesion}$, MPa
Ti-6Al-4V	0,5	20	10	1	11,4	1,4	42
	1.0				11,2	1,8	39
	1,5				10,1	3,7	42
	2,0				9,8	4,2	41
	2,5				9,1	4,8	39
	3,0				8,6	6,5	21
	3,5				8,0	13,3	2
	4,0				-	-	-
	4,5				-	-	-
	5,0				-	-	-

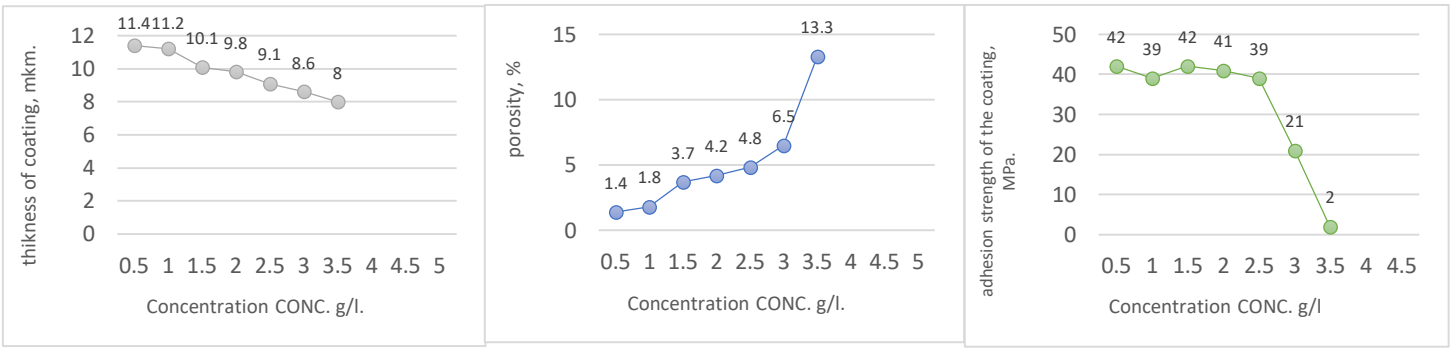

Fig.3.4. Dependence of the thickness, through porosity and adhesion strength of the coating on the concentration of CONC.

Table 3.3.

Alloy	Concentration, conc. g/l, г/л	τ, min.	j, A/d^2	I_k/I_a	$H_{coating}$, mkm	porosity, %	$\sigma_{adhision}$, МПа
Ti-6Al-4V	1,5	20	6	1	5,9	1,4	41
			8		8,2	3,1	41
			10		10,1	3,7	42
			12		11,7	5,0	41
			14		16,3	6,0	42
			16		18,1	9,1	40

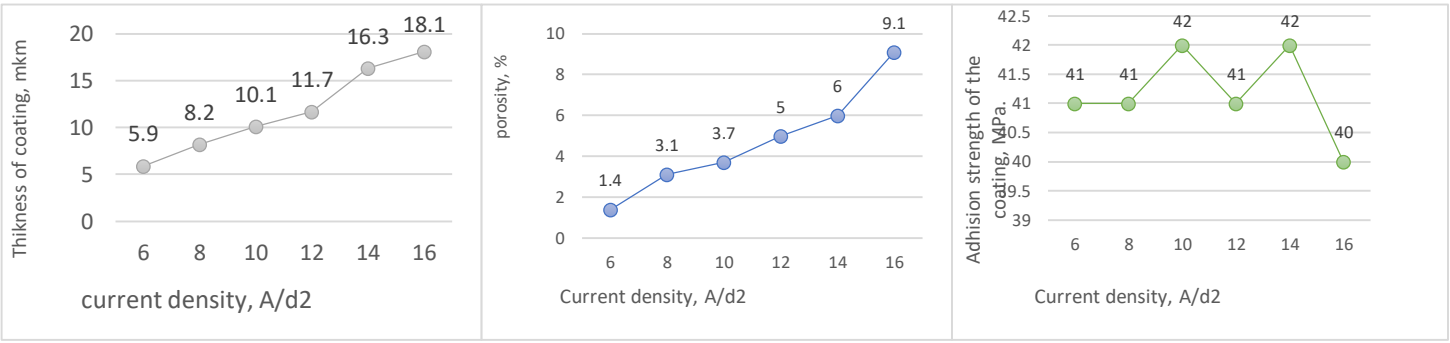

Fig.3.5. Dependence of the Thickness, through porosity and Adhesion strength of the coating on the Current density A/d^2.

Table 3.4.

Alloy	Concentration, conc. g/l	τ, min.	j, A/d^2	I_k/I_a	$H_{coating}$, мкм	porosity, %	$\sigma_{adhision}$, МПа
Ti-6Al-4V	1,5	20	10	0,7	15,0	2,1	12
				0,85	11,8	3,0	46
				1	10,1	3,7	42
				1,15	8,8	4,9	40
				1,3	4,3	-	-
				1,45	-	-	-

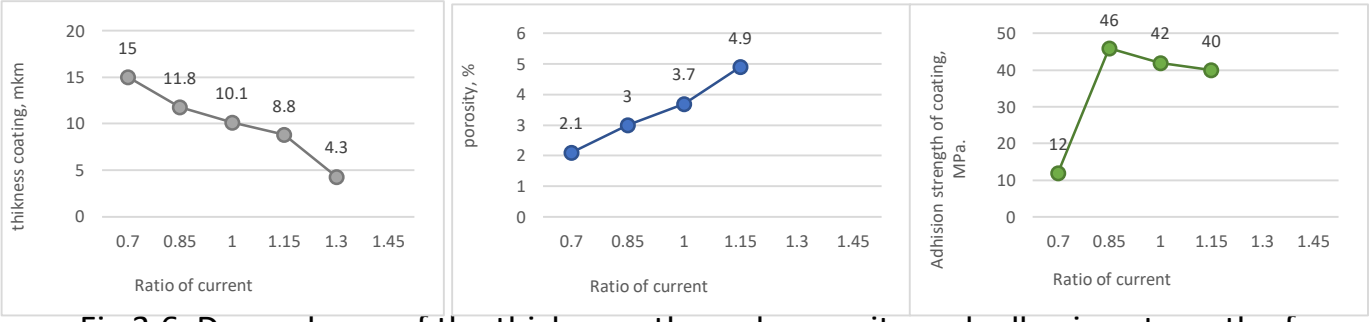

Fig.3.6. Dependence of the thickness, through porosity and adhesion strength of the coating on the ratio of currents.

It was found that the determining factor of the plasma electrolytic oxidation process is the composition and content of elements in the electrolyte. In particular, it was found that oxide coatings produced on titanium alloys in an ionic medium using KOH and NaAlO2 have a wide range of properties. This electrolyte contains aluminum ions, which, when anodically polarized, can integrate into the oxide layer, forming aluminum oxide and its various phase modifications, sometimes forming spinels with titanium dioxide.

Studies on the VT6 alloy have shown that the optimal concentrations of components in the KOH and NaAlO2-based electrolyte for creating oxide coatings should be in the ranges from 0.5 to 4 g/l and from 2 to 26 g/l, respectively. At these concentrations, under almost all acceptable technological conditions of PEO, oxide layers are formed that meet the minimum quality requirements. However, the most outstanding characteristics of the oxide layer are achieved under the following conditions:

for Ti 6Al 4V at KOH from 2 to 2.5 g/l, and NaAlO2 from 16 to 26 g/l.

3.3 Investigation of tribological and mechanical properties of PEO coatings.

As already noted in this paper (Figure 2.1), Titanium alloys are used in a wide variety of industries, such as aerospace, chemical and biomedical industries, due to their unique characteristics. These materials are characterized by low density, high mechanical strength and excellent corrosion resistance.

However, insufficient tribotechnical properties such as high coefficient of friction, tendency to jam and low wear resistance limit their use. [68].

To date, several studies have been conducted concerning the mechanical and tribological properties of PEO coatings on titanium alloys [69-79]. Most of these studies focus on the development of hard and wear-resistant oxide coatings and compared their tribological characteristics with uncoated substrates. It was reported that the bearing capacity of the coatings improved with increasing thickness, and this led to increased wear resistance.

However, at the moment there are practically no studies devoted to studying the effects of plasma electrolytic oxidation on the tribological properties of titanium alloy parts produced using electron beam melting (EBM) technology.

To carry out research work, samples in the form of disks measuring Ø 20×10 mm were created using electron beam melting (EBM) technology on an Arcam A2 apparatus made of VT6 alloy (Ti-6Al-4V) (Fig.3.1.).

Before the start of PEO treatment, the surface of the discs was sanded using silicon carbide (SiC) paper with a grain size of 800 and then degassed with acetone. PEO treatment was carried out in an aluminate-alkaline electrolyte medium with a concentration of KOH 2.2 g/l and NaAlO2 20 g/L. The procedure was performed using a useful configuration of anode and cathode with a current density of 10 A/dm2 at the anode and 20 A/dm2 at the cathode, and the duration of the process was 30 minutes.

The thickness of the modified layer was 24 and 39 microns, respectively. After the PEO process, the top porous coating layer was polished on a Tegramin-30 machine (Struers, Ballerup, Denmark) on SiC paper with a grain size of 800.

The wear resistance of the coatings was studied under dry friction conditions using the "ball on a flat surface" scheme (ball made of AL2O3 (Ø 6 mm), Fig. 3.7.

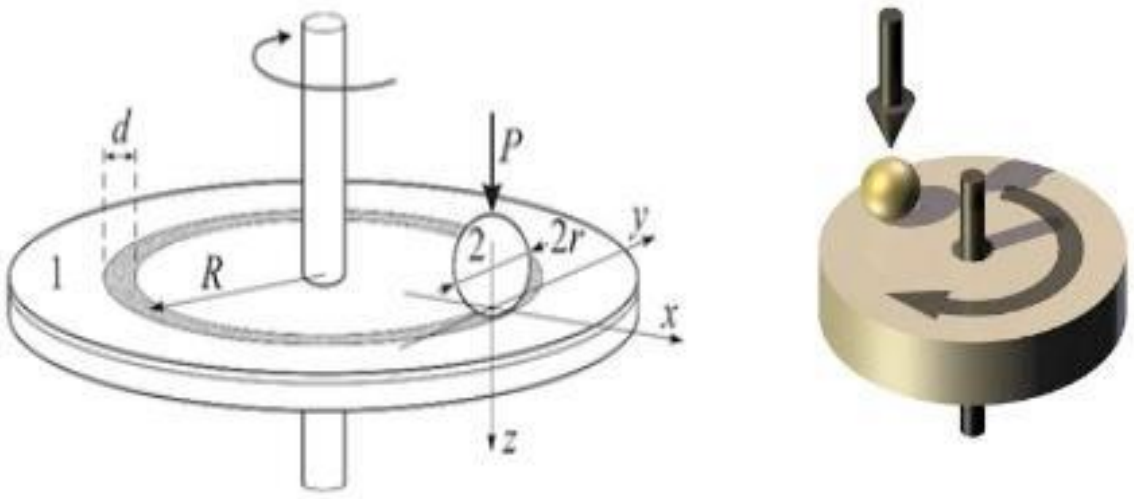

Fig. 3.7. The "ball on a flat surface" diagram.

The studies were carried out at normal loads of 5 and 10 N using a fixed sliding speed of 0.06 mm^{-1}(70 rpm) for each normal load on a friction track S = 500 m at room temperature T = 23°C and relative humidity 45...60%. Three tests were performed for each measurement.

The volume loss of the material was estimated by the profile of wear marks using a Talysurf CLI 500 surface profilometer (Taylor Hobson, Leicester, UK), which displays the measured area at the tip's contact with the sample surface in increments and scanning speeds of 0.01 microns and 0.1 $mm.s^{-1}$, respectively. In the case of a non-uniform wear mark, direct measurement of the wear volume using a profilometer is much more accurate than recommended in ASTM G-99. The profilometer Italy map software allows you to select only the wear zone and calculate the entire volume of the material to be removed. The wear rate was calculated using the following ratio:

W = V/(P·S) **(3.1.)**

Here, V is the volume loss after testing (mm^3), (P) is the applied load (N) and (S) is the sliding distance (m).

Since the rough outer (technological) layer is undesirable for tribological studies, this layer was removed by polishing to obtain a smooth surface.

A representative three-dimensional topography of a wear mark for a 0.5 M long sample after sliding on an aluminum oxide ball is shown in Figure 3.8.

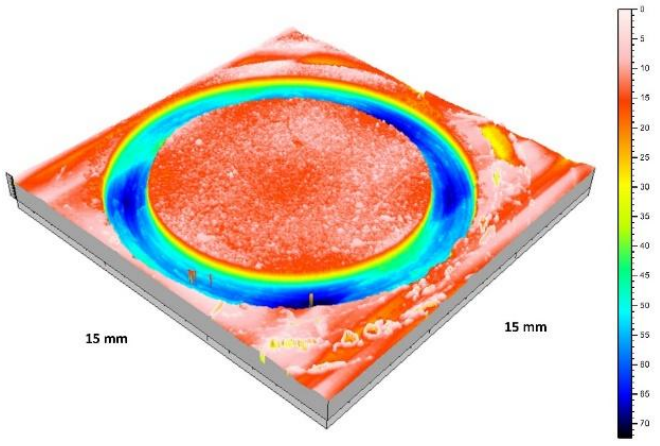

Fig.3.8 Image of the three-dimensional surface of the wear mark, indicating the depth in micrometers (color gradation).

Based on the obtained three-dimensional topography of the surface of the wear marks, the volume loss was calculated to determine the wear rate using Equation 3.1.

The coefficient of friction and the wear rate of the treated samples were, respectively:

Coefficient of friction - 0.76 ± 0.02

Wear rate, mm3/N·m - (18.04 ± 0.1)·10-4

While the wear rate of the untreated samples was (450-475) ± 0.1 mm3/Nm)·10-4, Fig. 3.9.

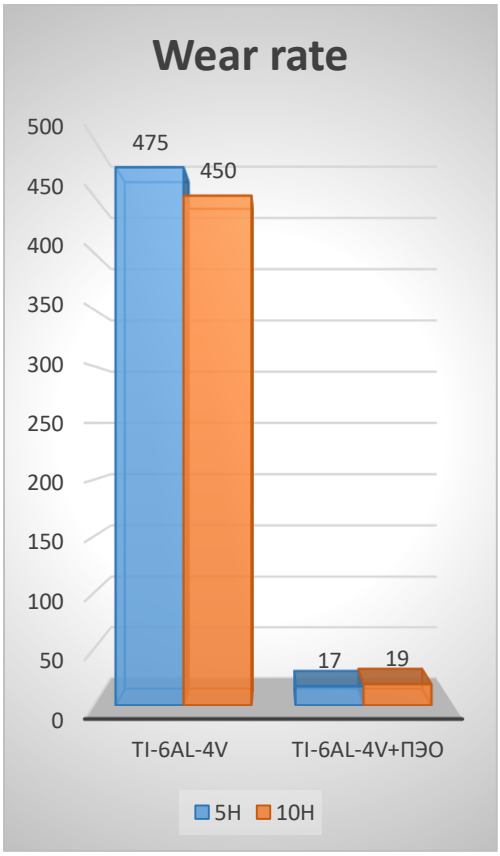

3.9 The wear rate of treated and untreated samples.

SEM images of wear marks on samples at 5N and 10N loads.

Accordingly, they are shown in Fig.3.10

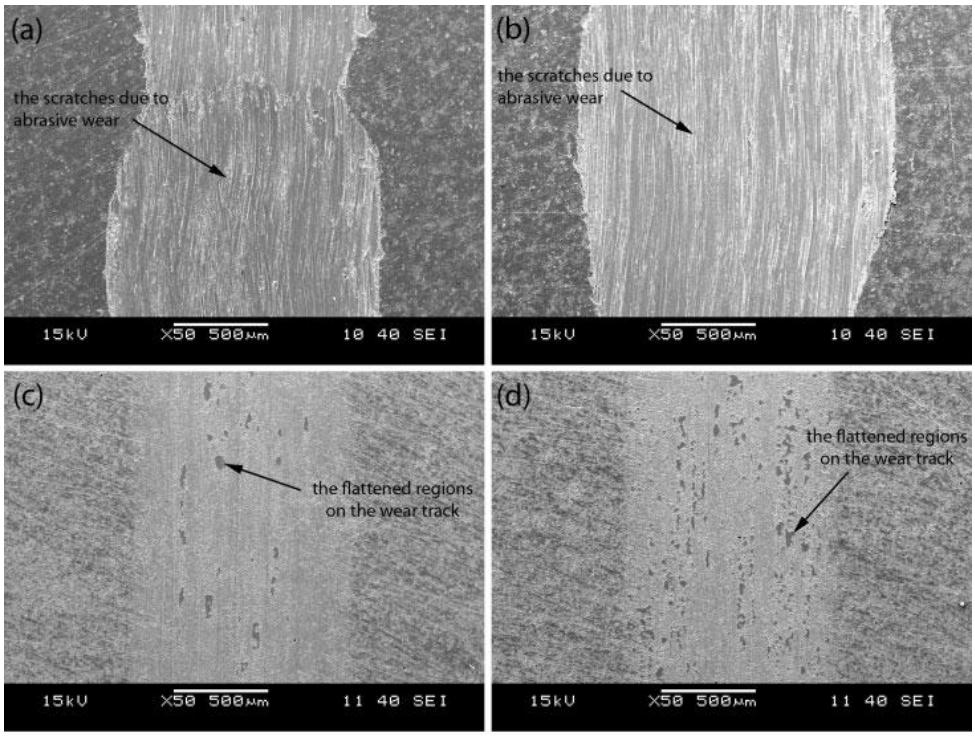

Fig.3.10. SEM images of wear marks on samples under load (a, c, - 5 N and b, d - 10 N, where a, b – VT6; c, d VT6 –PEO.

As can be seen from the presented data, the wear rate of the coating and its character on samples with PEO coating are significantly lower than that of the Ti6Al4V titanium alloy.

It should also be noted that the PEO coated samples show an increase in the coefficient of friction to 0.85 at the beginning of the test, followed by a slow decrease and fluctuation between 0.6 and 0.7 by the end of the wear test. In our opinion, the decrease in the coefficient of friction after passing a distance of ~ 10 m is due to the formation of a tribolayer at the interface of the rubbing surfaces.

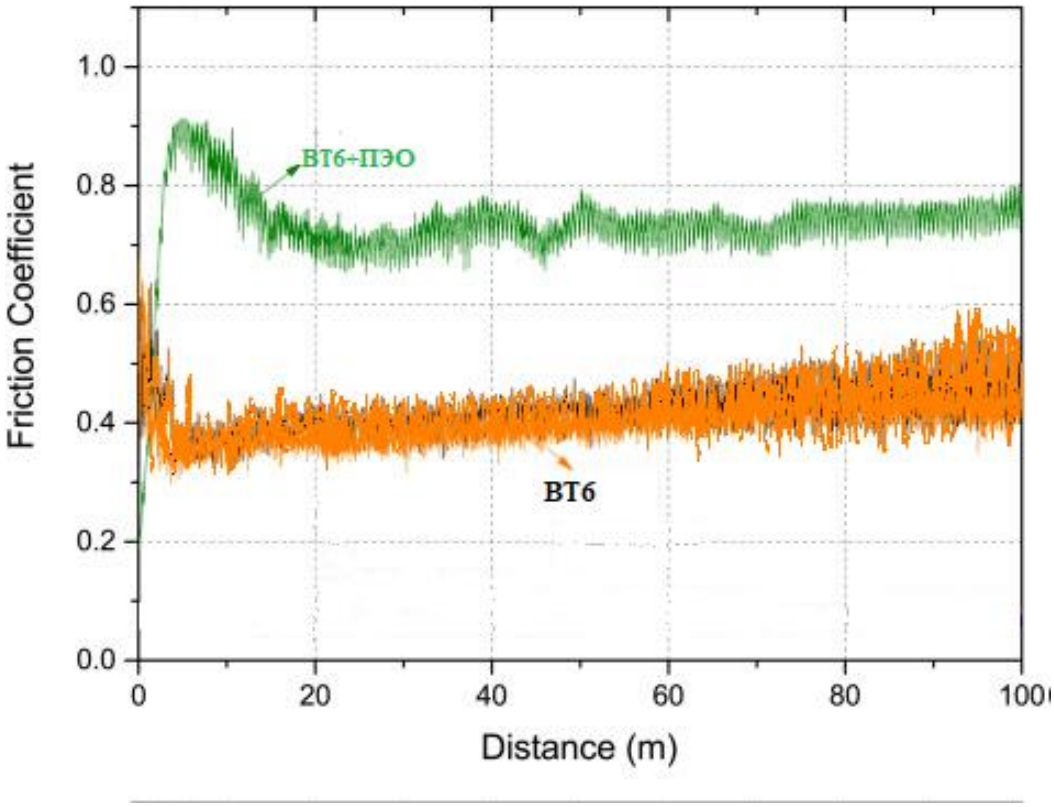

Figure 3.11. Change in the coefficient of friction during tribological wear tests of substrates with and without PEO coating.

3.4. Mechanical and corrosion properties of PEO coatings.

The mechanical properties of PEO coatings, such as microhardness, were evaluated using a QNESS Q10A microhardness tester according to the procedure described in the second chapter of this work.

The measurements were carried out on polished sections of the coating at peak loads reaching 100 mN. This was done so that the coating depth did not exceed 10% of the total coating thickness from the surface, which made it possible to avoid the influence of the properties of the substrate material on the depth data under load. The microhardness of the coating was evaluated directly on the surface and over the entire surface using a load of 100 g, which revealed a constant temperature range in all samples from 680 to 700 HV.

The results of corrosion studies conducted according to the methodology described in the second chapter showed that polarization tests of VT6 (Ti 6Al 4V) alloy samples with PEO coatings show the presence of a long-term passivation zone, which indicates their high resistance to corrosion. It was found that for samples made

of VT6 alloy, after applying a PEO coating, the current density in the passive zone decreases by about eight times. (see Figure 3.12).

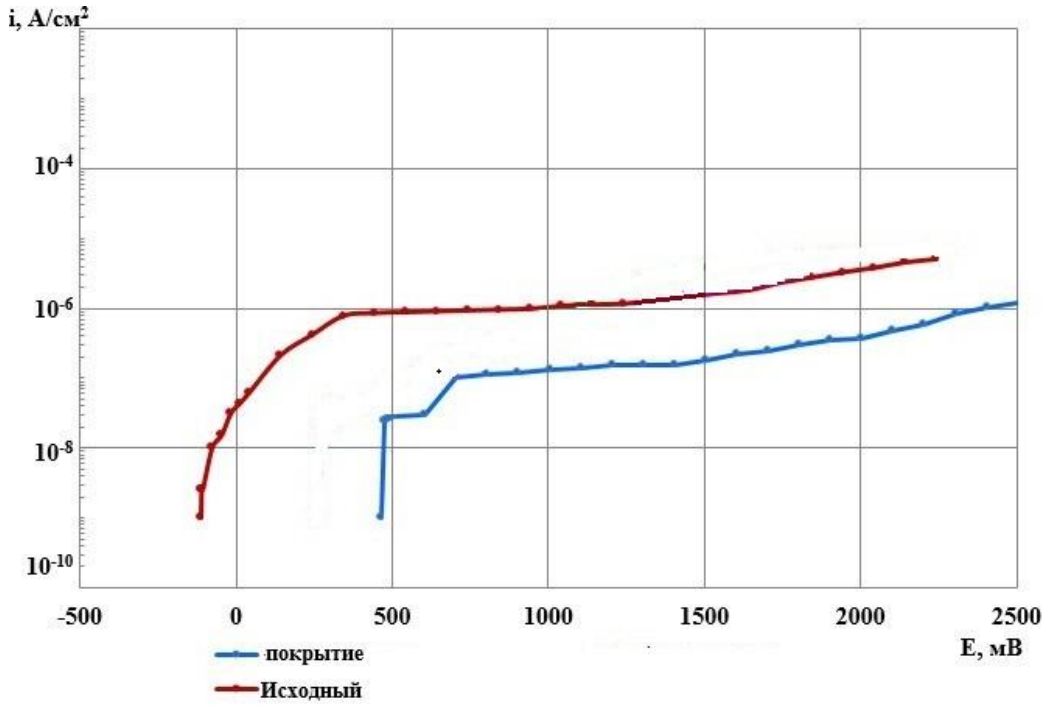

Fig. 3.12. Measurements of anode polarization curves of VT6 alloy samples.

3.5 Investigation of changes in structure and phase composition during plasma electrolytic oxidation (PEO).

Characteristics of oxide coatings obtained by plasma electrolytic oxidation (PEO). They are determined by their structural characteristics, elemental composition and phase structure, which depend both on internal factors (base material, heat treatment, etc.) and on external conditions (electrolyte composition, parameters and duration of the formation process).

The phase study of the coatings was carried out using X-ray analysis. An Empyrean X-ray diffractometer (Panalytical, Almelo, the Netherlands) with a Cu-Ka spectrum (wavelength 1.5405981 A) operating at 60 kV and a beam current of 30 mA was used. The scanning angle ranged from 2 = 20 to 80 degrees.

The cross-sectional structure of the samples was studied using a VEGA 2 LMH scanning electron microscope (SEM) manufactured by Tescan in Brno, Czech Republic, which was equipped with an energy dispersive X-ray spectrometer (EDS).

To prepare for the study of the microstructure, samples with cross-sections of PEO coatings were embedded in epoxy resin, after which the stages of sequential grinding and polishing took place. Grinding and polishing were performed on a Tegramin-30 device (Struers, Ballerup, Denmark).

SEM images in the cross-section of the coating thickness are shown in Fig. 3.13, a, and directly on the surface of the VT6 alloy after PEO, Fig. 3.13, b, and in Fig. 3.14. maps of the distribution of elements on the surface of the samples. As can be seen from the image, there are numerous small-scale micropores throughout the thickness of the coating. Micropores are most likely the result of gas capture in the exhaust channels during the PEO process, which may be due to the formation of powerful microarcs at later stages of PEO processing and their penetration into the substrate alloy. In addition, due to these powerful microarcs, the temperature gradient at the electrolyte interface may increase./coating, and cause rapid solidification of a large volume of molten oxides, which could form shrinkage cracks on the outermost layer of the coating.

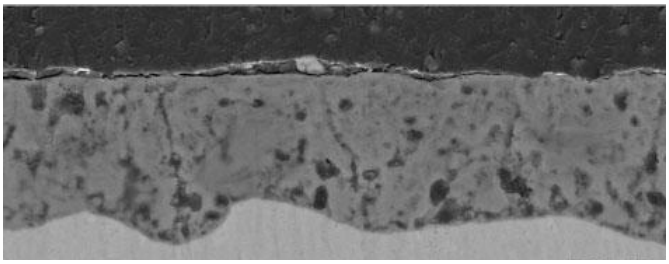
(a)

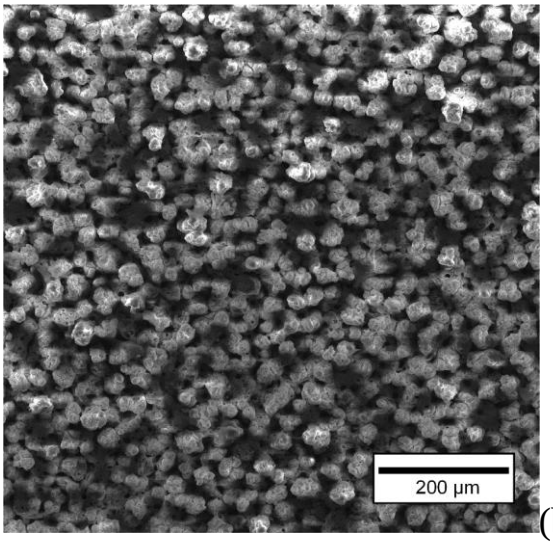

(b)

Fig. 3.13. SEM image (a) is the cross section of the PEO coating, (b) is the surface of the sample.

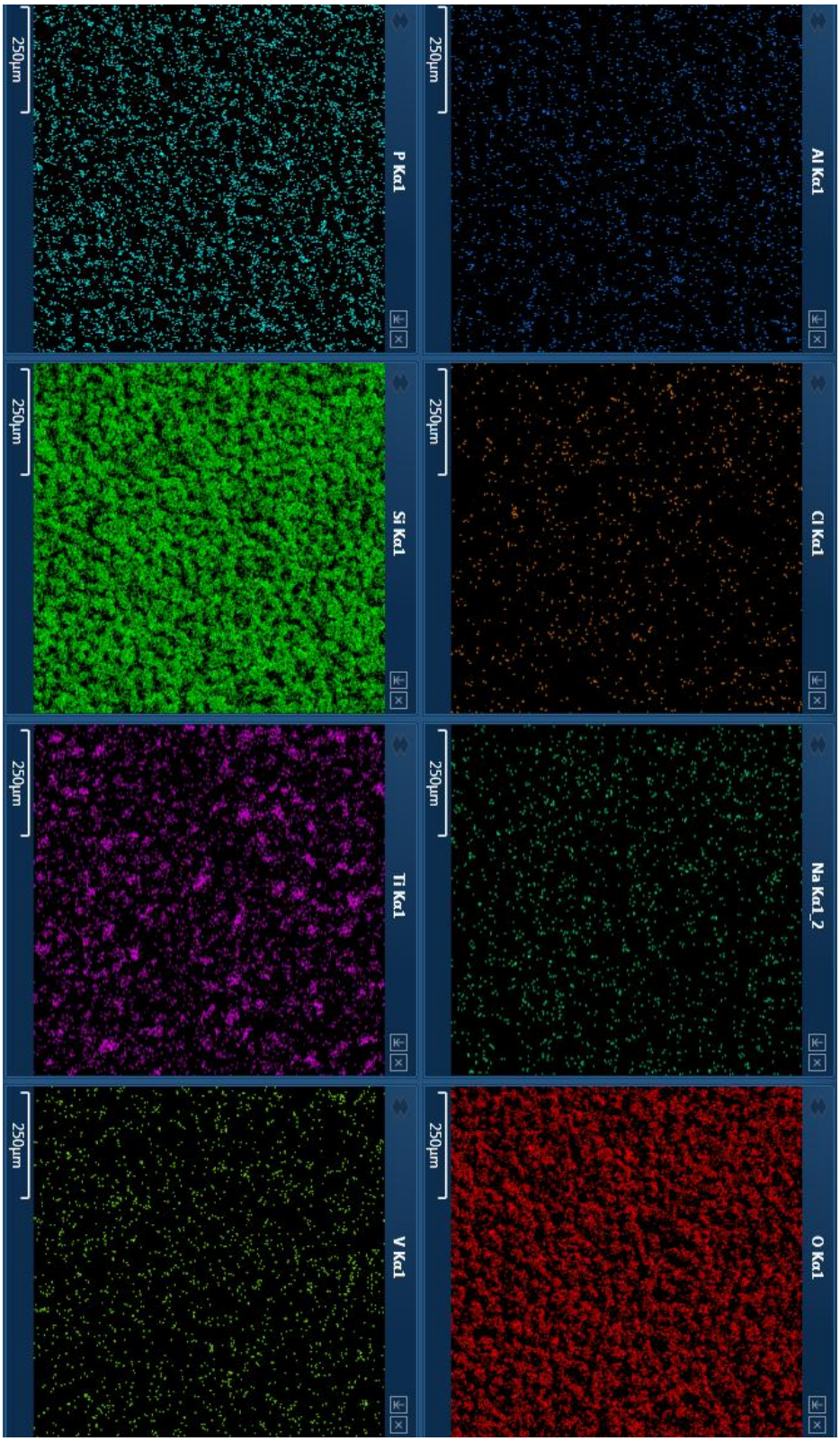

Fig. 3.14. Map of the distribution of elements on the surface of samples after PEO.

X-ray diffraction patterns of PEO coatings in Fig. 3.15 show that phase modifications of titanium oxide (TiO2) and aluminum α-Al2O3 are manifested in the PEO coating.This suggests that the anodic oxidation of the substrate metal mainly contributed to the growth of the coating. The presence of TiO2 in the coating only from the rutile phase indicates that the surface temperature was high enough to convert the metastable anatase to rutile. In our case, in addition to rutile, aluminum titanate (Al_2TiO_5). was observed in the structure. Aluminum titanate is formed as a result of the inclusion of electrolyte components in the coating structure, probably aluminum hydroxides through the exhaust channels. Upon contact of aluminum hydroxides with molten titanium oxide, a crystalline phase of aluminum titanate is formed in accordance with chemical reactions carried out using plasma, proposed by Erokhin and co-authors. [10].

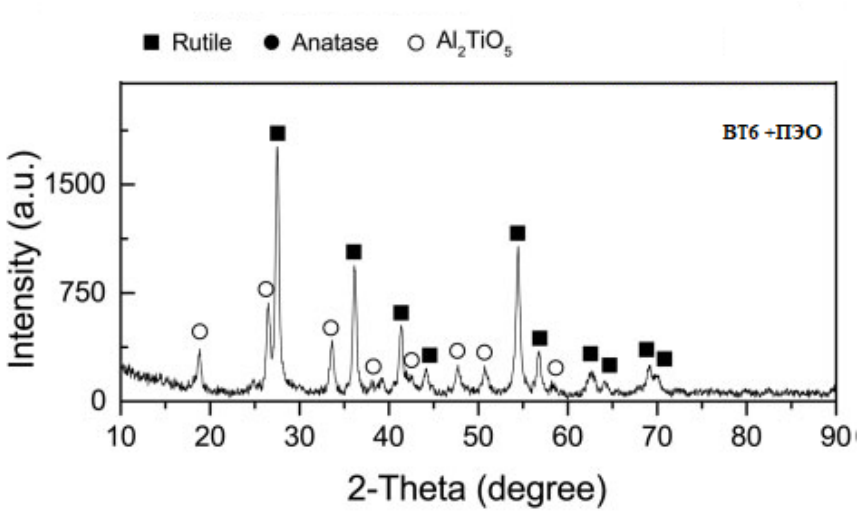

Fig. 3.15. X-ray phase diagram of samples after PEO.

In Figure 3.15, the X-ray images show the presence of two different crystalline phases in the substrate both before and after coating. After the PEO process, there is a significant decrease in the intensity of the α- and β-ti diffraction peaks, while the β-Ti phase tends to disappear completely.This is because during oxidation, the formed coating masks the original surface structure of the sample. At the same time, the preservation of the visibility of the α-phase is explained by the porosity of the created PEO coating.

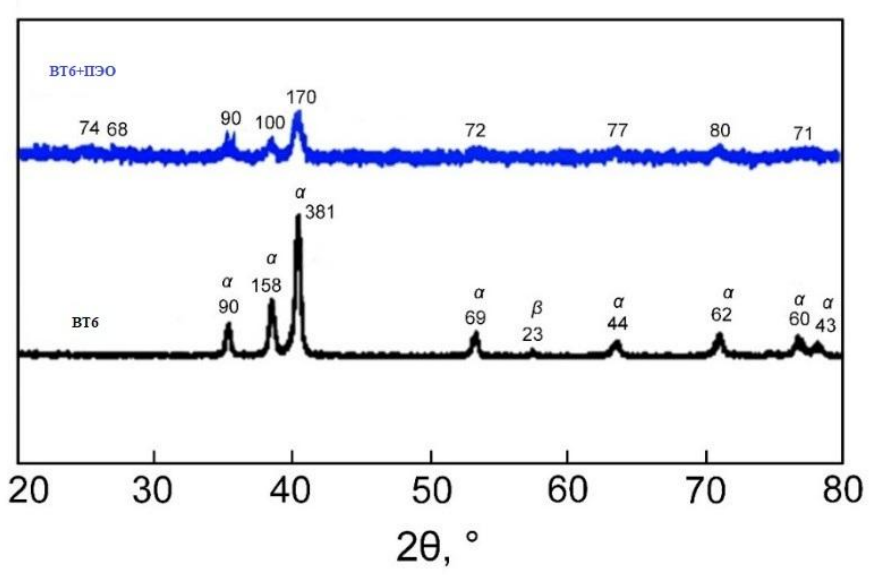

Figure 3.16. – Image of the X-ray diffraction pattern of a titanium alloy before and after performing the PEO procedure.

Information on the surface roughness of the studied samples is given in Table 3.1. Conclusions based on the results obtained are as follows: After the PEO procedure, the surface roughness decreased (Before applying the microarc oxide (MDO) coating, the sample was prepared): Ra=5.62 microns, Rz=32.12 microns; roughness after PEO coating: Ra=1.82 microns, Rz=10.04 microns, respectively). The decrease in surface roughness can be explained by the uniform distribution of the coating, which helps seal pores and defects that occur during electron beam evaporation.

Table 3.1 Differences in surface roughness of titanium samples subjected to the study.

Ti-6Al-4V without PEO coating.	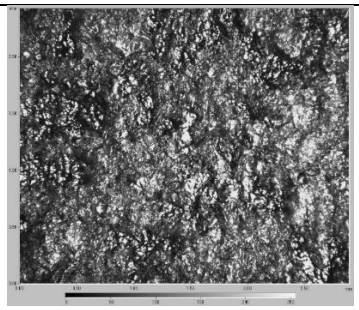	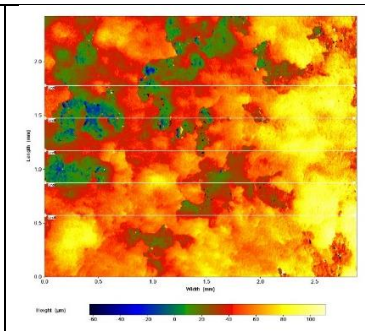	Ra, µm	Rz, µm
			5,62	32,12
Ti-6Al-4V with PEO coating.	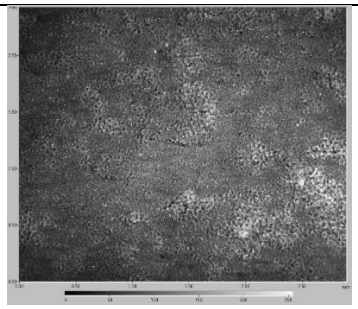	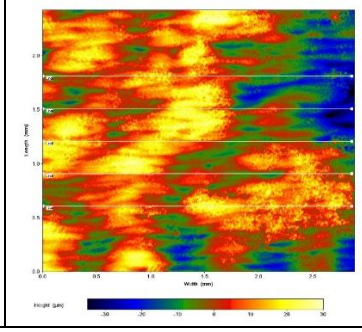	Ra, µm	Rz, µm
			1,82	10,04

3.6 Investigation of dielectric properties.

3.6.1. Investigation of electrical resistance.

To study the dielectric characteristics of PEO coatings, five samples were produced, each of which had a coating thickness from 5 to 25 microns, gradually increasing by 5 microns. The coatings were applied based on predefined parameters:

- current density of electricity j, A/dm^2: 10;

- The proportion of the unit to the electric jet that flows to the cathode from the electric jet that flows to the anode.Ik/Ia: 1,0;

- Processing time, min.: from 5 to 35;

- The concentration of potassium hydroxide (Con.) in a water-based solution used for the electrolysis process. C, g/l: from 3 to 5.

On the obtained coatings, using the E7-23 immitance meter, according to the methodology described in the second chapter of this work, the value of electrical resistance was measured, for which the E7-23 immitance meter was connected to the measuring cell (Fig. 3.17).

Figure 3.17. Connecting the E7-30 to the measuring cell.

The measurement data, as well as the average values of the measured parameters, are presented in Table 3.2.

Table 3.2 Resistance values of Ti-6Al-4V alloy with PEO coating.

Sample №	Material	Ti-6Al-4V + PEO
1	Resistance , Ohms	$1{,}8 \cdot 10^6$
2		$3{,}0 \cdot 10^6$
3		$1{,}5 \cdot 10^6$
4		$5{,}0 \cdot 10^6$
5		$4{,}0 \cdot 10^6$
Average resistance value, Ohms		$3{,}1 \cdot 10^6$

As can be seen from the data given in Table 3.2 PEO coatings on titanium alloy Ti-6Al-4V have significant resistance, which indicates good dielectric characteristics of the coating and the possibility of using it as an electrical insulation.

3.6.2. Investigation of the magnitude of the sustained voltage (electrical breakdown).

This parameter is key from the point of view of using coated products in nodes operating in conditions where it is necessary to provide electrical insulation of some nodes from others.

To determine the sustained voltage, samples prepared according to the technological parameters described at the beginning of this chapter were used.

For testing, the samples were mounted in a measuring cell, which in turn was connected to the GPT-79902 breakdown unit, the high-voltage connector to the measuring electrode, and the common outlet to the substrate of the test object (Fig.6.79). Measurement mode: test voltage up to 2000 VDC, maximum current up to 20 milliamps (mA), voltage rise time 10 seconds, test duration 60 seconds, manual mode.

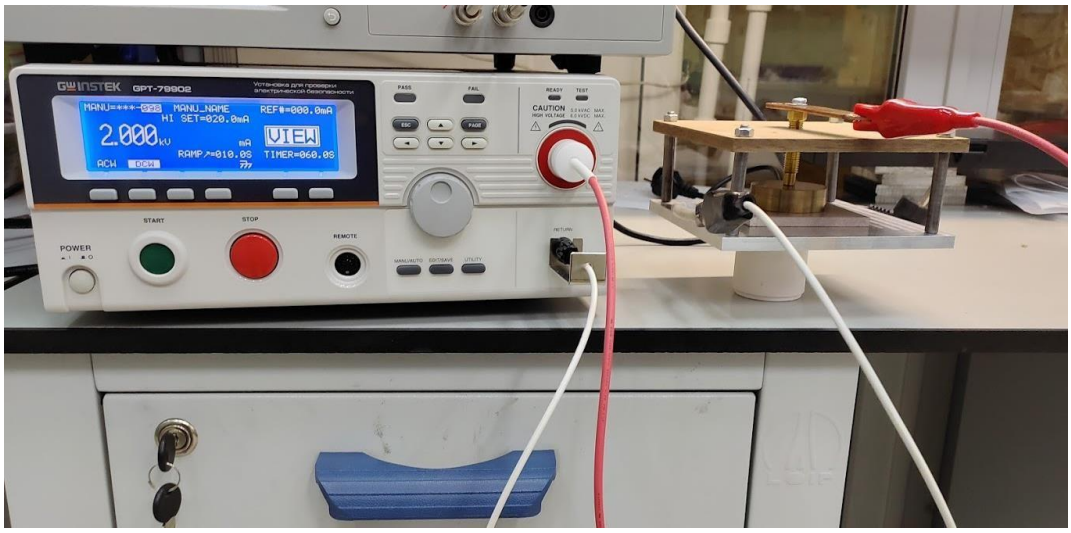

Figure 3.18. Connection of the measuring cell to the GPT- 79902 breakdown unit.

The breakdown test results are shown in Table 3.3.

Table 3.3 The results of testing PEO coatings for breakdown.

Sample №	Parameter	Ti-6Al-4V+PEO
1	breakdown voltage, V_B, V	180
2		225
3		200
4		175
5		202
The average value V_B, V		201

By analyzing the breakdown voltage, it is possible to determine the electrical strength of these films, taking into account the thickness of the dielectric films.

$$E_B = V_B / d \qquad (3.1)$$

where V_B is the breakdown voltage; *d* is the thickness of the dielectric film.

Table 3.4 shows the values of electrical strength calculated for the obtained PEO coatings, as well as the corresponding average values.

Table 3.4 The value of electrical strength.

Sample №	Parameter	Ti-6Al-4V+PEO
1	E_B V/м	$1{,}80 \cdot 10^9$
2		$2{,}25 \cdot 10^9$
3		$2{,}00 \cdot 10^9$
4		$1{,}75 \cdot 10^9$
5		$2{,}03 \cdot 10^9$
The average value E_B V/м		$2{,}01 \cdot 10^9$

Studies have shown that, in fact, the breakdown voltage is significantly affected only by the thickness of the coating and the condition of the sample. If the sample was rinsed in an ultrasonic bath for at least 180 minutes before testing, and dried in a vacuum dryer at 100 ° C for at least 24 hours, the results improve by about 20%, but the results worsen as moisture is saturated from the atmosphere.

In addition, the use of combined application modes does not actually lead to noticeable changes in breakdown voltage, the changes are less than the spread between measurements.

The data obtained indicate that in order to meet the requirements for PEO coatings in terms of increasing breakdown voltage, it is necessary to additionally fill the pores of the coating with a high-temperature polymer by vacuum infusion. Without this additional procedure, the maximum achievable breakdown voltage was 250 V for a PEO coating with a thickness of 20-25 microns.

Conclusions from Chapter 3

1. Using electron beam melting technology, samples were produced from Ti-6Al-4V titanium alloy, which were subsequently coated with plasma electrolytic oxidation (PEO). The dependences of the coating thickness, through porosity, and adhesion strength of the coating to the substrate, depending on the composition of the electrolyte, have been studied.
2. The dependences of the coating thickness, open porosity, and adhesion strength of PEO to the substrate depending on the electric current density have been studied.
3. The dependences of thickness are investigated, and the dependences of the through porosity and adhesion strength of the PEO coating to the substrate on the ratio of the anode and cathode current densities are investigated.
4. The relationships between the thickness, pore permeability, and adhesion strength of the PEO coating to the substrate and the time of the PEO process were studied.
5. Phase modifications of titanium oxide observed in PEO coatings obtained in an aluminate-alkali electrolyte indicate that the coating growth is mainly caused by anodic oxidation of the substrate metal. The presence of various compounds in an aqueous solution of an aluminate-alkaline electrolyte affects the coating structure and leads to an increase in thickness. This is due to the formation of the spinel phase of aluminum titanate (Al_2TiO_5). during the coating process.
6. It has been found that the adhesion of the PEO coating improves with increasing thickness, which provides better load-bearing capacity and leads to a significant, several-fold increase in wear resistance.
7. Studies have shown that in addition to the composition of the electrolyte and the concentration of its components, the characteristics of the oxide layers formed on

the VT6 titanium alloy play an important role. The temperature of the electrolyte, the oxidation time and the electrical parameters of the PEO process have a significant influence.

8. PEO treatment in an aluminate-alkaline medium helps to reduce the surface roughness of VT6 titanium samples made using ATM technology.
9. It is determined that, in fact, only the thickness of the coating and the condition of the sample significantly affect the electrical insulation characteristics of the PEO coating, and in order to increase the breakdown voltage, it is necessary to additionally fill the pores of the coating with a high-temperature polymer by vacuum infusion.

chapter 4

Development of a technological process for plasma-electrolyte oxidation (PEO) of Ti-6-Al-4V titanium alloy parts formed by electron beam melting (EBM).

The development of a technology for plasma-electrolyte processing of materials in order to obtain nanocomposite ceramic coatings on titanium alloy Ti6Al4V includes a range of work, namely: the development of requirements for coated surfaces, a description of basic operations, the development of a scheme of the technological site for applying PEO coatings and requirements for the arrangement of the technological site, as well as the sequence of technological operations for PEO (technological map).

4.1. Development of requirements for coated surfaces

As noted earlier, one of the advantages of PEO technology is the absence of special preliminary surface preparation: etching, lightening (except for the presence of a clad layer on the surface of aluminum alloys).

At the same time, the following requirements apply to the surfaces of parts and samples, depending on their functional tasks during PEO processing:

4.1.1 According to GOST 2789-73, the surface roughness of the base metal, measured in micrometers, should not exceed the specified value.:

- Ra 10 (Rz 40) — for applying protective coatings;
- Ra 2,5 (Rz 10) — for applying protective and decorative coatings;
- Ra 1,25 (Rz 6,3) — for application of hard, wear-resistant and electrical insulating coatings.

The surface roughness of the base metal for functional coatings must comply with the parameters specified in the regulatory, technical and/ or design documentation for the product, which must also be recorded in the Terms of Reference.

These requirements for surface roughness do not apply to non-working areas that are difficult to process and non-working internal surfaces of parts, threaded surfaces,

cut surfaces of stamped parts up to 4 mm thick, grooved surfaces, as well as parts whose base metal roughness is regulated by relevant standards. The need to bring the surface roughness to the specified values should be specified in the design documentation and reflected in the Terms of Reference.

4.1.2 Sharp corners and edges of parts, if not required for technical reasons, should be rounded with a radius of at least 0.3 mm; for parts designed for wear-resistant and insulating coatings, the radius of rounding should be at least 0.5 mm.

4.1.3 The presence of:

• the presence of oxides and growths is not allowed.;

• layering and cracking, including those that are detected after the processes of etse, polishing or sanding;

• Corrosion damage, porosity and cracks.

4.1.4 The surface of the printed parts must be free from gas and shrinkage defects, foreign inclusions, adhesions and cracks. Acceptable defects on such surfaces (type, size, and quantity) are defined in the relevant regulatory, technical, and design documents and must be specified in the Terms of Reference.

4.1.5 After machining, the surface of the parts must be clean, free of visible residues of grease or emulsion, metal shavings, burrs and corrosion products, as well as free of inclusions of particles of foreign material.

4.1.6 After abrasive treatment, such as hydroblasting, tilling and other methods, the surface of the parts must be free of pickling sludge, slag residues, corrosion products and burrs.

4.1.7 The surface of the parts after grinding and polishing must be smooth and uniform, without traces of nicks, dents, burns, scratches, burrs and defects resulting from the use of a straightening tool.

4.1.8 After heat treatment, there should be no nicks, scratches, cracks, bubbles, areas of corrosion, layering or curvature on the surface of the parts.

The use of PEO coatings on parts with soldered or glued joints is prohibited.

On the treated surface, the following features are not considered defects:

• color heterogeneity in areas with different heat and mechanical treatments;

• the presence of separate matte and light areas on the surface of parts that are not subject to decorative requirements;

• the disappearance of the oxide layer or a noticeable decrease in its thickness in hard-to-reach places such as crevices, gaps, blind holes up to 15 mm in diameter and through holes up to 10 mm, as well as in holes and depressions to which it is difficult to apply PEO treatment, unless otherwise specified in the design documentation or specified in the Technical Specification.

• traces of water stains;

• traces of contact with devices, appearing as matte and dark areas;

• if necessary, mechanical polishing of the points of contact with the devices and to achieve the exact dimensions of the part after processing;

• traces of mechanical processing of the base metal before PEO processing and other deviations permitted by the regulatory and technical documentation for the source material.

4.2. The process of performing PEO processing

The PEO process includes three stages: preparatory, basic and final operations.

Preparatory stages.

– The process involves the creation of an electrolyte of a certain composition and concentration in a functional solution (it is recommended to use high-quality water as a solvent).

– Adjusting the composition of the electrolyte that has been used for a certain period of time by adding the necessary components, such as water, to the initial level after chemical analysis of the results.

– Insulation of surfaces of parts that will not be processed by the PEO method, using specialized tools. (for example, the use of fluoroplastic gaskets or parts made of nylon, a fluoroplastic condenser film and vacuum rubbers) or using a high-temperature sealant (for example, silicone compound, heat-resistant tape).

– Installation of current-carrying elements on the parts. Current leads are usually made of aluminum (or titanium) and their alloys in the form of wires or rods (most often with a diameter of 4-6 mm) and fixed using threaded or other methods that provide mechanical strength and To ensure a reliable electrical connection, if necessary, additional stainless steel electrodes can be attached to the components using special tools.

– Extraction of adipose tissue from certain areas involves applying a heated (40-60 °C) soap solution or a cleaning agent (for example, a mixture containing 40 g/l Na3PO4 and 40 g/l Na2CO3 in water).

– Washing the components in cold running water.

– The placement of components equipped with electric current supply wires in a special electrical unit in an electrolyte solution is crucial.

– These elements must be completely immersed in the electrolyte. The particles are evenly distributed in the bath, so they do not come into contact with each other, the walls and floor of the bath, or with additional electrodes.

– It is also important to prevent the formation of air or gas bubbles in the voids of the components both during their positioning and during subsequent oxidation.

The main stages.

– Turn on the protective shield of the electrolyte bath, start the water cooling, activate the exhaust ventilation system, and begin the process of mixing the electrolyte, such as mechanical stirring, compressed air aeration, or circulation through a refrigeration device.

– Activate the process power supply, calibrate the main variables of the PEO process and consistently maintain them throughout the procedure using manual or automatic means.

– Throughout the oxidation process, it is important to observe and analyze currents and voltages at both the anode and the cathode.

– Upon completion of the PEO process, it is recommended to deactivate the power supply to the process source, turn off the ventilation, cooling and electrolyte mixing systems, and then open the protective barrier of the electrolyte bath (wait at least two minutes after disconnecting the capacitor current supply). Finally, proceed to removing the parts from the electrolyte bath.

The final stages.

– Rinsing the components with cold running water for 0.5 to 1.5 hours, depending on the duration of the MDO treatment.

– Removing impurities from the components by purging them with compressed air at a pressure of approximately 0.15 MPa until they dry completely from the outside, which is an additional step.

– Drying of components in a special case at a temperature range from 50 to 70 degrees Celsius for 30-40 minutes (alternatively, natural drying in the open air can also be used).

– Removal of existing fixtures, special tools, additional electrodes, seals and other parts in case of their installation.

– Removal of the technological layer of PEO coatings (if necessary) using abrasive blasting or grinding, followed by purging with compressed air.

– Monitoring of PEO coatings for the absence of visible defects (cracks, chips, burnouts, etc.), and then monitoring the main characteristics of coatings (thickness, microhardness), and, if necessary, changes in the final dimensions of parts, wear resistance, porosity, corrosion resistance, breakdown stress, etc.

– Packaging of finished parts.

The sequence of technological operations for PEO is presented below.

Table 4.1. Sequence of technological operations in PEO.

№	picture	operation	notes
1		Visual inspection	1. Upon detection of surface defects specified in clauses 1-1.10, the part is considered defective.
2	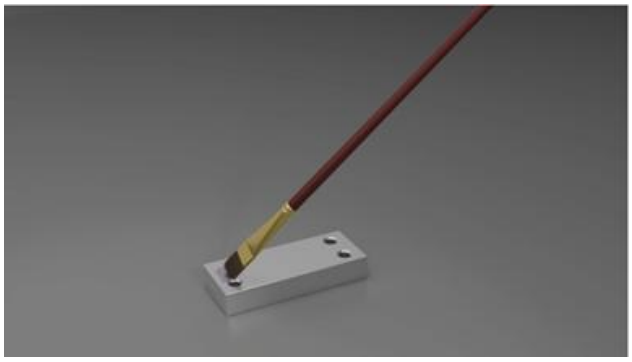	Removal of Greasy impurities	Dirty surfaces of parts should be cleaned of grease using a detergent or soap solution, usually heated to a temperature of 40 to 60 degrees Celsius, and may consist of substances such as 40 grams per liter of Na3PO4 and 40 grams per liter of Na2CO3 dissolved in water.
3	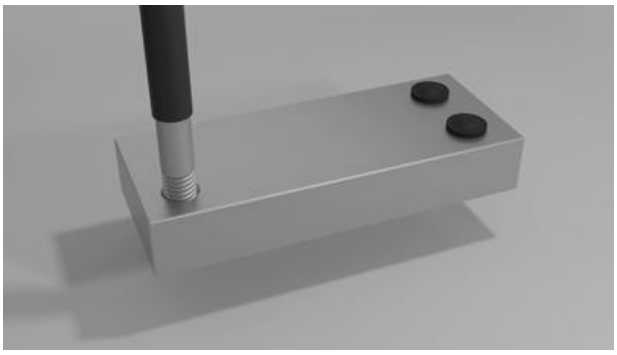	Installation of a current supply and protective equipment	1.Close the non-treatable areas with plugs. 2.Isolate the connection point of the current supply with the part with a fluoroplastic tape

4	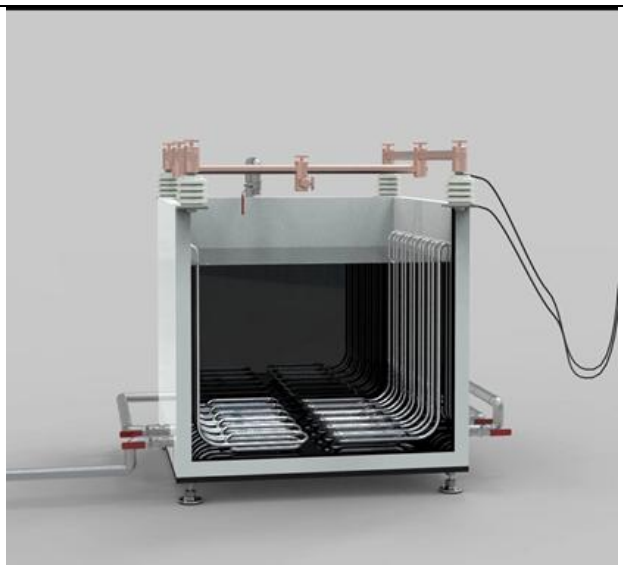	Filling the bath with the prepared electrolyte	The composition of the electrolyte for titanium alloy Ti6Al4V: 1.5 g/l KOH+15 g/l NaAlO2
5	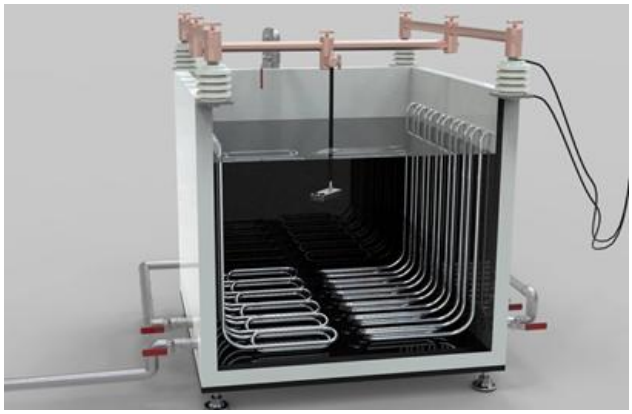	Fixing the part to the current supply on the current rails of the bath.	
6	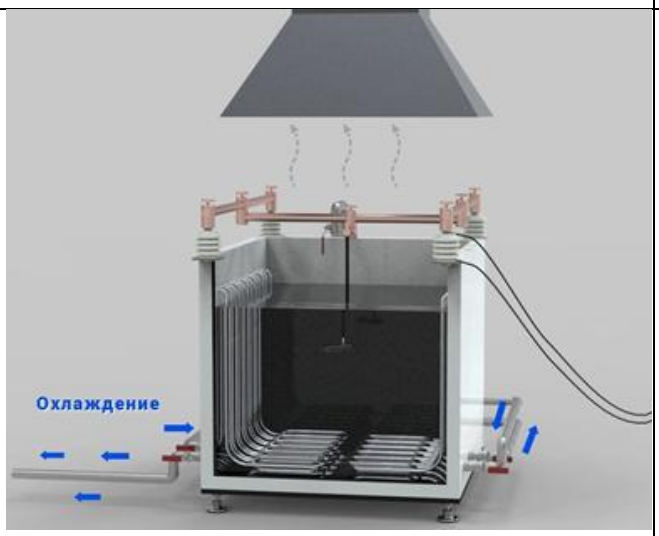	Inclusion of exhaust ventilation, bubbling and cooling system of the bath	All work should be carried out with the barrier closed.

7		Turn on the process current source and oxidize the part according to T3	Set the following modes to TIT: For Ti6Al4V titanium alloy: POE mode, the ratio range of cathode and anode currents Ik / Id = 0.78 – 1.0; total current density 1200 + 1400 A/m2. The processing time is 60-120 minutes.
8	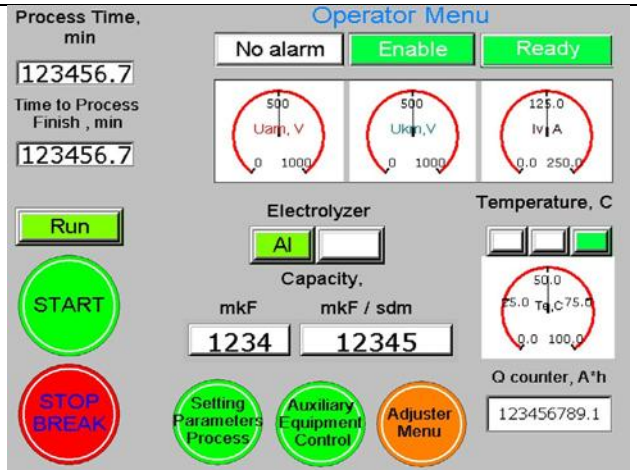	The progress of the technological process is monitored by the parameters on the operator panel	To carry out visual control of the process through a window in the fence or on a video monitor. 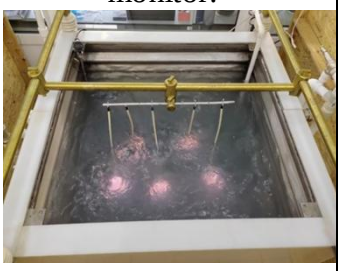
9		Turn off the process power source, turn off the ventilation, bubbling and cooling system of the bath	

10		Open the safety barrier, remove the part from the tub	
11		Rinse the part under running water	The rinsing time in running water is from 15 to 30 minutes
12	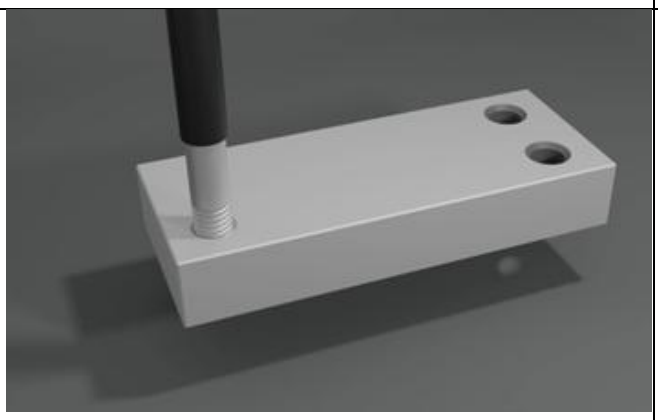	Disconnect the current leads and remove the snap-in	

13	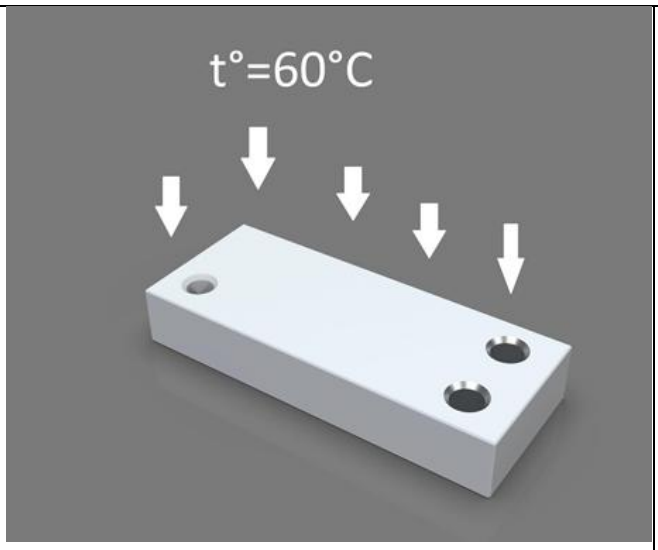	Install the part in the drying chamber (drying time is 60-120 minutes)	Air drying is allowed.
14		Measuring the thickness of the oxide layer with a thickness gauge	If necessary or according to the T3, remove the technological layer before measuring
15	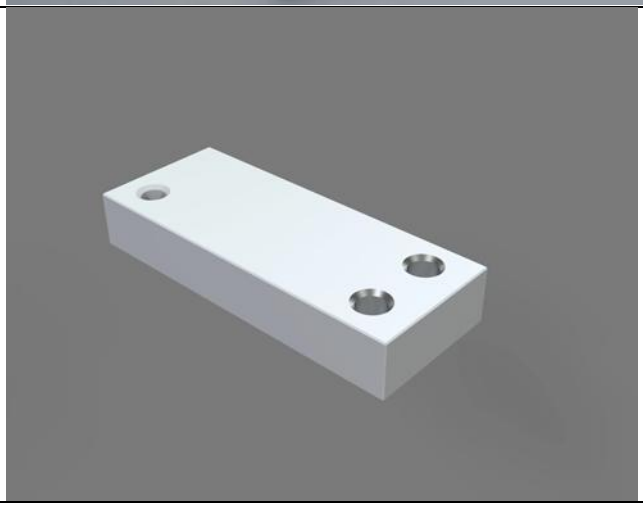	Item to label and pack	

4.4. Requirements for the arrangement of the technological site for the placement of equipment for the implementation of laboratory technology of plasma-electrolyte treatment.

General information

A set of laboratory-industrial electrotechnical and auxiliary equipment (hereinafter referred to as the Equipment) is intended and can be used for the development and implementation of laboratory and pilot-industrial electrochemical technological processes for the formation of multifunctional coatings and modified oxide coatings on the surfaces of products in various industries that provide protection against adhesion and jamming during friction, spraying and coating, corrosion (including fretting corrosion, contact corrosion and other types), erosion, cavitation, oxidative, corrosion-mechanical, hydrogen and other types of wear, as well as to impart decorative, biocidal and bioadaptive, thermal insulation, hygroscopic, dielectric, semiconductor and other functional properties of the work surface.

4.4.1 Typical composition of the plasma –electrolyte treatment site

Table 4.2 shows the design of the main equipment of the plasma–electrolyte treatment site.

It is suggested to specify other manufactured equipment, assembly units and products, as well as additional purchased components and materials, if necessary.

Table 4.2 – Design of the main equipment of the plasma – electrolyte treatment site.

№	Designation	Installed electric power, kVA
1	Technological current source	100
1.1	The basic hardware and software system for monitoring the technological parameters of the process (MDO-Monitor)	3
2	Electrolyte bath	-
2.1	Attachment device for electrical lines of parts	-
2.2	Electrolyte mixing device	-
2.3	Electromechanical electrolyte Discharge device	-
2.4	On-board electromechanical process gas removal device	-
3	Mixing bath	1
3.1	An automated electrolyte preparation and replacement device with a correction dosing system	-
4	Electrolyte cooling system (chiller)	30
5	Security fence	-
6	The ramp	-
7	Washing bath	-
8	Drying cabinet SHS-80-0	2
9	Distiller DE-25	20
10	A set of mounting, installation, electrical switching products and materials	-
11	A set of basic laboratory furniture and chemical utensils	-
12	A set of spare equipment and appliances	-

4.4.2 Technical description and characteristics of a typical site.

A sufficient recommended land area of at least 50 m2.

This square contains:

1. The preparation area for parts and accessories is at least 10 m2;
2. Processing area – at least 12 m2;
3. Electrolyte preparation area – at least 14 m2;
4. Control and storage area for blanks and finished products – at least 14 m2;

General requirements for placement:

1. Compressed air class 3 GOST 17433-80 (drying and cleaning of parts, bubbling), 6-8 bar, 1200 l/min;
2. 3-phase power supply network and dead-grounded neutral, 380V, 50Hz, 170kVA; if necessary, equalizing phase misalignment transformer.
3. Grounding on the site, no more than 4 ohms;
4. Technical water with a connection of at least 1 inch (in the case of flow cooling) and a flow rate of at least 100 l/min
5. Technical water with a connection of at least ½ inch (for washing parts and preparing the electrolyte) and a flow rate of at least 20 l/min.
6. Exhaust ventilation above the treatment area, at least 0.8 m3/min;
7. Exhaust ventilation in the electrolyte preparation area, at least 0.3 m3/min;
8. Supply ventilation of at least 1.5 m3/min;
9. The base of the location of the electrolyte bath must withstand

a constant calculated concentrated load from the electrolyte bath in the zone of maximum bending moment (in the case of overlaps), not less than 2.2 t / m2; the standard distributed load on the overlap is 1.6 t/ m2 or 0.8 t concentrated load from five supports.

10. The height of the room is clean, at least - 3m;

11. The floor covering is resistant to prolonged exposure to weak solutions of acids and alkalis – ceramic tiles, industrial linoleum, industrial laminate.
12. Availability of sewerage. There are no special requirements for the sewer pipeline system. All existing materials are acceptable (polypropylene, polyethylene, polyvinyl chloride, steel).
13. There are no special requirements regarding the disposal of the projected electrolyte solutions. No sewage treatment plants or additional equipment are required for disposal. The solutions of the designed electrolytes do not contain alkalis and acids, as well as other chemically and biologically active substances that consume oxygen, heavy metals and toxins in concentrations exceeding existing standards.

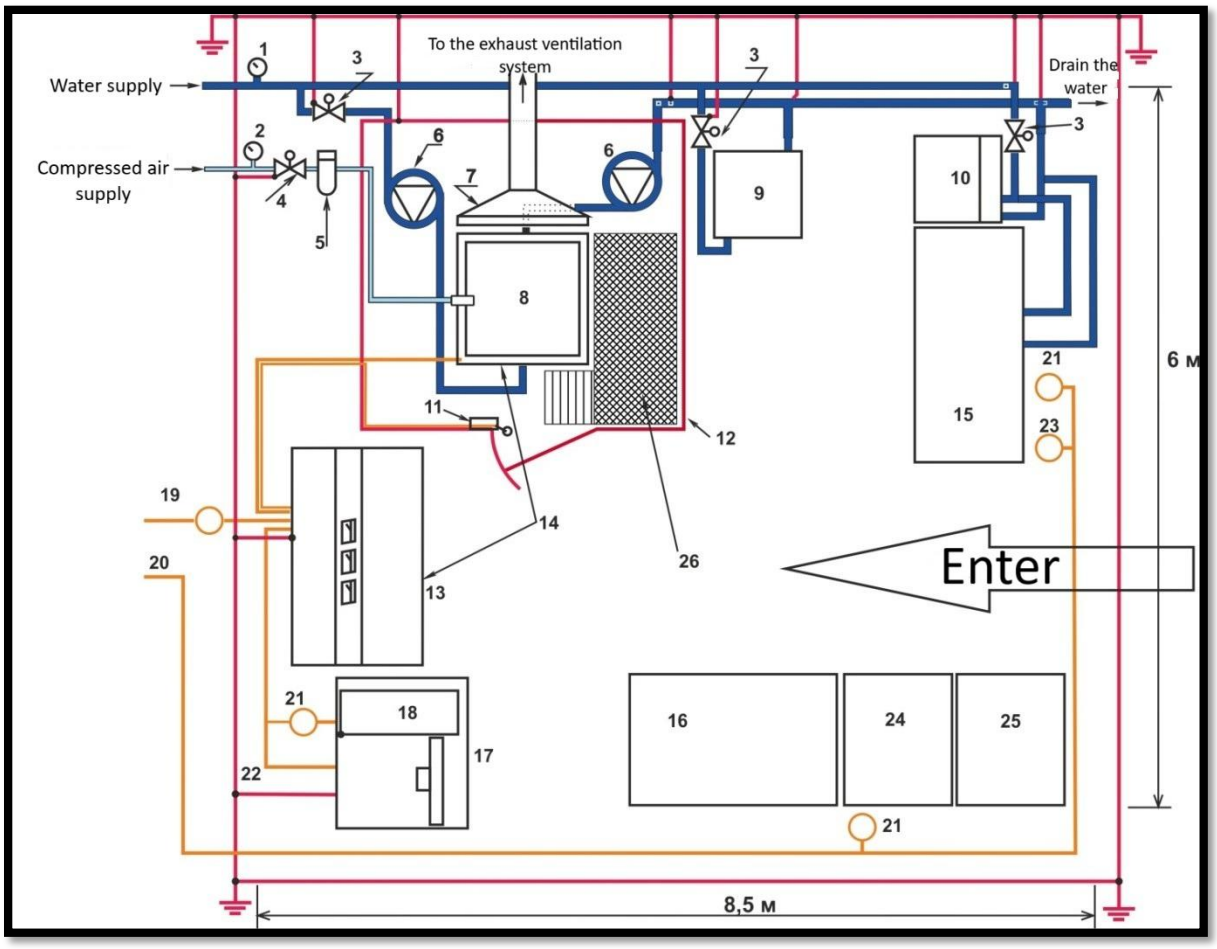

Figure 4.1. Recommended layout of the plasma-electrolyte treatment site

1. Water pressure gauge;
2. Air pressure gauge;
3. Water intake valve;
4. Air fittings;
5. Moisture and oil separator;
6. The hose rack;
7. On-board suction;
8. Main bath;
9. Washing bath;
10. Water sink + faucet;
11. Contact sensor;
12. Metal safety fence;
13. Power supply and control;
14. Package contents = Main bath + Power supply and control unit;
15. Electrolyte cooling system (chiller);
16. Workplace for monitoring output parameters;
17. Monitoring system;
18. Personal computer;
19. Electrical input ~ 220/380 V, phase-to-phase current 300 A;
20. Electrical input ~ 220/380 V, 15 kVA;
21. Two electrical outlets ~ 220 V, 1 kVA;
22. Protective earthing circuit;
23. Two electrical outlets ~ 220/380 V, 5 kVA;
24. Fume hood;
25. Reagent storage cabinet;
26. The ramp.

The main elements of the site are a power and control source (13) and an electrolyte bath (8).

The power source is designed to monitor and control the technological parameters of the plasma-electrolyte treatment process.

The electrolyte bath is placed inside a metal grounded enclosure (12). Access control inside the fence is carried out using a contact sensor (11). Observation windows are provided in the enclosure for visual control of the process. The floor covering inside the enclosure must be non-conductive. A ramp with a height of at least 80 mm is provided around the electrolyte bath.

After the end of the process, the parts are moved to the washing bath (9), and then to the workplace for monitoring the output parameters (16).

With the help of the monitoring system (17), the main technological parameters of the process are monitored, visualized and archived.

In general, when preparing the sites, the possibilities of providing the following infrastructure are being considered:

- preparation of the electrolyte;
- neutralizing the electrolyte before disposal;
- preparation (washing baths, etc.) and loading (manipulator) of products;
- compressed air treatment (6-8atm, 1200 l/min, class 3 GOST 17433-80);
- preparation of deionized water (TDS~0mg/L, G>4M*cm);
- preparation of demineralized water (distilled TDS<7mg/L, G>0.1 MOm*cm);
- purification of the aspiration medium;
- cold treatment;
- energy supply;
- strapping of the site (other materials and accessories).

To visualize the technological site, a standard 3D model was developed, shown in Figures 4.2.-4.3.

Figure 4.2 is a 3D model of a typical equipment placement site for implementing PEO technology. General view,

Figure 4.3. – 3D model of a typical site for the placement of equipment for the implementation of PEO technology. An additional view.

4.5. Complex technology for creating products using the AT method from Ti6Al4V alloy with PEO coating.

Based on the research carried out in this work, a comprehensive technology for creating products using the AT method from Ti6Al4V alloy with PEO coating is shown in Fig. 4.4 and combines both the AT and PEO processes.

Fig.4.4 Sequence of technological operations of the developed technology.

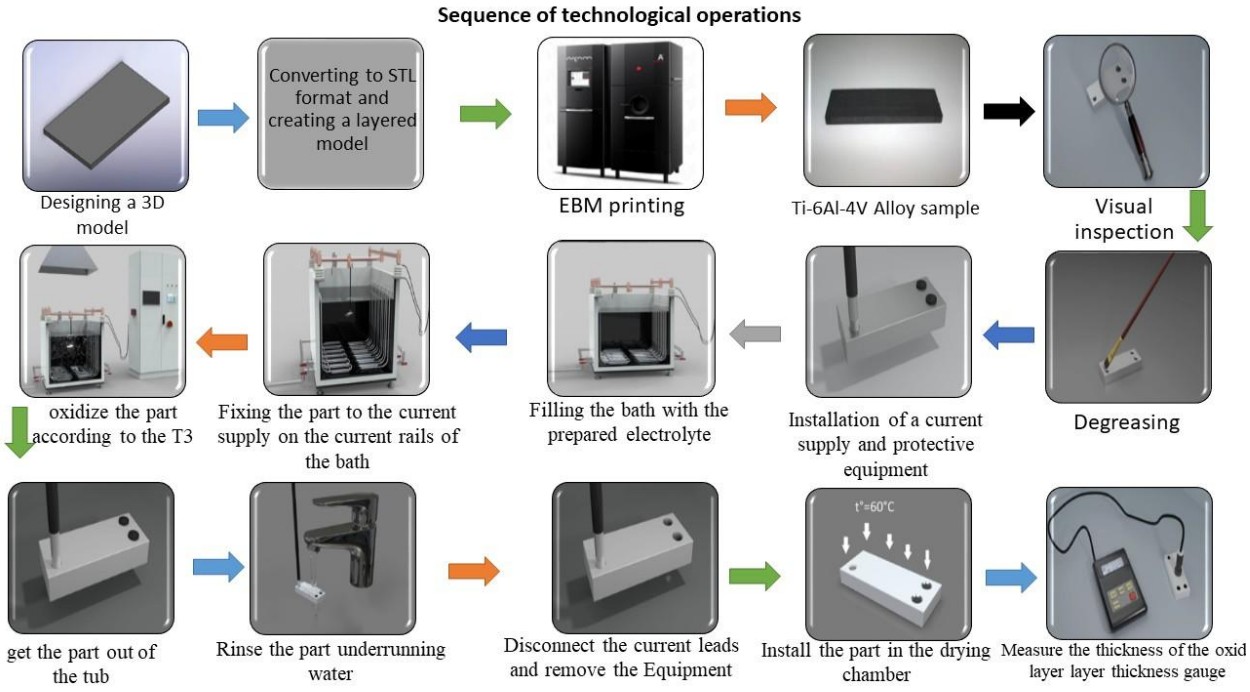

Conclusions according to Chapter 4.

1. A method of plasma-electrolyte oxidation (FEO) on the components of titanium alloy Ti-6-Al-4V obtained by electron beam melting (EBM) has been created.

2. The requirements for the surfaces to be coated are formulated.

3. It is established that the technological process of PEO should contain three groups of operations: preparatory, basic and final.

4. The sequence of technological operations in PEO is determined.

5. The requirements for the arrangement of the technological site for the placement of equipment and the implementation of laboratory technology of plasma-electrolyte treatment are formulated.

6. The draft of the main equipment of the plasma – electrolyte treatment site is presented and the requirements for its placement are formulated, as well as a 3D model of a typical site.

7. The order of operations (technological map) for the complex technology of creating products using the AT method from Ti6Al4V alloy with PEO coating is given.

Conclusion

As a result of the theoretical and practical research, an important scientific and technical problem was solved, which is significant for both the machine engineering and medical industries. The task was to develop processes for manufacturing various products from titanium alloy [VT6] using additive technologies, such as electron beam melting (EBM).

A review of the literature showed that the most preferred method for producing titanium components using additive technologies is the electron beam melting (EBM) method. The EBM device demonstrates considerable effectiveness in production. The thermal operation of the equipment reduces internal stresses that arise during the manufacturing of products, thus eliminating the need for thermal treatment to improve mechanical properties and remove residual stresses, which is required in the SLM process. However, maintaining the necessary vacuum level is associated with additional costs.

Increasing the durability and reliability of titanium alloy products using technological processes is a crucial task in the field of machine engineering. Plasma electrolytic oxidation (PEO) is a promising approach to protect titanium alloys from wear in friction units and harsh chemical environments. Among the various methods studied for applying protective and wear-resistant coatings, PEO stands out.

Plasma electrolytic oxidation (PEO) is a process in which the outer layer of components undergoes transformation into oxide ceramic due to the use of electroplasma-chemical conditions. This method allows creating universal coatings on the surface of titanium components with such notable characteristics as increased wear resistance, corrosion resistance, excellent electrical insulation properties, and favorable adhesion properties.

Plasma electrolytic oxidation using anodic-cathodic PEO allows creating coatings with greater thickness and lower porosity. This method is currently the main one in surface treatment.

An analytical review of the literature showed a relatively low level of development in the selected area of work and confirmed the relevance of the research. Based on the analysis of titanium alloys used in the aviation industry, the widely used alloy VT6 (Ti6Al4V) was chosen for the research.

Specialized equipment was selected that allows conducting the necessary experimental work. This equipment can be used to implement anodic and plasma-electrolytic oxidation processes, as well as their combinations, in industrial applications.

The selected tools and equipment can be successfully applied in the industry for integrating anodic oxidation processes followed by plasma electrolytic oxidation treatment of titanium alloys. This aligns with one of the objectives of the work, which is to implement technologies into production.

Samples made of titanium alloy VT6 (Ti-6Al-4V) were fabricated using the electron beam melting method, after which they were coated by plasma electrolytic oxidation (PEO).

The dependencies of the coating thickness, through porosity, and the adhesion strength of the PEO coating to the substrate were studied with respect to the concentration of electrolyte components.

The dependencies of the coating thickness, through porosity, and adhesion strength of the PEO coating to the substrate on the current density, the ratio of cathodic and anodic currents, and the duration of the PEO process were studied.

PEO coatings obtained in an aluminate-alkaline electrolyte show changes in the titanium oxide phase, indicating that the anodic oxidation of the base metal primarily influences the coating development. Additionally, it was observed that substances present in the aqueous solution of the aluminate-alkaline electrolyte play a role in the coating composition and increase its thickness, facilitating the formation of the spinel phase of aluminum titanate (Al_2TiO_5).

It was found that the adhesion of the PEO coating improves with an increase in thickness, which ensures better load-bearing capacity and results in a significant, several-fold, increase in wear resistance.

The research demonstrated that, in addition to the electrolyte composition and its concentration, the characteristics of the oxide layers formed on the titanium alloy Ti6Al4V (VT6) are significantly influenced by the electrolyte temperature, the oxidation process duration, and the electrical parameters of the plasma electrolytic oxidation method.

PEO treatment in an aluminate-alkaline electrolyte leads to a reduction in the surface roughness of titanium alloy VT6 (Ti6Al4V) samples produced by additive technology.

It was determined that the electrical insulation characteristics of the PEO coating are significantly influenced only by the coating thickness and the condition of the sample, and to increase the breakdown voltage, it is necessary to additionally fill the pores of the coating with a high-temperature polymer by vacuum infusion.

A method for plasma electrolytic oxidation (PEO) was developed for the treatment of titanium alloy Ti-6Al-4V components produced by the electron beam melting (EBM) method.

Requirements for the coated surfaces were formulated.

It was established that the PEO technological process should consist of three groups of operations: preparatory, main, and final.

The sequence of technological operations in PEO was determined.

Requirements for the arrangement of the technological area for the placement of equipment and the implementation of laboratory plasma-electrolytic processing technology were formulated.

A project for the main composition of equipment for the plasma-electrolytic processing area was provided, and requirements for its placement, as well as a 3D model of a typical area, were formulated.

A set of operations (technological map) for the integrated technology of manufacturing products using additive technology from Ti6Al4V alloy with PEO coating was presented.

Publications.

1) Dhiaa H.Hilfi , Suminov Igor «Additive Manufacturing Using Material Ti-6AL-4V Titanium Alloy: Review», NEUROQUANTOLOGY | March 2023 | Volume 21 | Issue 5| Page 1530-1556| doi: 10.48047/nq.2023.21.5.NQ222145

2) Dhiaa H.Hilfi, Suminov Igor «Microsturctural Characteristics and Mechanical Properties of Ti 6Al 4V Alloy in Additive Manufacturing», International Journal of Membrane Science and Technology, 2023, Vol. 10, No. 2, pp 3665-3681

3) Суминов И.В., Хилфи Диаа Х.Ч. «Аддитивные технологии в современной промышленности: применение и перспективы на примере титановых сплавов», обзор, Кузнечно-штамповочное производство, обработка материалов давлением, №3, 2024 год, стр.36-44.

4) Суминов И.В., Хилфи Диаа Х.Ч. «Экспериментальное исследование влияния технологических параметров процесса электрохимическое оксидирование на свойства оксидного слоя и его эксплуатационные характеристики», испытания, измерения и контроль, Кузнечно-штамповочное производство, обработка материалов давлением, №4, 2024 год, стр.51-57.

5) Суминов И.В., Хилфи Диаа Х.Ч. «Технологии плазменно-электролитной обработки поверхностей изделий машиностроения из титанового сплава ВТ6, сформированных аддитивными технологиями», испытания, измерения и контроль, Кузнечно-штамповочное производство, обработка материалов давлением, №4, 2024 год, стр.58-62.

Reference list:

1. Микродуговое оксидирование (теория, технология, оборудование) / И.В. Суминов, А.В. Эпельфельд, В.Б. Людин и др. — М.: ЭКОМЕТ, 2005. — 368 с. 3.
2. Малышев, В.Н. Упрочнение поверхностей трения методом микродугового оксидирования: Автореф. дис…докт. техн. наук / В.Н. Малышев. — Москва, 1999. — 53 с.
3. Attaran, M. The rise of 3-D printing: The advantages of additive manufacturing over traditional manufacturing [Text] / M. Attaran // Business Horizons. – 2017. – Vol. 60. – Iss. 5. – P. 677-688.
4. Василюк, В.П. Использование аддитивных технологий при восстановлении дефектов лицевого скелета [Текст] / В.П. Василюк, Г.И. Штраубе, В.А. Четвертных / Пермский медицинский журнал. – 2013. – Т. 30. – № 3. – С. 60-65.
5. Зленко, М.А. Аддитивные технологии в машиностроении [Текст]: пособие для инженеров / М.А. Зленко, М.В. Нагайцев, В.М. Довбыш. – М.: ГНЦРФ ФГУП «НАМИ», 2015. – 220 с.
6. Чемодуров, А.Н. Применение аддитивных технологий в производстве изделий машиностроения [Текст] / А.Н. Чемодуров // Известия ТугГУ.Технические науки. – 2016. – № 8. – С. 210-217.
7. Additive Manufacturing [Text] / compiled by A. Bandyopadhyay, S. Bose. – N.Y.: CRC Press, 2015. – 389 p.
8. Noorani, R. 3D Printing: Technology, Applications, and Selection [Text] / R. Noorani. – N.Y.: CRC Press, 2017. – 271 p.
9. Quinlan, H.E. Industrial and Consumer Uses of Additive Manufacturing: A Discussion of Capabilities, Trajectories, and Challenges [Text] / H.E. Quinlan, T. Hasan, et.al. // Journal of Industrial Ecology. – 2017. – Vol. 21. – P. 15-20.
10. Кузнецов, П.А. Аддитивные технологии на базе металлических порошковых материалов для российской промышленности [Текст] / П.А. Кузнецов, О.В. Васильева и др. // Новости материаловедения. Наука и техника.– 2015. – № 2 (14). – С. 4-10.
11. Dawes, J. Introduction to the Additive Manufacturing Powder Metallurgy Supply Chain.

Exploring the production and supply of metal powders for AM processes [Text] / J. Dawes, R. Bowerman, R. Trepleton. // Johnson Matthey Technol. Rev. – 2015. – Vol. 59. Iss. 3. – P. 243–256.

12. Wohlers Report 2018. 3D Printing and Additive Manufacturing State of the Industry. Annual Worldwide Progress Report [Text] / compiled by I. Campbell, O. Diegel, J. Kowen and T. Wohlers. – Fort Collins: Wohlers Associates, Inc, 2017. – 344 p.
13. Attaran, M. The rise of 3-D printing: The advantages of additive manufacturing over traditional manufacturing [Text] / M. Attaran // Business Horizons. – 2017. – Vol. 60. – Iss. 5. – P. 677-688.
14. Смуров, И.Ю. О внедрении аддитивных технологий и производства в отечественную промышленность [Текст] / И.Ю. Смуров, С.Г. Конов, Д.В. Котобан // Новости материаловедения. Наука и техника. – 2015. – № 2 (14). –С. 11-22.
15. Kruth, J.P. Binding Mechanisms in Selective Laser Sintering and Selective Laser Melting [Text] / J.P. Kruth, P. Mercelis, L. Froyen, M. Rombouts // Rapid Prototyping Journal. – 2005. – Vol. 11. – Iss.1. – P. 26-36.
16. Milewski, J.O. Additive Manufacturing of Metals. From Fundamental Technology to Rocket Nozzles, Medical Implants, and Custom Jewelry. Springer Series in Materials Science 258 [Text] / J.O. Milewski. – Cham: Springer International Publishing AG, 2017. – 343 p.
17. Meier, H. Experimental studies on selective laser melting of metallic parts [Text] / H. Meier, C. Haberland // Materialwissenschaft und Werkstofftechnik. – 2008. – Vol. 39. – No. 9. – P. 665-670.
18. Волосова, М.А. Пути оптимизации процесса селективного лазерного плавления при помощи выбора стратегии обработки лазерным лучом [Текст] / М.А. Волосова, А.А. Окунькова // Известия Самарского научного центра Российской академии наук. – 2012. – Т. 14. – № 4 (2). – С. 587-591.
19. Килина,П.Н. Исследование режимов селективного лазерногоплавления металлических порошков [Текст] / П.Н. Килина, Е.А. Морозов и др. // Современные проблемы науки и образования. – 2014. – № 6. – С.133.
20. Krol, M. Surface quality in selective laser melting of metal powders [Text] / M. Krol, L.A.

Dobrzanski, L. Reimann, I. Czaja // Archives of Materials Science andEngineering. – 2013. – Vol. 60. – Iss.2. – P. 87-92.
21. Смуров, И.Ю. Аддитивное производство с помощью лазера [Текст] / И.Ю. Смуров, И.А. Мовчан и др. // Вестник МГТУ “Станкин”. – 2011. – № 4 (16). – С. 144-146.
22. Hebert, R.J. Viewpoint: metallurgical aspects of powder bed metal additive manufacturing [Text] / R.J. Hebert // J Mater Sci. – 2016. – Vol. 51 – P. 1165–1175.
23. Байтимеров, Р.М. Определение оптимальных параметров селективного лазерного сплавления титанового сплава TiAl6V4 углекислотным лазером [Текст] / Р.М. Байтимеров, П.А. Лыков и др. // Вестник ЮУрГУ. Серия «Машиностроение». – 2017. – Т. 17. – № 3. – С. 36-40.
24. Vandenbroucke, B. Selective laser melting of biocompatible metals forrapid manufacturing of medical parts [Text] / B. Vandenbroucke, J.P. Kruth // Rapid Prototyping Journal. – 2007. – № 4 (13). – P. 196-203.
25. Байтимеров, Р.М. Определение оптимальных параметров селективноголазерного сплавления титанового сплава TiAl6V4 углекислотным лазером [Текст] / Р.М. Байтимеров, П.А. Лыков и др. // Вестник ЮУрГУ. Серия «Машиностроение». – 2017. – Т. 17. – № 3. – С. 36-40.
26. Смуров И.Ю. Аддитивное производство с помощью лазера. Проведение экспериментальных работ [Текст] / И.Ю. Смуров, И.А. Ядройцев и др. // Вестник МГТУ “Станкин”. – 2012. – № 1 (18). – С. 36-38.
27. Смуров, И.Ю Экспериментальное аддитивное прямое производство с помощью лазера [Текст] / И.Ю. Смуров, И.А. Мовчан, И.А. Ядройцев и др. // Вестник МГТУ “Станкин”. – 2012. – № 2 (20). – С. 48-50.
28. Литунов, С.Н. Обзор и анализ аддитивных технологий. Часть 1 [Текст] / С.Н. Литунов, В.С. Слободенюк, Д.В. Мельников // Омский научный вестник. – 2016. – № 1 (145). – С. 12-17.
29. Murr, L.E. Metal fabrication by additive manufacturing using laser and electron beam melting technologies [Text] / L.E. Murr, S.M. Gaytan, D.A. Ramirez, et.al. // J. Mater. Sci. Technol. – 2012. – Vol. 1 (28). – P. 3-16.

30. Kirchner, A. Process window for electron beam melting of Ti-6Al-4V [Text] / A. Kirchner, B. Klöden, J. Luft, et.al. // Powder Metallurgy. – 2015. – Vol. 4 (58). – P. 246-249.

31. Lancaster, R. Structural Integrity of an Electron Beam Melted Titanium Alloy [Text] / R. Lancaster, G. Davies, et.al. // Materials. – 2016. – Vol. 9. – P. 470.

32. Швец, А.А. Сравнительный анализ устройств для объемной печати[Текст] / А.А. Швец, А.Р. Авдеев, А.В. Дроботов // Известия Волгоградского государственного технического университета. – 2015. – № 1 (156). – С. 76-79.

33. Упрочнение поверхности деталей из алюминиевых, титановых и циркониевых сплавов микродуговым оксидированием/ А.Е. Розен, А.Ю. Артемьев, А.В. Прыщак, А.И. Лопухова// Тез. докл. I собр. металловедов России (Пенза, 22-24 сент. 1993 г.). Пенза: 1993. Ч. II. С. 45-46.

34. Многофункциональные защитные покрытия на металлах и сплавах/ С.В. Гнеденков, П.С. Гордиенко, С.JI. Синебрюхов и др.// Тез. докл. междунар. науч.-техн. симпозиума «Наукоемкие технологии и проблемы их внедрения на машиностроительных и металлургических предприятиях Дальнего Востока». (Комсомольск-на-Амуре, 19-24 сент. 1994 г.). Комсомольск-на-Амуре: 1994. С. 53.

35. Формирование износостойких покрытий на титане/ П.С. Гордиенко, С.В. Гнеденков, О.А. Хрисанфова и др.// Электронная обработка материалов. 1990. №5. С. 32-35.

36. Гордиенко П.С. Формирование покрытий на ряде металлов и сплавов в электролитах при микроплазменных процессах: Дис. ... д-ра техн. наук. 1991. 683 с.

37. Малоцикловая усталость титановых сплавов после МДО/ Е.Д. Шехов- цев, П.С. Гордиенко, С.В. Гнеденков, Н.И. Лошакова// Защитные покрытия. Способы получения и свойства. Владивосток. 1989.

38. Образование рутила и анатаза при микродуговом оксидировании титана в водных электролитах/ П.С. Гордиенко, О.А. Хрисанфова, Т.П. Яровая и др.// Электронная обработка материалов. 1990. №4. С. 19-22.

39. Кузовлева К.Т., Гордиенко П.С. Потенциодинамическое исследование анодного оксидирования титана при высоких потенциалах// Электронная обработка материалов. 1989. №5. С. 44-47.

40.Баковец В.В. Оксидные покрытия, полученные микродуговой обработкой титанового сплава в кислых электролитах// Неорганические материалы. 1987. Т. 23. №7. С. 1226-1228.

41.Электролит для микродугового оксидирования титана и его сплавов: А.с. 1788793 РФ: МКИ С25 Д11/26.

42. Электролит для формирования покрытий на вентильных металлах: Пат. №2046156 РФ: МКИ С25 Д11/04.

43.Новое явление в электролизе/ А.В. Николаев, Г.А. Марков, Б.И. Пе- щевицкий.- Изв. СО АН СССР. Сер. хим. науки, 1977. Вып. 5. № 12. С. 32-34.

44.Технология получения покрытий микродуговым оксидированием/ Э.С. Атрощенко, И.А. Казанцев, А.Е. Розен// Новые промышленные технологии. 1996. № 1.С. 28-33.

45.Получение покрытий анодно-искровым электролизом/ В.И. Черненко, JI.A. Снежко, И.И. Папанова - Л.: Химия. Ленингр. отд-ние, 1991. 126 с.

46.Свойства оксидных пленок, сформированных переменным напряжением на титановом сплаве ВТ-1/ Е.К. Черненко, Л.А. Янов, В.И. Черненко// Электрохимия. 1971. Т.VII. Вып. 9. С. 1374-1377.

47.Микродуговые и дуговые методы нанесения покрытий/ О.П. Терлеева, Г.А. Марков, Е.К. Шулейко// Тр. ин-та. Московский ин-т нефтехимической и газовой промышленности. 1985. Вып. 185. С. 55-64.

48.Способ анодирования металлов: А.с. 534525 СССР: МКИ С25 Д11/26.

49.Барыкин Н.В. Разработка технологии восстановления и упрочнения деталей из алюминиевых сплавов микродуговым оксидированием: Дис. ... канд. техн. наук. 1994. 173 с.

50.Способ микродугового оксидирования металлических изделий и устройство для его осуществления: Пат. №2070947 РФ: МКИ С25 Д11/04.

51.Малышев В.Н. Особенности формирования покрытий методом анодно-катодного микродугового оксидирования// Защита металлов. 1996. Том 32. №6. С. 662-667.

52.Особенности строения и свойства покрытий, наносимых методом микродугового оксидирования/ В.Н. Малышев, Г.А. Марков, В.А. Федоров и др.// Химическое и нефтяное машиностроение. 1984. №1. С. 26-27.

53.Микродуговое оксидирование/ Г.А. Марков и др.// Наука и человечество: Международный ежегодник. М.: Знание, 1981.

54.Электролит для микродугового оксидирования титана и его сплавов: А.с. 1788793 РФ: МКИ С25 Д11/26.

55.Электролит для анодирования титана и его сплавов: Пат. №1156409 РФ: МКИС25 Д11/26.

56. Мусин Р.А., Конюшков Г.В. Соединение металлов с керамическими материалами. М.: Машиностроение, 1991. 224 с.

57. ГОСТ 19807-91 Титан и сплавы титановые деформируемые. Марки.

58. ОСТ 1.92077-78 Сплавы титановые. Марки.

59. https://www.splav-kharkov.com/mat_start.php?name_id=129860.Плазменно электролитическое модифицирование поверхности металлов и сплавов/ И.В. Суминов, П.Н. Белкин, А.В. Эпельфельд и др.; под общей ред. И.В.Суминова. В 2-х томах. Т.2. М.: Техносфера, 2011. - 512с.

61.Толщиномер ВТ-201, https://www.ntcexpert.ru/uc/tolshhinamery-pokrytij/639-tolshhinomer-pokrytij-vt-201, дата посещения 13.05.2022

62.Микротвердомеры, твердомеры Виккерса, http://www.s-i.ru/mikrotverdomery-tverdomery-vikkersa/, дата посещения 13.02.2022

63. Эпельфельд А.В., Людин В.Б., Суминов И.В., Крит Б.Л., Борисов А.М., Григорьев С.Н. Микродуговое оксидирование / А. В. Эпельфельд, В. Б. Людин, И. В. Суминов [и др.].

– Москва: Московский государственный технологический университет "СТАНКИН", 2020. – 94 с.

64. Планирование эксперимента при поиске оптимальных условий/ Ю.П. Адлер и др. М.: изд-во 'Паука" , 1971. 287 с.
65. Финки Д. Введение в теорию планирования экспериментов. Перев. с англ. Главная редакция физико-математической литературы изд-ва "Наука", 1970.
67. Жуков С.В. Исследование процессов и разработка технологии формирования многофункциональных покрытий методом микродугового оксидирования на титановых сплавах в приборостроении: Дис. ... канд. техн. наук. Москва, 2009. 228 с.
68. A. Molinari, G. Straffelini, B. Tesi and T. Bacci: Wear, 1997, 208, (1-2), 105–112.
69. L. Ceschini, E. Lanzoni, C. Martini, D. Prandstraller and G. Sambogna: Wear, 2008, 264, (1-2), 86–95.
70. X.-J. Li, G.-A. Cheng, W.-B. Xue, R.-T. Zheng and Y.-J. Cheng: Mater. Chem. Phys., 2008, 107, (1), 148–152.
71. X.-Z. Lin, M.-H. Zhu, J.-F. Zheng, J. Luo and J.-L. Mo: Trans. Nonferr. Met. Soc. China, 2010, 20, (4), 537–546.
72. C. Martini, L. Ceschini, F. Tarterini, J. M. Paillard and J. A. Curran: Wear, 2010, 269, (11-12), 747–756.
73. Y. M. Wang, B. L. Jiang, L. X. Guo and T. Q. Lei: Appl. Surf. Sci., 2006, 252, (8), 2989–2998.
74. Y. M. Wang, B. L. Jiang, T. Q. Lei and L. X. Guo: Surf. Coat. Technol., 2006, 201, (1-2), 82–89.
75. J. M. Wheeler, C. A. Collier, J. M. Paillard and J. A. Curran: Surf. Coat. Technol., 2010, 204, (21-22), 3399–3409.
76. A. L. Yerokhin, A. Leyland and A. Matthews: Appl. Surf. Sci., 2002, 200, (1-4), 172–184.
77. A. L. Yerokhin, X. Nie, A. Leyland and A. Matthews: Surf. Coat. Technol., 2000, 130, (2-3), 195–206.
78. Y. K. Qin, D. S. Xiong, J. L. Li and R. Tyagi: Surf. Eng., to be published.
79. S. L. Sinebryukhov, A. S. Gnedenkov, O. A. Khrisanfova and S. V. Gnedenkov: Surf. Eng., 2009, 25, (8), 565–5

80. Цвиккер У. Титан и его сплавы. Берлин - Нью-Йорк, 1974. Пер. с нем. М.: Металлургия, 1979. 512 с.

81. Еременко В.Н. Титан и его сплавы.- Киев: Изд-во АН УССР, 1960. 500 с.

82. Тимошенко А.В . Защитные неметаллические и неорганические покрытия и материалы. Курс лекций, институт стали и сплавов, № 484, 1990 г.

83. Прикладная техника обработки поверхности металлических материалов: Справ, изд. Г. Симон, М. Тома. Пер. с нем./ Под ред. А.Ф. Пименова. - Челябинск: Металлургия, Челябинское отделение, 1991. 368 с.

84. Кудинов В.В. Нанесение покрытий напылением. Л., 1970. 35 с.

85. Simon H. und Suchentrunk R. Werkstoffe und Schichten für hohe Beanspruchungen in der Luft- und Raumfahrt// Galvanotechnik. 1996. № 2. S.396-411 .

86. РД 5.95066-90. Термическое оксидирование (антифрикционное и защитное) деталей из сплавов типа ПТ-3В.

87. Упрочнение поверхности деталей из алюминиевых, титановых и циркониевых сплавов микродуговым оксидированием/ А.Е. Розен, А.Ю. Артемьев,

88.А.В. Прыщак, А.И. Лопухова// Тез. докл. I собр. металловедов России (Пенза, 22-24 сент. 1993 г.). Пенза: 1993. Ч. II. С. 45-46.180

89. Грилихес С.Я., Тихонов К.И. Электролитические и химические покрытия: Теория и практика. Л,: Химия. Ленингр. отд-ние, 1990. 288 с.

90. Кудинов В.В., Иванов В.М. Нанесение плазмой тугоплавких покрытий. М.: Мап1ИНостроение , 1981. 192 с.

91. Савочкин В.Р., Нагай Й.Н. Напряжение пробоя и защитные свойства окисных пленок на титане// Защита металлов. 1981. Том XVII. №3 . С. 318-321.

92. Гнеденков СВ . Формирование покрытий на титане методом микродугового оксидирования, их состав и свойства: Дис. ... канд. хим. наук. 1988. 165 с.

93. Формирование износостойких покрытий на титане/ П.С. Гордиенко, С В . Гнеденков, О.А. Хрисанфова и др.// Электронная обработка материалов. 1990. №5. С. 32-35.

94. Гордиенко П.С. Формирование покрытий на ряде металлов и сплавов в электролитах при микроплазменных процессах: Дис. ... д-ра техн. наук. 1991. 683 с.

95. Малоцикловая усталость титановых сплавов после МДО/ Е.Д. Шеховцев, П.С. Гордиенко, СВ . Гнеденков, Н.И. Лошакова// Защитные покрытия. Способы получения и свойства. Владивосток. 1989.

96. Федоров В.А. Модифицирование микродуговым оксидированием поверхностного слоя деталей// Сварочное производство. 1992. №8. С. 29-30.

97. Образование рутила и анатаза при микродуговом оксидировании титана в водных электролитах/ П.С. Гордиенко, О.А. Хрисанфова, Т.П. Яровая и др.// Электронная обработка материалов. 1990. №4. С. 19-22.

98. Кузовлева К.Т., Гордиенко П.С. Потенциодинамическое исследование анодного оксидирования титана при высоких потенциалах// Электронная обработка материалов. 1989. №5. С. 44-47.

99. Баковец В.В. Оксидные покрытия, полученные микродуговой обраоткой титанового сплава в кислых электролитах// Неорганические материалы. 1987. Т. 23. №7. С. 1226-1228.

100. Технология получения покрытий микродуговым оксидированием/ Э.С. Атрощенко, И.А. Казанцев, А.Е. Розен// Новые промышленные технологии. 1996. № I.e . 28-33.

101. Получение покрытий анодно-искровым электролизом/ В.И. Черненко,

102.Л.А. Снежко, И.И. Папанова - Л.: Химия. Ленингр. отд-ние, 1991. 126 с.

103. Герций О.Ю. Технологическое обеспечение качества обработки детаей машин методом микродугового оксидирования на основе раскрытия наледственных связей между заготовкой и деталью: Дис. ... канд. техн. наук. 1996. 254 с.

104. Свойства оксидных пленок, сформированных переменным напряжением на титановом сплаве ВТ-1/ Е.К. Черненко, Л.А. Янов, В.И. Черненко// Электрохимия. 1971. Т.VII. Вып. 9. С. 1374-1377.

105. Малышев В.Н. Особенности формирования покрытий методом анодно-катодного микродугового оксидирования// Защита металлов. 1996. Том 32. №6. С. 662-667.

106. Особенности строения и свойства покрытий, наносимых методом микродугового оксидирования/ В.Н. Малышев, Г.А. Марков, В.А. Федоров и др.// Химическое и нефтяное машиностроение. 1984. №1 . С. 26-27.

107. Руднев В.С. , Гордиенко П.С. Зависимость толщины покрытия от потенциала МДО// Защита металлов. 1993. Т.29. №2. С. 304-307.

108. Оптимизация режимов получения и свойств оксидных покрытий на алюминиевом сплаве с использованием метода мультифрактального анализа/ В.Н. Малышев, А.Г. Колмаков, И.Ж. Бунин// Физика и химия обработки материалов. 1997. №5. С. 77-84.

109. Некоторые закономерности формирования микродуговых покрытий/ А.И. Слонова, О.П. Терлеева, Е.К. Шулепко, Г.А. Марков// Электрохимия. 1992. Т.28. Вып. 9. С. 1280-1285. 18

110. Справочник по триботехнике. В 3-х т. Т. 3. Триботехника антифрикционных, фрикционных и сцепных устройств. Методы и средства триботехнических испытаний/ Под общ. ред. М. Хебды, А.В. Чичинадзе. М.: Машиностроение, 1992. 730 с.

111. P. Pesode, S. Barve, Surface modification of titanium and titanium alloy by plasma electrolytic oxidation process for biomedical applications: a review, Mater. Today: Proc. (2020).

112. LEON A, LEVY G K, RON T, SHIRIZLY A, AGHION E, The effect of strain rate on stress corrosion performance of Ti6Al4V alloy produced by additive manufacturing process [J]. Journal of Materials Research and Technology, 2020, 9: 4097−4105.

113. Isaev A., Grechishnikov V., Kozochkin M. [et al.] Structure and machinability of thin-walled parts made of titanium alloy powder using electron beam melting technology / A. Isaev, V. Grechishnikov, M. Kozochkin [et al.] // IOP Conference Series: Materials Science and Engineering. – Miskolc-Lillafured: Institute of Physics Publishing, 2016. – P. 012044.

114. Facchini L, Microstructure and mechanical properties of Ti-6Al-4V produced by electron beam melting of pre-alloyed powders/ Facchini L, Magalini E, Robotti P, Molinari A// - Received 2009. - p 171-178.

115. J. Wang, H. Fan, H. Zhang, Q. Chen, Y. Liu, W. Ma, Anodizing process of titanium and formation mechanism of anodic TiO_2 nanotubes, Progr. Chem. 28 (2016) 284–295.

116. J.D.C. Tardelli, C. Bolfarini, A.C. Dos Reis, Comparative analysis of corrosion resistance between beta titanium and Ti-6Al-4V alloys: a systematic review, J. Trace Elem. Med. Biol. (2020), 126618.

117. WANG Ya-ming, JIANG Bai-ling, LEI Ting-quan, JIA De-chang, ZHOU Yu. Research progress of wear resistant coating on Ti6Al4V alloy surface [J]. Journal of Materials Engineering, 2016, 3: 38−43.

118. X. Zhang, Z. Yao, Z. Jiang, Y. Zhang, X. Liu, Investigation of the plasma electrolytic oxidation of Ti6Al4V under single-pulse power supply, Corros. Sci. 53 (2011) 2253–2262.

119. D. Quintero, O. Galvis, J.A. Calderon, M.A. Gomez, J.G. Castano, F. Echeverría, H. Habazaki, Control of the physical properties of anodic coatings obtained by plasma electrolytic oxidation on Ti6Al4V alloy, Surf. Coat. Technol. 283 (2015) 210–222

120. A.L. Yerokhin, X. Nie, A. Leyland, A. Matthews, S.J. Dowey, Plasma electrolysis for surface engineering, Surf. Coat. Technol. 122 (1999) 73–93.

121. Y. Han, S.-H. Hong, K. Xu, Porous nanocrystalline titania films by plasma electrolytic oxidation, Surf. Coat. Technol. 154 (2002) 314–318.

122. V.S. Rudnev, Micro- and nano-formations on the surface of plasma electrolytic oxide coatings on aluminum and titanium, Surf. Coat. Technol. 235 (2013) 134–143.

123. M. Shokouhfar, C. Dehghanian, A. Baradaran, Preparation of ceramic coating on Ti substrate by Plasma electrolytic oxidation in different electrolytes and evaluation of its corrosion resistance, Appl. Surf. Sci. 257 (2011) 2617–2624.

124. H. Jiang, Z. Shao, B. Jing, Effect of electrolyte composition on photocatalytic activity and corrosion resistance of micro-arc oxidation coating on pure titanium, in, Procedia Earth Planet. Sci. (2011) 156–161.

125. Y. Jiang, J. Wang, B. Hu, Z. Yao, Q. Xia, Z. Jiang, Preparation of a novel yellow ceramic coating on Ti alloys by plasma electrolytic oxidation, Surf. Coat. Technol. 307 (2016) 1297–1302.

126. M. Echeverry-Rendon, O. Galvis, D. Quintero Giraldo, J. Pavon, J.L. Lopez- Lacomba, E. Jimenez-Pique, M. Anglada, S.M. Robledo, J.G. Castano, F. Echeverría, Osseointegration improvement by plasma electrolytic oxidation of modified titanium alloys surfaces, J. Mater. Sci. Mater. Med. 26 (2015) 1–18.

127. O.A. Galvis, D. Quintero, J.G. Castano, H. Liu, G.E. Thompson, P. Skeldon, F. Echeverría, Formation of grooved and porous coatings on titanium by plasma electrolytic oxidation in H2SO4/H3PO4 electrolytes and effects of coating morphology on adhesive bonding, Surf. Coat. Technol. 269 (2015) 238–249.

128. W. Ping, W. Ting, P. Hao, G.X. Yang, Effect of NaAlO2 concentrations on the properties of micro-arc oxidation coatings on pure titanium, Mater. Lett. 170 (2016) 171–174.

129. J. Baszkiewicz, D. Krupa, J. Mizera, J.W. Sobczak, A. Bilinski, ´ Corrosion resistance of the surface layers formed on titanium by plasma electrolytic oxidation and hydrothermal treatment, Vacuum 78 (2005) 143–147.

130. “Additive Manufacturing Using Material Ti-6AL-4V Titanium Alloy:Review”, NeuroQuantology. Dhiaa H.Hilfi, Suminov Igor, 25- March -2023, DOI:10.48047/nq.2023.21.5.NQ222145

131. M. Aliofkhazraei, D.D. Macdonald, E. Matykina, E.V. Parfenov, V.S. Egorkin, Applied Surface Science Advances, Volume 5, 1 September 2021, 100121.

132. Dhiaa H.Hilfi , Suminov Igor «Additive Manufacturing Using Material Ti-6AL-4V Titanium Alloy: Review», NEUROQUANTOLOGY | March 2023 | Volume 21 | Issue 5| Page 1530-1556| doi: 10.48047/nq.2023.21.5.NQ222145

133. Dhiaa H.Hilfi, Suminov Igor «Microsturctural Characteristics and Mechanical Properties of Ti 6Al 4V Alloy in Additive Manufacturing», International Journal of Membrane Science and Technology, 2023, Vol. 10, No. 2, pp 3665-3681

134. Суминов И.В., Хилфи Диаа Х.Ч. «Аддитивные технологии в современной промышленности: применение и перспективы на примере титановых сплавов», обзор, Кузнечно-штамповочное производство, обработка материалов давлением, №3, 2024 год, стр.36-44.

135. Суминов И.В., Хилфи Диаа Х.Ч. «Экспериментальное исследование влияния технологических параметров процесса электрохимическое оксидирование на свойства оксидного слоя и его эксплуатационные характеристики», испытания, измерения и контроль, Кузнечно-штамповочное производство, обработка материалов давлением, №4, 2024 год, стр.51-57.

136. Суминов И.В., Хилфи Диаа Х.Ч. «Технологии плазменно-электролитной обработки поверхностей изделий машиностроения из титанового сплава ВТ6, сформированных аддитивными технологиями», испытания, измерения и контроль, Кузнечно-штамповочное производство, обработка материалов давлением, №4, 2024 год, стр.58-62.